ANALYSIS OF PROTEINS AND PEPTIDES BY ON-COLUMN PRECONCENTRATION CAPILLARY LIQUID CHROMATOGRAPHY AND CAPILLARY ELECTROPHORESIS

By

HONG SHEN

A DISSERTATION PRESENTED TO THE GRADUATE SCHOOL
OF THE UNIVERSITY OF FLORIDA IN PARTIAL FULFILLMENT
OF THE REQUIREMENTS FOR THE DEGREE OF
DOCTOR OF PHILOSOPHY

UNIVERSITY OF FLORIDA

1998

To my dearest wife Qing and son Kevin

ACKNOWLEDGMENTS

I would like to thank my advisor, Bob Kennedy, for his generous support and outstanding guidance during my stay at the University of Florida. I would also like to thank the members of the Kennedy group for the wonderful time I had in my daily work. Special thanks go to my parents and my parents-in-law for their selfless support that led me through all the difficulties in the past 5 years. I would like to give my sincerest thanks to my dear grandmother, Peiheng Hu, for the early scientific education and all her understanding and love over the past 30 years.

TABLE OF CONTENTS

page

Abstract of Dissertation Presented to the Graduate School
of the University of Florida in Partial Fulfillment of the
Requirements for the Degree of Doctor of Philosophy

ANALYSIS OF PROTEINS AND PEPTIDES BY ON-COLUMN PRECONCENTRATION CAPILLARY LIQUID CHROMATOGRAPHY AND CAPILLARY ELECTROPHORESIS

By

Hong Shen

May 1998

Chairman: Robert T. Kennedy
Major Department: Chemistry

Capillary liquid chromatography has been used as a separation based microanalysis method due to its low mass limit of detection and improved resolution compared to conventional high performance liquid chromatography (HPLC). While the mass limit of detection is in the low attomole range, the concentration limit of detection of these methods is typically in the nanomolar to high picomolar range, which is insufficient for analysis of many proteins and peptides *in vivo* due to their low concentrations. This deficiency is because the typical sample volume that can be loaded onto capillary columns is limited to the nanoliter scale. In order to improve the concentration limit of detection, the capability of loading large volume samples (preconcentration) is required.

In this dissertation, the development of different on-line preconcentration techniques will be addressed. A dual-microcolumn immunoassay (DMIA) technique was

developed and applied to insulin variants determination in various sample matrices. While the separation and detection were performed on the second reversed phase column, the first immunoaffinity column was used to selectively preconcentrate insulin variants from sample matrices as complicated as serum. With up to 500 μL sample loaded onto the DMIA system, a concentration limit of detection of 20 pM was achieved with simple UV/Vis detection.

In addition to the analysis of peptide hormones by DMIA, a single-column capillary liquid chromatography/electrochemical detection (capillary LC/EC) system was developed for *in vivo* monitoring of neuropeptides using microdialysis sampling. With over 100-fold on-column preconcentration of analytes, the concentration limit of detection was improved from nanomolar to picomolar range. Coupled with a microdialysis probe, this capillary LC/EC method was applied to *in vivo* met-enkephalin monitoring, improving the temporal resolution 6-fold compared to radioimmunoassay. Application of this capillary LC/EC system was extended to non-electroactive neuropeptides using a pre-column biuret derivatization. With biuret reaction, peptide as low as 30 pM can be derivatized by the copper(II) at basic pH. It has been shown that this system can be used to monitor both electroactive and non-electroactive neuropeptides with improved temporal resolution.

In order to better understanding the formation and oxidation of peptide copper biuret complexes, capillary electrophoresis (CE) was used to couple with both UV absorbance and electrochemical detection to investigate the electroactivity of peptide copper biuret complex in different forms.

CHAPTER 1
INTRODUCTION

Proteins and peptides are important biomolecules that are involved in a variety of significant biological functions. The importance of understanding their functions has been constantly addressed but this task relies heavily on the improvement of currently available analytical methods. The *in vivo* concentrations of some very important proteins, such as insulin, and neuropeptides such as met-enkephalin, vasopressin and bradykinin, are typically in the low picomolar range and in a complicated sample matrix; this combination presents a great analytical challenge. For *in vivo* monitoring of these neuropeptides, currently available methods that utilize microdialysis coupled with radioimmunoassay (RIA) can achieve temporal resolution as fast as 30 min [Boa83, Hat92, Lud92, Lud93, Lan91, Mai89, Ver92]. The temporal resolution is limited by the mass sensitivity of the methods. While these temporal resolutions already require sub-femtomole mass limit of detection, it limits the capability of monitoring the *in vivo* changes of these neuropeptides in the 30 min time interval. In order to study the biological behaviors of these peptides at short time intervals, the capability of higher temporal resolution *in vivo* monitoring is required. To improve the temporal resolution of *in vivo* monitoring, a method with better mass limit of detection is essential.

Miniaturization is a general trend in analytical science, particularly so in the field of chemical separations. The development of microcolumn separations in the last few

years has been widely embraced in the field of analytical chemistry and biotechnology [Jor81, Jor83, Nov88, Ken89]. The microcolumn has been used for separation based microanalysis method due to its low mass limit of detection and improved resolution in comparison to conventional high performance liquid chromatography (HPLC). Microcolumns are ideal in micro scale analysis where sample volumes are small and limited, such as in single cell analysis [Wal88, Ken89, Coo92, Ewi93], or very recently, single vesicle analysis [Chi98].

While the mass sensitivity of microcolumn separations is in the low attomole range [Ole90, Slo93], the concentration limit of detection of these methods is usually in the nanomolar to upper picomolar range (500 pM for catechol) [Lu93], which is insufficient for analysis of many proteins and peptides *in vivo*. In addition to detector sensitivities, small sample volumes that a capillary column can accommodate also attribute to this deficiency of high concentration limit of detection. Typically the sample volume that can be loaded onto capillary columns is limited to the nanoliter scale. One way of improving the concentration limit of detection of this capillary column based method is to increase the sample volume (preconcentration). Part of this dissertation will explore the feasibility of applying on-column preconcentration capillary column separation to *in vivo* protein and peptide analysis.

Microcolumn Separation

Among many different microcolumn separation modes, capillary liquid chromatography (capillary LC) and capillary electrophoresis (CE) are two capillary based separation techniques. In the research presented in this dissertation, both packed capillary column liquid chromatography and capillary electrophoresis have been used to develop

separation based microanalysis systems to analyze biologically important proteins and peptides. Due to the difference in the separation mechanisms, each separation mode has its own advantages as outlined below.

Capillary Electrophoresis (CE)

Currently, the most popular and widely studied microcolumn separation technique is capillary electrophoresis. Although its principles are well documented [Tse59], capillary electrophoresis is a relatively new separation technique compared to liquid chromatography. In capillary electrophoresis the separation is based on the difference of electrophoretic mobility μ of analyte ions in an electric field. The electrophoretic mobility can be approximated as

$$\mu = \frac{z}{m^{\frac{2}{3}}} \qquad 1 - 1$$

where z is the charge of the analyte in its the separation form and m is mass of the analyte [Chu92]. The separation efficiency of an analyte can be described as the number of theoretical plates, N. When diffusion is the major source of band broadening, N can be expressed as

$$N = \frac{(\mu + \mu_{osm})V}{2D} \qquad 1\text{-}2$$

where D is the diffusion coefficient of the analyte, V is the potential applied across the separation capillary and μ_{osm} is the mobility of the separation buffer.

The resolution R_s of two analytes that are separated by the electric field can then be expressed as

$$R_s = \frac{N^{1/2}}{4} * \frac{\mu_1 - \mu_2}{\mu_{av} + \mu_{osm}} \qquad 1\text{-}3$$

where μ_1 and μ_2 are the electrophoretic mobilities of the analytes and the μ_{av} is the average of the two. Rearranging equations 1-2 and 1-3:

$$R_s = \frac{1}{4}\left(\frac{V}{2D}\right)^{1/2} \frac{\Delta\mu}{(\mu_{av} + \mu_{osm})^{1/2}} \qquad 1\text{-}4$$

$\Delta\mu$ is the difference of the electrophoretic mobilities of the two analytes. For given analytes, as expressed in equations 1-2 through 1-4, the higher the electric field, V, the higher the number of theoretical plates and the higher the resolution R_s. In addition, R_s is also proportional to $\Delta\mu$. The high number of theoretical plates is mainly attributed to the flat profile of the electroosmotic flow which causes less zone dispersion than laminar flow in pressure driven separations. This separation scheme has achieved extremely high resolution, especially for protein and peptide separations. As many as 10^6 plates for protein separations have been reported [Lau86]. As can be seen in equation 1-3, the resolution of separating two analyte is proportional to the square root of the number of theoretical plates. The factor that increases N will also be beneficial to R_s, such as the separation potential, V, and diffusion coefficient, D.

In addition to its high resolving power, CE is also a fast separation technique:

$$t_m = \frac{L^2}{(\mu + \mu_{osm})V} \qquad 1\text{-}5$$

Here t_m is the migration time of the analyte in the separation capillary in the electric field, L is the capillary length between the injection and the detection. By increasing the electric field strength, i.e. V/L, the migration time will decrease accordingly. With small i.d. fused silica capillaries (5 - 50 μm i.d.), very high electric fields can be applied without severe heating problems. It is reported that electric field as high as 1200 V/cm

has been used for DNA analysis [Dov97]. High field strength capillary electrophoresis has also been used in our lab to shorten the separation time to sub-second level [Tao98].

Among its many applications, CE has been used to separate ligand from complex in affinity assays and has been successfully applied to an immunoaffinity based insulin assay [Sch95, Tao96]. In addition to separating ligand from complex, CE can also separate complexes with different numbers of ligands attached. In this dissertation, CE was used as a method to separate biuret (copper-peptide) complexes with different numbers of bound copper. Coupling to electrochemical detection, the electroactivity of these biuret complexes can be determined.

Packed Capillary Column Liquid Chromatography

For packed capillary column liquid chromatography, depending on the stationary phase particles used, all conventional liquid chromatographic separations, such as reversed phase, ion-exchange, hydrophobic interaction, affinity chromatography and size-exclusion, can be performed on a much smaller scale. The separation mechanisms are identical to their conventional counterparts. Bulk transport is achieved using a pressure gradient just as that in conventional liquid chromatography. However, there are several advantages of capillary columns compared to conventional columns.

High resolution. One of the important indices to measure the success of the separation of two components is resolution, R_s, which can be defined by following equation

$$R_s = \frac{X_2 - X_1}{2(\sigma_1 + \sigma_2)} \qquad 1\text{-}6$$

where X_1 and X_2 are the center locations of the two zones, and $\sigma 1$ and $\sigma 2$ are their respective zone variances. Zone variance σ is related to theoretical plate height, H, by

$$H = \frac{\sigma^2}{X} \qquad 1\text{-}7$$

it can be seen that the smaller the H, the higher the R_s. According to the Knox equation, reduced plate height (h), which is the ratio of plate height H over packing particle diameter, can be expressed as [Ken72]

$$h = Av^{0.33} + \frac{B}{v} + Cv \qquad 1\text{-}8$$

At a specific reduced velocity (v), the reduced plate height will be determined by the parameters *A, B* and *C*. It has been shown that both *A* and *C* will decrease with the decrease of column inner diameter for given particle size while *B* term slightly increases [Kar88, Col93]. Among these three, the most striking changes appeared in the *A* term, which decreased rapidly with decreasing column inner diameter. According to Eq 1-8, as A term decreases, the reduced plate height (h) will decrease and so does the theoretical plate height (H). This decreased H results the increasing of resolution R_s.

Improvement on concentration-sensitive detection. The most important and commonly used LC detectors (such as UV absorbance, fluorescence, and sometimes electrochemical detection) are concentration sensitive, so that the decrease in peak volume of small-diameter columns is beneficial in terms of substantially improved mass sensitivity. This phenomenon can be understood by the smaller volumetric peak variance (σ_{column}^2) inside the capillary column [Nov88]

$$\sigma_{column}^2 = (\pi r^2 \varepsilon_T)^2 HL \qquad 1\text{-}9$$

where ε_T is the total porosity of the column packing material, r is the column radius, and L is the column length. It is clear that the smaller the column radius, the smaller the volumetric peak variance. As volumetric peak variance decreases, the concentration of a given amount of analyte eluted from a capillary column will increase. This increased analyte concentration will generate a larger response in concentration-sensitive detector such as UV/VIS, electrochemical and fluorescence detection and thus increase mass sensitivity.

Preconcentration. One difference between capillary liquid chromatography and capillary electrophoresis is the on-line preconcentration capability of packed capillary column. A sample volume that exceeds 100 times the column volume can be loaded onto the capillary column system without detrimental effect on the separation efficiency [Kar74, She97b]. For a given mass sensitivity, the concentration detection limit can be improved several hundred fold from previous nanomolar to picomolar through preconcentration. With this decreased concentration detection limit, many biologically important proteins and peptides in living systems can be analyzed without off-line preconcentration steps. One major purpose of the research described here is to develop capillary liquid chromatography based separation techniques to be utilized in the analysis of low concentration proteins and peptides in biological samples through preconcentration.

Other advantages. There are other advantages of capillary liquid chromatography over conventional HPLC. This includes smaller sample requirements, low volumetric flow rate compatibility, and less solvent consumption. This miniaturized system is ideal for micro-scale analysis where sample volume is small and limited as mentioned before.

The low flow rates used in capillary column make it compatible to interfacing to mass spectrometry, which has gained substantial interest due to its ability to obtain both qualitative and quantitative information on the analytes. As it is today, capillary column based separation has already become a very attractive method in microanalysis.

In order to perform microanalysis, both a compatible detector and a sampling technique are needed. In accordance with miniaturization of the separation column, sampling and detection must also be miniaturized to accommodate the overall small sample volume. In addition to the commercially available UV/VIS detector, a carbon fiber microelectrode based detector has been widely used in conjunction with capillary columns to detect electroactive analytes [Kne84, Wal87, Ken89, Coo92]. For the biological application of this microcolumn separation system, a microdialysis probe is usually used to acquire *in vivo* samples. A brief introduction of microelectrode detection and microdialysis sampling will be given in the following two sections.

Microelectrode Detection

Electrochemical detection has been successfully used in conventional scale separation due to its simplicity, selectivity and high sensitivity. Electrochemical detection is also a concentration sensitive technique and its potential can be better achieved when coupled with microcolumn separations, which improves mass detection limits. There are three basic modes of electrochemical detection: amperometry, conductimetry and potentiometry. Of these three detection modes, amperometry is the easiest to use and is also one of the most popular detection schemes used in chromatography. In amperometry mode, the analyte is oxidized or reduced through the

loss or gain of electrons at the electrode surface. The current through the electrode surface is directly proportional to the concentration of analyte present.

Carbon fiber based microelectrodes were initially used for the *in vivo* determination of dopamine in the rat brain [Gon80, Day81]. Typically, the carbon fiber microelectrode has a diameter of several micrometers to sub-micrometer, making it ideal for analysis in micro-environments. In addition to the spatial resolution advantage, the microelectrode also has smaller double layer capacitance, which allows rapid signal transition [Day81]. The cylindrical geometry of the carbon fiber based microelectrode (see Figure 1-1) makes it an ideal detector for capillary column separations [Ken89, Coo92]. For capillary electrophoresis coupled with microelectrode, a mass detection limit of 0.5 amol for dopamine has been reported [Ole90]. In this is dissertation, the characterization of carbon fiber microelectrodes coupled with a capillary column separation system will be discussed.

Microdialysis Sampling

Microdialysis is a technique developed recently in the field of neuroscience research for sampling regions of the brain with high spatial resolution and moderate temporal resolution. Figure 1-2 shows a schematic of a microdialysis probe. The dimensions of the microdialysis probe are typically in several mm range. The analyte diffuses through a size selective dialysis membrane that allows only small analyte molecules to pass while blocking large molecules. The size of the molecule allowed to pass through the membrane is determined by the pore size of the dialysis membrane. The perfused analyte is then carried away by dialysis flow and collected for analysis. Because of its small dimensions, the microdialysis probe is suitable to be used in micro-

environment sampling with minimum disturbance to the subject. It has been widely used as an *in vivo* sampling technique followed by HPLC with/or Radioimmunoassay (RIA) determination [Mai89, Ken90, Mai91, Emm95].

In measuring the efficiency of microdialysis sampling, both absolute recovery and relative recovery are used. The absolute recovery is the index that measures the amount of analyte the microdialysis probe acquired in a period of time while the relative recovery measures the ratio of the concentration of acquired analyte to that in the sample solution. Both indices will be affected by the dialysis sampling flow rate. For a given microdialysis probe and analyte, the higher the sampling flow rate, the higher the absolute recovery and the lower the relative recovery. At a certain flow rate, the absolute recovery will begin to level off while the relative recovery will continuously decrease limiting the maximum useful flow rate.

For coupling with a mass sensitive detector, absolute recovery is the main consideration since detection requires minimum amounts of analyte. This is the case for microdialysis coupling with the RIA determination of proteins and peptides. Although RIA has been widely used in coupling with microdialysis for biological tasks, their mass limits of detection were typically in the medium to upper amol range [Boa83, Hat92, Lud92, Lud93, Lan91, Mai89, Ver92]. In addition to their moderate limit of detection, the radiation protection as well as the radioactive waste disposal remains as other major drawbacks. On the other hand, HPLC based detection schemes have also been used to quantitate microdialysis samples [Her93, St.85]. Many detectors used in HPLC are concentration sensitive such as fluorescence, electrochemical detection (ECD), etc. For concentration sensitive analytical scheme such as LC/ECD, the relative recovery of the

microdialysis probe will be the main concern. In order to achieve higher relative recovery in microdialysis sampling, a lower flow rate will be required. The flow rate used in microdialysis sampling is typically several microliters per minute. While the sample volume obtained at this flow rate in a reasonable time is too small to be easily manipulated in conventional HPLC analysis, the relative recovery is already very low, usually less than 10% [Mai89, Ken90, Mai91, Emm95].

On the other hand, capillary column separations require very small volumes of sample to perform the analysis. The coupling of microdialysis and microcolumn separations will take full advantage of the small sample volume acquired by the microdialysis probe at low flow rates with the high relative recovery and the high sensitivity detection provided by microcolumn separations [She97b]. Part of the research presented in this dissertation is method development for capillary liquid chromatography to monitor neuroactive peptides in the brain with microdialysis as a sampling tool.

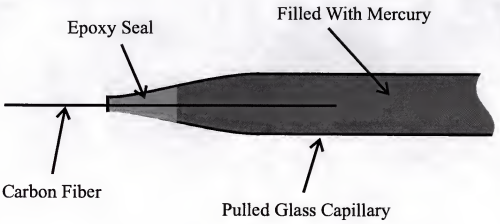

Figure 1-1. Schematic of cylindrical carbon fiber microelectrode.

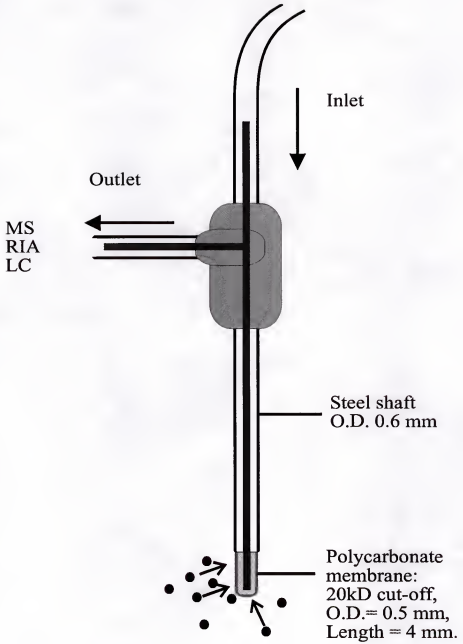

Figure 1-2. Schematic of microdialysis probe.

CHAPTER 2
DUAL MICROCOLUMN IMMUNOAFFINITY / REVERSED PHASE CHROMATOGRAPHY DETERMINATION OF INSULIN VARIANTS

Introduction

Due to the increasing complexity of modern analytical tasks, there are large demands on the improved separation power of modern chromatographic techniques. One common way of doing this is to decrease the inner diameter of the separation column as stated in the last chapter. In addition to improve the resolution power of each specific separation column, combining distinct separation modes to achieve the separation of very complicated samples is clearly a fruitful approach [Jan88, Jan89a, Jan98b, Flu93, Col95, She97a]. By using multi-column separation schemes, two analytes that can not be separated by the first column can sometimes be separated by the second column that based on different separation mechanism. With the use of a dual microcolumn separation system, not only do we have the benefit of multi-column separation, but also we can take advantage of the enhanced resolution power of the capillary liquid chromatography (see chapter 1). In this chapter, a study based on development of dual microcolumn immunoaffinity chromatography will be presented. A capillary immunoaffinity chromatographic column will be used as the first column to preclean and preconcentrate the analytes and a reversed phase capillary column will be used as the second dimension of the separation system to achieve better separation of analytes that co-eluted from the

first immunoaffinity column. Figure 2-1. shows the principles of dual microcolumn immunoassay.

Immunoaffinity Chromatography

Immunoaffinity chromatography is based on biospecific binding interactions between a ligand chemically bound to the chromatographic packing and a target molecule in the sample. An immobilized ligand may include either proteins or small molecules that interact specifically with the target molecule of interest. Immunoaffinity chromatography has been widely used in the field of biotechnology and biochemistry and is an important tool for both purification and determination of trace biological molecules in complex sample matrices [Fau84, Jan88, Jan89a, Jan89b].

Antigen-antibody interaction. An antibody is a protein substance produced in the blood or tissues in response to a specific antigen, such as a bacterium or a toxin. As a result, an antibody usually has an extraordinarily high binding constant to its specific antigen. The forces involved in the binding include the same ionic and hydrophobic interactions that cause nonspecific ion-exchange and hydrophobic interaction binding. However, the charged and hydrophobic groups are arranged on both antigen and antibody in a unique orientation; thus, the two fit into each other like a lock and key, with a very high degree of specificity. Therefore, the antigen-antibody interaction is extremely strong in comparison to other ordinarily nonspecific interactions. As a result, very low concentration of antigen in a very complicated sample matrices can be "picked up" by its specific antibody together with very limited amount of other interferences. The interaction between antigen and antibody has been used to pre-clean and preconcentrate

the analytes from complicated sample matrices [Jan88, Jan89a, Jan98b, Flu93, Col95, She97a].

Immunoaffinity chromatography. Immunoaffinity chromatography is a separation technique that based on the biospecific binding of the analyte molecule to the immobilized ligand. In immunoaffinity chromatography, one of the ligand pair (antibody or antigen) is immobilized (covalently coupled) as a bound phase. This immobilized ligand forms a highly selective stationary phase that, in theory, will only bind to the other molecule (either antigen or antibody) of the ligand pair. In a typical immunoaffinity chromatographic assay, the analyte is selectively retained by the antibody while non-binding components of a sample are washed out of the column. The bound substances are then eluted and detected following injection of an agent, such as low pH buffer, which disrupts the antibody-antigen interaction.

Preconcentration. In addition to their role in separation, immunoaffinity interaction can also be used in preconcentrating low concentration analytes of interest. Due to their high binding constant between antigen and antibody, a very low concentration of antigen or antibody can be retained on the stationary phase through immunoaffinity interaction. After a large volume of sample is loaded onto the immunoaffinity column, a desorbing reagent will be introduced to break the bond between antigen and antibody. Usually the eluted volume is much smaller than the loaded sample volume and thus the low concentration analyte is selectively enriched. The capacity of this preconcentration process will only be limited by the binding constant and the amount of immobilized ligand available.

Pre-cleaning. This preconcentration technique not only preconcentrates the analyte of interest, but also removes the majority of interference that does not bind with the immobilized ligand. The effluent obtained this way is relatively clean because the majority of interference substances is removed. However, due to the nonspecific binding between the immobilized ligand and other interference of the sample, there are usually some interference substances co-eluting with the analyte. Coupled with the other separation technique, the analyte can then be separated from its co-eluting interference substances and determined.

Dual-Microcolumn Immunoassay

Dual-microcolumn chromatography. As samples get more and more complicated, one column (single dimension) separation technique may not be able to resolve all the components in it. With the development of dual-column separation (two-dimensional separation) technique, the peak capacity is greatly increased as stated by the following equation:

$$n_T = n_1 \times n_2 \qquad 2\text{-}1$$

where the n_T is the total peak capacity of the dual-column separation system, and the n_1, n_2 are the peak capacity of individual separation dimensions. The above calculation assumes the two separation dimensions are based on completely different mechanisms (i.e. their separation mechanisms are "perpendicular" to each other). The co-eluted components from first separation column will be given the chance to be separated and detected on the second column, because of different separation mechanisms.

There are several types of dual-column separation techniques investigated. To try to analyze all the components in the sample, the effluents from the first column must be

collected in either temporal or spatial sequences and be introduced into the second separation column. There are, however, some cases in which only one or two of the components in the sample of interest. In these cases, the first column will serve as both pre-separation and pre-cleaning step to eliminate most of the interfering components for the easy separation and determination of analytes on the second column. This method is extremely useful when dealing with complicated sample matrices such as serum and other biological fluid. Part of the work present here is the development of a dual-microcolumn immunoassay technique applied to different biological samples to determine insulin concentration.

Dual-microcolumn immunoassay (DMIA). In spite of the great selectivity possible with antibody stationary phases, interferences frequently degrade detection limits in single column immunoassay. For example, the desorbing agent can cause a baseline disturbance when using UV absorbance detectors. This disturbance can hinder observation of the analyte peak at low levels and worsen detection limits. Similarly, nonspecifically adsorbed components or cross-reactive antigens can interfere with detection of the analyte. In addition, slow desorption kinetics can have a detrimental effect on detection limits due to dilution of the analyte zone during elution.

To avoid the limitations of single column immunoaffinity assays, Janis and coworkers [Jan88, Jan89a, Jan98b] introduced the concept of dual-column immunoassays (DCIAs). In this type of assay, a second chromatography column, typically reversed-phase, is placed in-line with the immunoaffinity column. The system collects the desorbed zone from the immunoafffinity column and injects it onto the second reversed phase column where it is reconcentrated and separated from desorbing buffer,

nonspecifically adsorbed components, and cross-reactive analytes. The combination of reconcentration and added separation dimension result in significant improvement in selectivity and detection limit for DCIAs relative to one-column immunoassays. DCIAs have proven to be versatile as well and have been used for determining antigens in a complex mixture, characterizing protein variants and determining antibody titers [Jan88, Jan89a, Jan98b].

Presented here is the development of a dual-column assay that utilizes packed capillary columns which brings the advantages of microcolumns to DCIA. Using microcolumns instead of conventional HPLC columns gives higher mass sensitivity, better compatibility with mass spectrometry, and less consumption of reagents and stationary phases. Only one previous example of a dual-column affinity assay that utilizes microcolumns has been described [Flu93]. In that work, the affinity column was used to retain high concentration interfering substances in order to simplify the reversed-phase separation of the unretained components. In this work, we describe the development and application of a dual microcolumn immunoassay for insulin. It is found that the multiple stages of preconcentration allow low concentration detection limits for antigens, even with a UV absorbance detector in the microcolumn. In addition, the preconcentration steps simplify the instrumental requirements of the system.

Bioanalytical Applications

With the development of the dual microcolumn immunoassay system, two bioanalytical applications were performed. As a demonstration, the assay is explored for determination of insulin in serum and insulin secretion from single rat islet of Langerhans.

Determination of rat insulin secretion from single rat islet. Islets are microorgans containing about 3000 cells each and are dispersed throughout the pancreas. Islets are responsible for secreting insulin and other hormones regulating glucose metabolism; thus, the measurement of insulin secretion from islets is important in the study of diabetes and other metabolic diseases. It is often desirable to measure insulin release at the level of single islets since insulin release at the level of single islets since insulin secretion from islets may vary due to differences in islet size or position within the pancreas. In addition, islets are difficult to obtain and the ability to work at the single islet level saves considerable resources required to isolate islets. Typically, insulin secretion from islets is measured by radioimmunoassay (RIA) which can take over one day to complete. Therefore, more rapid and more sensitive assays for insulin may be of interest in diabetes research.

In our work, we utilize rat islets which benefit in another way from analysis by a dual-column assay. Rats are unusual among mammals in that they synthesize and release two insulin variants (rat insulin I and II) with slightly different amino acid sequences. Most secretion measurements by RIA do not distinguish between the forms; the functional significance of their existence has not been determined.

Determination of insulin in serum. In addition to the single rat islet insulin secretion analysis, the determination of insulin level in the serum is also carried out on this DMIA system. Serum is considered one of the most complicated biological systems in terms of the difficulties for analysis. However, the direct analysis of insulin in the serum represents great importance in the study and treatment of diabetes. Currently, the most commonly used method is still RIA as stated before. The dual microcolumn

immunoaffinity assay system has the concentration detection limit for the direct measurement of insulin level in serum and therefore can be used on the determination of insulin in serum.

Experimental

Reagents

Rat insulin and human insulin were obtained from Eli Lilly and company (Indianapolis, IN, USA). Antibodies used in this work were monoclonals from Balb/c mice and were originally described by Schroer et al [Sch83]. Two different antibodies (designated antibody 1 and 2) were used and their properties are summarized in Table 2-1. The antibodies were obtained in phosphate buffered saline following purification from ascites fluid using protein G affinity chromatography by the University of Florida Hybridoma Laboratory. Unless specified otherwise, all other reagents used were from Sigma. All solutions were filtered with 0.22-μm nylon filters (MSI, Westboro, MA, USA) before use.

Preparation of Capillary Reversed-Phase Columns

Reversed-phase capillary columns were prepared using a previously described technique [Col93]. Fused- silica capillaries (Polymicro Technologies, Phoenix, AZ, USA), 15 cm long with 150 μm I.D. and 360 μm (O.D.), were used as column blanks. Approximately 0.5 to 1 cm of the polyimide coating on one end of the capillaries was removed with a flame. Frits were installed by gently tapping the stripped end of the capillary into a pile of 15-μm glass beads (Duke Scientific, Palo Alto, CA, USA). This process was continued until a 0.1-0.2 mm section of the capillary was filled with beads. This section was then briefly heated with a match flame to sinter the beads in place.

Table 2-1. Properties of Antibodies used

Antibody	Name[a]	Insulin immunogen	Isotype	Affinify constant K_o (L/M)[b]	Bovine I_{50}[c]	Human I_{50}	Porcine I_{50}	Rat I_{50}[d]
1	DB9G8	Bovine	IgG_{2a}	$5X10^7$	1	1	0.5	3
2	AE9D6	Human	IgG_1	$3X10^8$	113	1	0.3	38

a. Designation assigned by original developer of antibody in Ref. [Sch83].
b. Data from Ref. [Sch83].
c. I_{50} is the ration of insulin variant to antigen required to inhibit binding of 50% of the immunogen to the antibody.
d. No distinction was made between Rat I and Rat II insulin in this test.

Capillaries with frits installed were slurry packed at 1000 to 1500 p.s.i. from a high-pressure bomb equipped with a pneumatic amplifier pump (Alltech Model 1066). The slurry solvent was 50% acetonitrile – 50% 20 mM phosphate buffer (pH 2.5) and used in a ratio of 100:1 (ml solvent/g packing materials); 5 μm particles with 300 A pores modified with octyl stationary phase (Deltabond, Keystone Scientific, Bellafonte, PA, USA) were used for most of the work. For serum analysis, columns were packed with 10 μm Poros IIR particles modified with octadecyl stationary phase (PerSeptive Biosystems, Cambridge, MA, USA).

Preparation of Capillary Immunoaffinity Columns

Capillary immunoaffinity columns were packed in a fashion identical to that described above except the slurry solvent was 20 mM pH 2.5 phosphate buffer and the particles were 20 μm diameter perfusion particles modified with recombinant protein G (Poros 20 G, PerSeptive Biosystems).

The antibody was loaded onto a protein G packed capillary by pumping a 60 μl slug of 0.375 mg/ml antibody (either antibody 1 or antibody 2 or a 1:1 mixture of the two) in 20 mM pH 6.5 phosphate buffer ("loading buffer") at 5 μl/min using a syringe pump (ISCO Model 100DM, ISCO, Lincoln, NE, USA) through the capillary. The antibody-loaded column was rinsed with several column volumes of loading buffer. The antibody was cross-linked to the protein G phase [Hor87] by pumping 200 μl of 50 mM dimethylpimelimidate dihydrochloride (Pierce Chem., Rockford, IL, USA) in 0.2 M triethanolamine (pH 8.2) through the capillary column at 5 μl/min. The column was then rinsed with 0.2 M ethanolamine at 30 μl/min for 10 min. Several column volumes of desorbing buffer (20 mM phosphate at pH 2.5) were injected onto the column to remove

any unbound antibody. For simple illustration, see figure 2-2. The column was stored in 10 mM pH 6.5 phosphate buffer containing 10 mM sodium azide at 4°C. Columns prepared in this fashion had an average binding capacity for insulin of 130 ± 15 pmol (n=5).

Apparatus

Figure 2-3 shows a block diagram of the DMIA instrument. The system was equipped with two six-port injection valves (C6W, Valco Instruments, Houston, TX, USA). Valve 1 was used to load samples onto the immunoaffinity column (injection loop volume depended on the experiment). The second valve (fitted with a 5-µl loop) was used to collect the elution peak from the immunoaffinity column and inject it onto the reversed-phase capillary column. Teflon tubing (Alltech, Deerfield, IL, USA) with 0.0625 in. (1 in.=2.54 cm) O.D. and 0.010 in. I.D. was used as a sleeve over the fused-silica tubing for connection to the injection valve ports. Flow through the immunoaffinity column was controlled by an ISCO 100DM syringe pump. Flow through the reversed-phase column was generated by an SSI 222D pump (Scientific Systems, State College, PA, USA). In order to maintain a smooth baseline, a post-pump mixing coil (stainless steel tubing 300 cm X 1.0 mm I.D.) was used to enhance mixing of the mobile phase components. A splitter (10 cm X 50 µm i.d. fused-silica capillary) was used between the gradient LC pump and the second injection valve to generate low flow rates in the capillary reversed-phase column.

Detection was accomplished on-column using a Thermo Separation Products (Fremont, CA, USA) model Spectra 100 variable-wavelength UV absorbance detector set at 210 nm. The rise time of the detector was set at 1 s for all chromatograms. A

computer (Gateway 2000 4DX2-66) equipped with a National Instruments data acquisition board (AT- MIO-16F-5) was used to collect data and analyze the chromatograms. The detector was directly connected to the immunoaffinity column for characterization.

Procedure for DMIA

Samples up to 500 µl dissolved in loading buffer were loaded through an on-line filter frit into the loop of injection valve 1 and then injected. Unless stated otherwise, the sample was injected at 35 µl/ min and the pump then adjusted to 5 µl/min. While the flow rate was stabilizing (typically about 5 min was required), the immunoaffinity column was rinsed with loading buffer for over 10 column volumes. The immunoaffinity column was then rinsed with desorbing buffer at 5 µl/min. The desorbed zone was collected into the second sample loop by switching valve 2 at the appropriate time. For initial characterization studies using bovine insulin as a test analyte, the reversed-phase mobile phase was an 80:20 mixture of 0.1% trifluoroacetic acid : acetonitrile. For gradients, the mobile phase was stepped to 35% acetonitrile at 5.00 min. Conditions for the second separation for more complex mixtures of insulin are given for each sample.

Determination of Insulin Secretion from Single Islets

Islets, obtained from male Sprague-Dawley rats using a previously described procedure [Sch95], were incubated at 37°C in the presence of 5% CO_2 for one to five days prior to use. For secretion experiments, a single rat islet was incubated in 70 µl of 3 mM glucose in Kreb's Ringer Buffer (KRB: 118 mM NaCl, 5.9 mM KCl, 2.54 mM $CaCl_2$, 1.19 mM $MgSO_4$, 1.19 mM KH_2PO_4 and 25 mM $NaHCO_3$) for 30 min. A 60-µl volume of the supernatant was removed for analysis. The same islet was then incubated

with 70 µl of 8 mM glucose in KRB for another 15 min after which 60 µl was removed for analysis. The procedure was then repeated with 20 mM glucose on the same islet. The supernatants were injected directly onto the DMIA system and analyzed as described above except the sample loading was performed at 5 µl/min. The immunoaffinity column used for the insulin secretion measurement was loaded with a 1:1 mixture of both antibody 1 and 2. For the reversed-phase separation of rat insulins, solvent A was 20 mM phosphate buffer pH 6.5 and solvent B was 40% solvent A with 60% acetonitrile. The initial mobile phase was 37% B. For the gradient, the mobile phase was increased to 55% B over 5 min, and then maintained at 55% B for 3 min.

Determination of Insulin in Serum

Serum samples were prepared by reconstituting lyophilized human serum as described by the supplier (Sigma). For calibration studies, insulin was spiked into the serum at appropriate concentrations. Reconstituted serum was directly injected onto the immunoaffinity column and assayed as described above with two modifications. First, the immunoaffinity column used for serum determinations was 15 cm long, but only 1.5 cm was packed. It was found that this short bed had sufficient capacity and much less nonspecific adsorption than the fully packed capillary. Second, a larger rinsing volume (over 20 column volumes) was used after injection of serum onto the immunoaffinity column. For the reversed-phase separation, solvent A was pH 2.5 20 mM phosphate buffer and solvent B was 40/o solvent A and 60% acetonitrile. The initial mobile phase was 30% B. For the gradient, the mobile phase was linearly increased to 60% B in 5 min then linearly increased to 100% B in 5 min.

Results and Discussion

Characterization of DMIA

Effect of loading and desorbing conditions on insulin recovery. It is desirable to use high loading and desorbing flow rates in order to minimize overall analysis times. The loading flow rate is especially important when preconcentrating large volume samples (up to 500-µl samples were used in our experiments) on capillary columns. The loading flow rate cannot be increased arbitrarily because (1) the capture efficiency may decrease if insufficient time is given for binding and (2) the pressure limits on the packing material may be exceeded. We found that recovery of insulin from injection of 20 µl of 1 nM insulin was 100% over the loading flow rate range of 1 to 35 µl/min, see Table 2-2 and Figure 2-4.

Higher flow rates could not be used because of the pressure limits of the packing materials (2000 psi). As with the loading flow rate, high desorbing flow rates are desirable in order to minimize analysis time. However, increasing the desorbing flow rate causes greater dilution of the eluted antigen zone due to the relatively slow kinetics of desorption [Car86]. We measured desorbing peak volumes and time required for desorption using desorbing flow rates of 1 to 10 µl/min as summarized in Table 2-3 and Figure 2-5. As expected, the lower flow rates yielded lower volume, and therefore more concentrated, antigen zones that required longer elute times. The longer elution times were compounded by a technical difficulty. Specifically, several minutes were required for the flow rate to stabilize after changing from the loading flow rate to a lower desorbing flow rate. The stabilization time increased with decreasing desorbing flow rate as illustrated in Table 2-3. The effects of pH and ionic strength of loading buffer were

Table 2-2. Recovery Effect of Loading Flow Rate

Loading Flow rate (μL/min) (Insulin 1 μM, 20 μL loading)	UV Absorbance of Desorbing Peak (Arbitrary Unit)*	Relative Recovery** (%)
1.0	74.2	100.0
3.0	68.2	91.9
5.0	76.5	103.1
10.0	78.8	106.2
10.0***	4.47	100.9
35.0***	4.40	99.2

* The UV absorbance readings were corrected by desorbing flow rate and the AUFS setting.

** Assuming the insulin recovery with 1 μL/min loading flow rate was 100%.

*** Different insulin concentration and total sample volume (0.2 μM, 500 μL with different AUFS setting).

also investigated for their effect on recovery. The pH could be increased to 7.4 and the ionic strength could be varied between 0.02 and 0.2 M (ionic strength was varied by addition of Na_2SO_4) with no decrease in recovery from our standard loading buffer. Increasing the ionic strength to 3 M and higher, however, reduced loading efficiency by over 50%. Therefore, samples with extremely high ionic strength may need to be desalted before being used with this antibody.

Injection volume for reversed-phase column. As discussed above, higher desorbing flow rates result in dilution of the desorbed zone. The desorbed zone, however, can be reconcentrated on the second column. Using the injection system described in the Experimental Section, we found that up to 5 µl of insulin dissolved in the desorbing buffer could be injected onto the second column with only a 10% decrease in theoretical plates over that found for a 1-µl injection volume. The ability to inject this large volume is due to preconcentration by reversed-phase retention. Since desorbing buffers tend to be aqueous solvents, it is likely that many proteins could be similarly preconcentrated on reversed-phase columns in the second dimension.

Based on this experiment and the results in Table 2-3, we elected to use desorbing flow rates of 5 µl/ min. The elution volume of 1.9 µl at this flow rate (see Table 2-3) was well within the tolerable injection volume range of the reversed-phase column. In addition, with the desorbed peak volume this small, it was straightforward to reliably capture the entire peak in a 5-µl loop for injection onto the reversed- phase column despite the dead volume of the valves and variation in the desorption time from the first column.

Table 2-3. Effect of Desorbing Flow rate

Desorbing Flow rate (μL/min)	Desorbing Peak Volume[1] (μL)	Total Desorbing Time[2] (min)	System Equilibrium Time[3] (min)
1.0	1.0	4.33	15.0
3.0	1.5	1.50	8.0
5.0	1.9	1.10	3.0
10.0	2.6	0.67	2.0

1. The total volume of the desorbing peak; 2. Time needed from the injection of desorbing buffer to the complete elution of antigen; 3. Approximate time the capillary immunoaffinity column needed to reach the specified desorbing flow rate from the higher loading flow rate (35 μL/min here).

Detection limit and calibration. A goal of this work was to use the dual-column system for quantitative analysis in biological samples. Therefore, we characterized the linearity of the peak area for bovine insulin obtained by DMIA following 500-µl injections of 0.1 to 5 nM bovine insulin dissolved in loading buffer. A chromatogram used in the calibration is illustrated in Figure 2-6. The response was apparently linear (correlation coefficient of 0.992) with a slope of 0.026 nM/unit area and an intercept of –0.24 nM. Peak areas had relative standard deviations of 5% for 500-µL injections. In general, the response was linear up to binding capacity of the immunoaffinity column.

The detection limit, calculated as the concentration that would give a peak height three times the peak-to-peak noise was 20 pM for a 500-µl injection. This corresponds to a 10 fmol detection limit which is typical for UV detectors with capillary columns. The low concentration is directly attributable to the significant preconcentration possible with the two columns. In previous work, we had described a similar assay which utilized capillary electrophoresis in the second dimension [Col95]. That assay had a detection limit of about 25 nM, which is well above that described here. The improved detection limit is due to the ability to inject and concentrate the entire desorbed antigen zone on the reversed-phase column. In the CE case, on-line preconcentration in the second dimension was not readily accomplished and only a small portion of the antigen zone eluted from the affinity column could be injected.

Simultaneous detection of insulin variants. An important advantage of DCIA is the ability to simultaneously determine multiple, cross-reactive protein variants [Jan88, Jan89a, Jan98b]. Figure 2-7 illustrates a DMIA of 4 insulin variants, all of which cross-react with antibodies used in the first column. In developing this assay, it was found that

antibody 1 preferentially recovered rat insulin II. Therefore, we investigated antibody 2 for the immunoaffinity column which we found recovered both rat insulins equally, but gave lower recovery overall. Maximum recovery was obtained by immobilizing a 1:1 mixture of the two antibodies. Compared to a column that utilized just antibody 1, a column with a 1:1 mixture of antibody 1 and 2 had the same recovery for rat insulin II and a 40% increase for rat insulin I. The insulin from other species was unaffected by the use of a mixed antibody column.

Applications of DMIA for Insulin

Determination of insulin secretion from single islets. Figure 2-8 illustrates a DMIA for insulin secreted from an islet stimulated with 8 mM glucose. As shown, the two rat insulins were well-resolved and their peaks were above the detection limit allowing for quantitative measurements. A summary of the quantification of insulin secretion is given in Table 2-4. The total amounts of insulin released are in agreement with previous studies of insulin secretion assayed by RIA coupled with HPLC from rat islets under similar conditions. For example, Ma reported that rat islets stimulated with 22 mM glucose secrete 0.83 pmol insulin/islet/30 min [Ma95]. For comparison, the results in Table 2-4 for 20 mM glucose stimulation, expressed in the same units, would be 0.92 pmol insulin/islet/30 min (recall that a 15-min stimulation was used in our case). Finally, insulin quantified by DMIA gave results with relative standard deviation of 3.2% (n =4). The results in Table 2-4 indicate that rat insulin I and II are released differentially, but at a constant ratio regardless of the glucose concentration. This result is also in agreement with previous studies. For example, in experiments that utilized 40 to 150 islets pooled together, Gishizky et al. showed that 85% [Gis87] of the insulin released

Table 2-4. Single Rat Islet Insulin Secretion with Different Glucose Stimulation Level

Stimulating Glucose Level (mM)	Insulin I ± σ (fmole)	Insulin II ± σ (fmole)	Total Insulin ± σ (fmole)	Percentage of Insulin I (%)
3 (n=4)	96 ± 19	19 ± 2	114 ± 21	83 ± 3
8 (n=3)	196 ± 29	30 ± 6	226 ± 35	88 ± 3
20 (n=3)	389 ± 119	70 ± 40	460 ± 154	85 ± 3

was rat I compared to 83% to 88% for our results. The agreement with previous results illustrates that the DMIA provides quantitative information that is consistent with RIAs. The previous measurements were made by separating the insulins by HPLC, collecting the fractions, and assaying them for insulin by RIA. This is a laborious, time consuming process (the RIA required 8 h). By comparison, the assay used here required 45 minutes and the analysis could easily be automated. Further improvement in the analysis could be obtained by using a more sensitive detection scheme (requiring less sample to inject) or by improving the separation speed. Furthermore, the assay could readily be adapted to other islet hormones by using multiple antibodies on the affinity column.

DMIA for insulin in serum. Another application that we explored with the dual-column system was determination of insulin in serum. The complexity of serum samples presents a challenge to the selectivity of the dual-column method. This is illustrated by the DMIA chromatograms of serum samples in figure 2-9. Trace A. shows a serum blank (i.e., a serum sample with no insulin added). As seen, a number of peaks appear in the reversed-phase chromatogram suggesting nonspecific adsorption to the immunoaffinity column. In order to decrease this effect, the column length was shortened to 1/10 of the length used for the islet studies. This was done to reduce the nonspecific adsorption sites while maintaining a sufficient insulin capacity. The shorter column reduced the overall background peaks to the level seen in figure 2-9, trace A. The height of the largest serum blank peak (the largest peak is not shown in the chromatograms in figure 2-9 decreased from 0.16 absorbance units (a.u.) with a 15 cm packed bed to 0.02 a.u. with the 1.5 cm packed used for figure 2-9 trace A. We attempted to further reduce the number of interfering peaks by several sample treatments prior to injection onto the immunoaffinity

columns. Sample pretreatments examined include: (1) extraction of lipids with 1,1,2-trichlorotriflouroethane, (2) removal of immunoglobulins by solid-phase extraction with Protein G particles, and (3) reduction of nonspecific adsorption by adding 0.2% Tween 20 to the sample and loading buffer. These treatments decreased some of the peaks that appeared later in the chromatogram, but they did not reduce those in the range of 4 to 5 min, which is the expected retention time of insulin. Thus, for the further experiments we used untreated serum.

In spite of the interfering peaks at the insulin retention time, it was still possible to clearly observe a peak for insulin at 200 pM as illustrated by comparing figure 2-9, trace A to trace B and C. The detection limit in the serum was set by the variability of the co-eluting peak. We calculated a detection limit of 100 pM as the insulin concentration that would give a signal three times the standard deviation of the co-eluting interfering peak. This detection limit is nearly sufficient to reliably measure basal levels of insulin in serum which can be between 47 and 150 pM. A calibration performed by spiking insulin at concentrations of 0.2 to 3.0 nM into serum samples was linear with a slope of 6.27 nM/peak height and intercept of -0.10 nM with a linear correlation coefficient of 0.996.

It was found that the amount of insulin recovered on the reversed-phase column when insulin was dissolved in serum was 50 ± 9.8% (n=4) of that found for insulin dissolved in loading buffer which resulted in a decrease in sensitivity. This decrease in recovery is possibly due to competition for binding sites with large amounts of nonspecifically adsorbed material. It was also found that the immunoaffinity column capacity for insulin loading decreased by 18% after 14 serum sample loadings. The

decrease in loading capacity is attributed to blocking of antibody binding sites by high concentration proteins or peptides found in the serum.

It is apparent that use of the system for real serum analysis would require some improvements. One possibility would be to use the standard addition method to determine the insulin concentration in the presence of the matrix peaks. A preferable choice would be to completely eliminate the co-eluting interference peak by optimizing the mobile phase gradient or eliminating the nonspecific adsorption on the immunoaffinity column with an appropriate pretreatment. The co-eluting interfering peak may include some native insulin, however attempts to reduce it by treating the sample with anti-insulin modified particles did not reduce the peak significantly.) In addition, the use of more selective detection, such as fluorescence (perhaps with post-column derivatization) would allow for more freedom from interferences and improved detection limits. These results suggest that the dual microcolumn assay may be used for samples as complex as serum; however, trace-level substances, such as insulin and other hormones, will be difficult to determine without effort spent to optimize the separation and/or detection.

Conclusion

The development of a DMIA system which utilizes capillary immunoaffinity column coupled with capillary reversed-phase column is presented. The system can be used for many of the applications that have already been described for dual-column assays such as characterization of protein variants, determination of multiple antigens and antibody titers [Jan88, Jan89a, Jan89b]. In addition, several advantages of this system compared to conventional DCIA were apparent. For example, the microcolumn system

uses less materials. This is especially significant for expensive chromatographic packings like protein G-modified particles. The system also has good mass sensitivity which allows insulin release from single islets to be readily measured. The preconcentration capability of the DMIA allowed islets to be manipulated in convenient volumes (incubation volumes were about 70 μl) without concerns about excessive dilution of the analyte. These advantages are achieved without sacrifice in convenience of operation. Typically microcolumn systems require extensive modifications to conventional HPLC equipment. In this case, the use of preconcentration allowed conventional injection valve to be used. Relatively high flow rates in the immunoaffinity column allowed a readily available syringe pump to be used. The main modifications that were still required were a on-column detector cell and a splitter for the mobile phase flow in the reversed phase column. With capillary reversed-phase column, the mass detection limit was improved in comparing with conventional column. The DMIA system has insulin mass detection limit of 10 fmole with simple UV/Vis detection and can accommodate up to 500 μL sample, which is 100 times of the column volume.

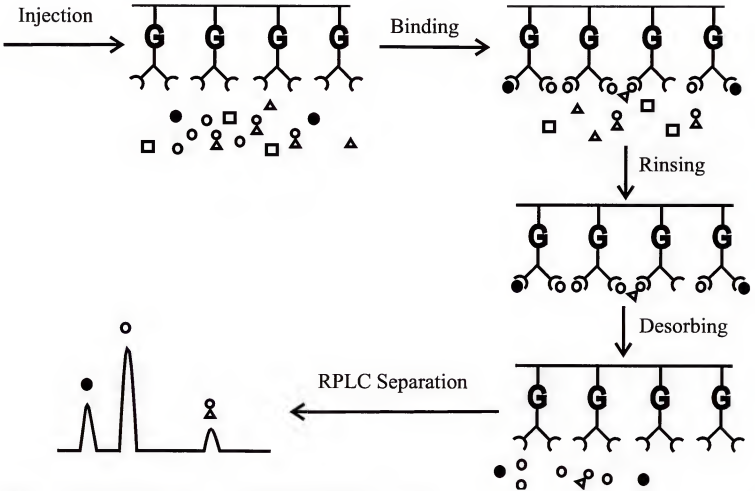

Figure 2-1. Principle of dual-microcolumn immunoaffinity assay.

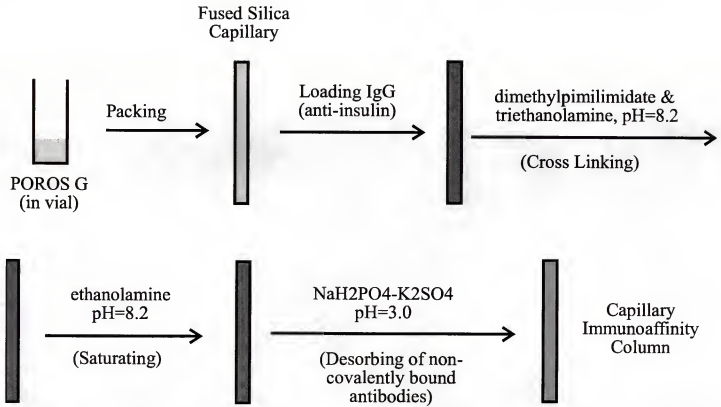

Figure 2-2. Schematic of immunoaffinity chromatographic column preparation.

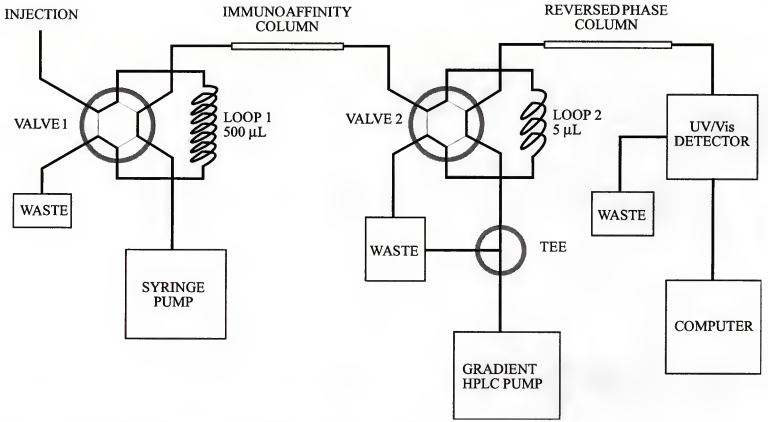

Figure 2-3. Block diagram of DMIA instrument.

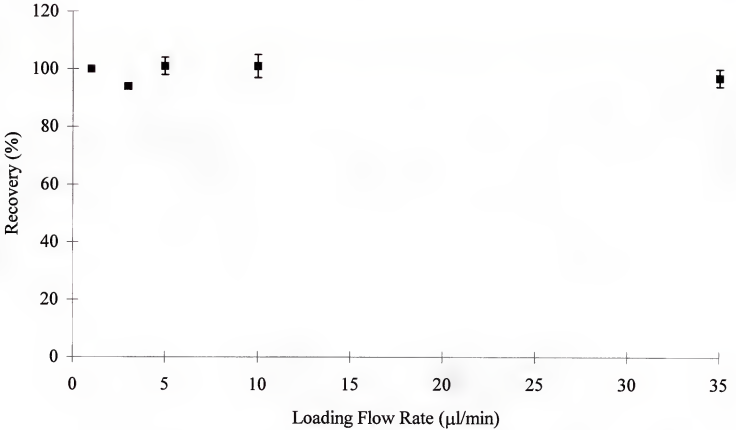

Figure 2-4. Effect of recovery on different loading flow rate. Experimental condition described in table 2-3.

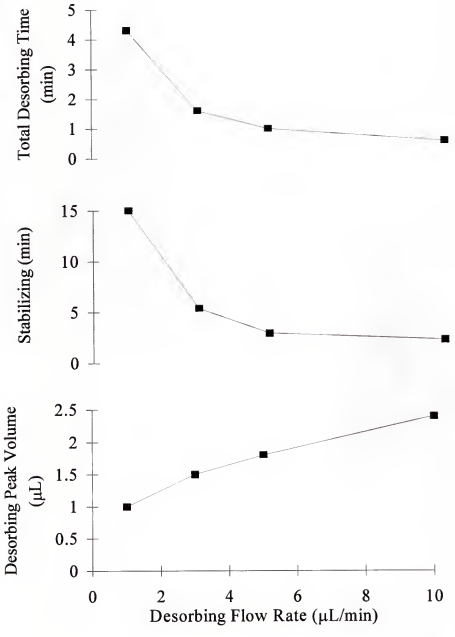

Figure 2-5. System performance affected by the desorbing flow rate. (A) peak desorbing time, (B) system stabilizing time and (C) total volume of desorbing peak.

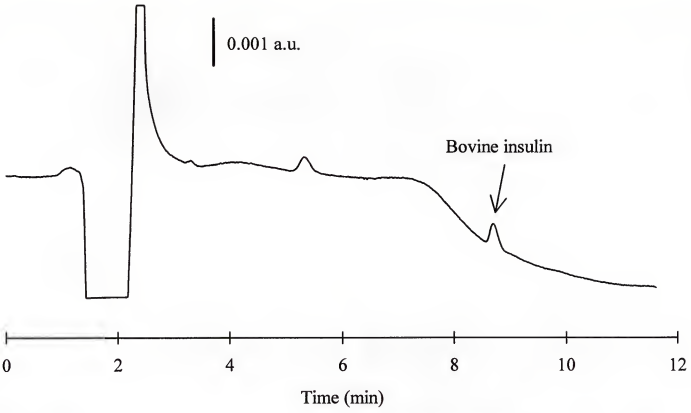

Figure 2-6. DMIA chromatogram of 100 pM bovine insulin in 500 µl loading buffer. Mobile phase conditions are given in the experimental section.

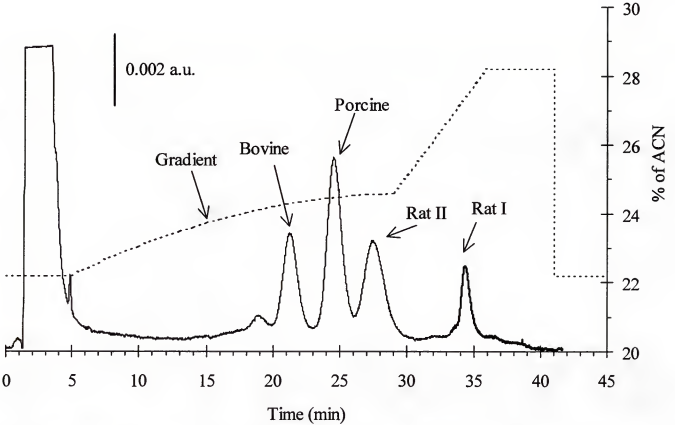

Figure 2-7. DMIA separation of insulin variants. Sample injected was 60 µl bovine (30 nM), porcine (45 nM), rat I (100 nM) and rat II (100 nM) insulins in loading buffer. Mobile phase solvent A and B are the same as for separation of rat insulins (see experimental section) and the gradient is indicated by the dashed line

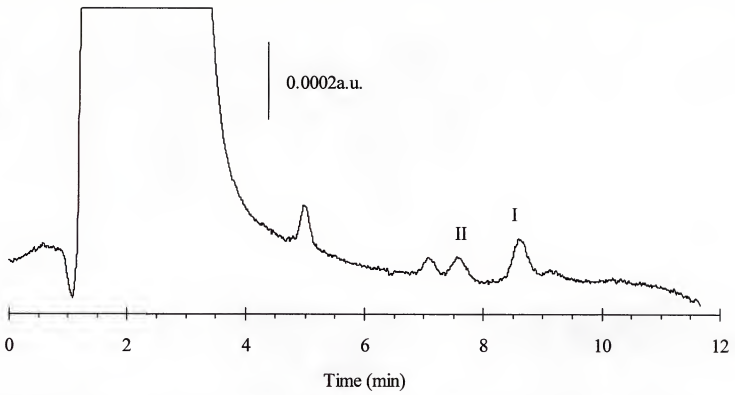

Figure 2-8. DMIA chromatogram of supernatant from single rat islet stimulated with 8 mM glucose. Labeled peaks indicate rat insulin II and I as shown. Unlabeled peaks are either due to buffer or unknowns from the sample.

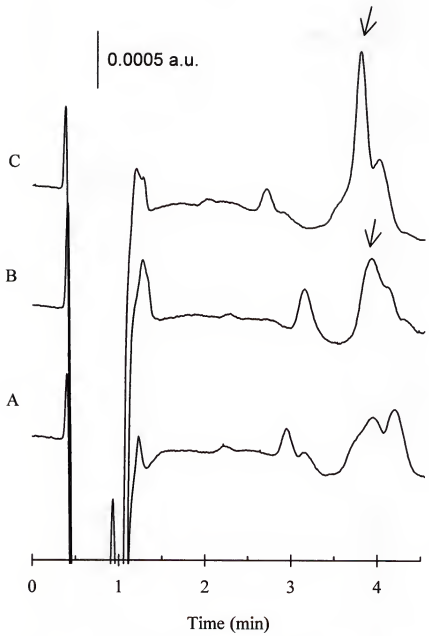

Figure 2-9. DMIA of 500 µl serum samples. (A) Serum blank (no insulin added), (B) serum with 200 pM human insulin added and (C) serum sample with 1 nM human insulin added. The arrows indicate the human insulin peaks.

CHAPTER 3
ON-LINE PRECONCENTRATION CAPILLARY LIQUID CHROMATOGRAPHY/ELECTROCHEMICAL DETECTION (LC/ECD) MONITORING OF MET-ENKEPHALIN WITH MICRODIALYSIS SAMPLING

Introduction

Neuropeptides are an important group of neuroactive substances which can act as neurotransmitters, neuromodulators, and neurohormones throughout the central nervous system [Bra86]. Compared to other types of neurotransmitters, such as monoamines or amino acids, neuropeptides are much more difficult to detect and monitor in the brain because they tend to be found at much lower concentrations than the other neurotransmitters. For example, peptides are typically in the 1-150 pM range while monoamines may be present at a few nM and the amino acids are present at micromolar concentrations [Rob91].

An important example of the neuroactive peptides is the opioid peptide met-enkephalin [Mai89, Boa83, Ken90] which has been implicated in several diseases. For example, met-enkephalin levels have been correlated to neurological disorders such as Huntington's Disease [Wag86, Che95] and Parkinson's Disease [Dur91, Mon94, Lad96]. Met-enkephalin has also been implicated in regulation of several important physiological functions. It has been found, for example, that met-enkephalin can decrease pain-related impulses to the brain by inhibiting the release of substance P [Adv93]. Met-enkephalin also regulates the secretion of prolactin by blocking dopaminergic inhibition [Zho95].

As with other peptides, a greater understanding of met-enkephalin is hindered by the difficulty of monitoring it *in vivo*. The difficulty in monitoring is partially due to the fact that *in vivo* met-enkephalin concentration is low; for example, in the globus pallidus, a region rich in met-enkephalin, the extracellular concentration is estimated to be approximately 150 pM [Her93, St.85]. By far the most common method for monitoring met-enkephalin and other peptides is by microdialysis sampling coupled with radioimmunoassay (RIA). In some cases, HPLC is used prior to the RIA to gain further selectivity [Her93, St.85]. The use of microdialysis sampling exacerbates the difficulty of detecting peptides because of fairly low relative recoveries. For detection of met-enkephalin for example, if a dialysis flow rate of 2.7 μL/min is used, the relative recovery might be ~9% requiring detection of low picomolar in dialysates from the globus pallidus [Her93]. At this low of a concentration, RIA is the preferred method for detection because of its concentration detection limits allow direct determination in the dialysates. The mass detection limits for RIA's of small peptides are typically 0.1 - 0.2 fmol. This detection limit, combined with typical absolute recoveries of the probes, allow sampling frequencies of 30 minutes [Her93].

Since neuronal events occur on much faster time scales than current methods can follow, it is of interest to develop alternative approaches to monitoring that allow better temporal resolution. Temporal resolution possible with microdialysis sampling is usually limited by the mass detection limit of the assay used with the probe. The mass detection limit of RIA, while quite low, is not as good as what can be achieved by capillary separation methods. For example, capillary liquid chromatography with electrochemical detection (LC/EC) has mass detection limits of a few attomoles [Hur95, Sau84], thus the

use of this technique offers the opportunity to significantly improve temporal resolution. A problem with capillary LC/EC is that concentration detection limits are not sufficient to detect basal levels of peptides in dialysates. This paradox is caused by the fact that capillary separation techniques normally utilize minuscule injection volumes on the order of a few nanoliters. Recently, some work has focused on using large volume injections and on-column preconcentration in order to improve the concentration detection limit in capillary LC [Dru85, Oat89]. As presented in last chapter, a two-stages of preconcentration has been developed to yield low picomolar detection limits in 500 μL samples for insulin using UV absorbance detection [Oat89].

In addition to use immunoaffinity preconcentration technique presented in last chapter, direct on-column reversed phase preconcentration can also be achieved [Vis96, She97b]. With this preconcentration capability, the sample volume limitation of the capillary reversed phase separation can be avoided. As the sample volume increases, concentration detection limit of the capillary LC can be greatly improved. This improvement will allow capillary LC be used in low concentration analyte determination, such as brain neuropeptide analysis.

On a reversed phase column, small organic molecules and large protein molecules behave differently on their retention and separation. Usually there are two different major interactions between the analyte molecules and stationary reversed phase: partition and adsorption/desorption. For small organic molecules, the retention and separation is mainly based on their partition between stationary phase and mobile phase. Analytes are separated due to their different partition coefficients between the two phases. But for

protein and peptides, their retention and separation is dominated by adsorption/desorption rather than partition. This can be better illustrated in figure 3-1.

For small organic molecule, such as biphenyl, its capacity factor k' gradually decreases as the content of organic modifier increases. This trend is maintained through a wide range of organic modifier concentration. However, the capacity factor *k*'s of the protein and peptide such as myoglobin, lysozyme and insulin, behave differently. For example, insulin, an peptide hormone with about 50 amino acid, when the organic modifier content changes from 34% to 33%, the capacity factor of insulin changes from 7 to 16, which is more than doubled. This means that the retention of analyte will be twice as longer if the organic modifier percentage decreases only 1%. For the same insulin, as the organic modifier content increases above 40%, its capacity factor approaches 1 and the change is limited. This phenomenon can be understood by the interaction between those proteins or peptides and stationary reversed phase [Gen94]. During separation, protein or peptide molecules are first adsorbed onto stationary phase due to their hydrophobicity to the reversed phase. These molecules will stay on the stationary phase until organic modifier content in the mobile phase reaches the critical percentage for specific protein or peptide. Only at this critical organic modifier concentration, the specific protein or peptide starts to elute. This provide the bases that proteins and peptides can be preconcentrated on a stationary reversed phase with very low or no organic modifier in the sample.

In the work presented here, large on-column preconcentrations in conjunction with capillary LC/EC is utilize to monitor met-enkephalin in dialysates with 5 min temporal resolution. This 6-fold improvement in temporal resolution over that possible

with RIA is due to the high mass sensitivity of capillary LC/EC. The method should be generally applicable to monitoring a variety of tyrosine and tryptophan-containing oligopeptides in the brain. The possibility of further improvement in temporal resolution is also discussed.

Experimental

Reagents and Mobile Phase

Unless specified otherwise, all chemicals were purchased from Sigma (St. Louis, MO, USA). The aqueous portion of the mobile phase (solvent A) for reversed-phase capillary liquid chromatography was 1 mM phosphate buffer in 10 mM sodium sulfate adjusted to pH 7.0. The organic phase (solvent B) was prepared by mixing 40% (v/v) of aqueous buffer with 60% acetonitrile. Artificial cerebral spinal fluid (aCSF) used for microdialysis perfusion consisted of 145 mM NaCl, 2.68 mM KCl , 1.01 mM $MgSO_4$, and 1.22 mM $CaCl_2$. The high K^+ perfusate solutions for stimulation experiments consisted of 2.62 mM NaCl and 145 mM KCl with other salts the same as aCSF.

Preparation of Capillary Reversed Phase Columns

Capillary columns were prepared by previously described techniques [Ken89] using 7 to 8 cm lengths of 25 μm inner diameter (i.d.), 360 μm outer diameter (o.d.) fused silica capillaries (Polymicro Technologies, Phoenix, AZ, USA) as the column blanks. Columns were slurry-packed with 5 μm Alltima C-18 (Alltech, Deerfield, IL, USA) reversed-phase particles (slurries consisted of 10 mg packing material in 3 ml acetonitrile) at 1.2 to 1.4 MPa using a pneumatic amplifier pump (Cat. No. 1666, Alltech).

Capillary LC

A schematic of the LC system used in this work is shown in Figure 3-2. Mobile phase flow was generated using a SSI 232D HPLC gradient pump (Scientific Systems, State Collage, PA, USA) through a splitter tee. A two valve injection system was designed to minimize both waste of sample and dead volume between sample and column. The first six-port two position valve (Valco Instruments, Houston, TX, USA) was used to connect the sample capillary and the pump. The outlet of the sample capillary was connected to a cross (Valco) which was constructed so that 360 μm o.d. capillaries fit snugly inside. One port of the cross was connected to a second six-port switching valve, another was connected to the column, and the last port was normally plugged. The sample capillary and column were positioned inside the cross (see figure 3-3) under a microscope with a small gap between them in order to minimize dead volume. After the capillaries were correctly positioned, the last port of the cross was sealed with a plug. The use of a cross instead of a tee facilitated capillary positioning. The second six-port switching valve allowed the cross to be connected to two different splitter capillaries, the larger one 50 μm i.d. by 15 cm long and the smaller one 25 μm i.d. by 6 cm long.

Injections were made by switching the sample capillary from the high pressure flow path using the first valve. The second valve was connected to the larger i.d. splitting capillary and a micro syringe used to load sample into the sample capillary. Such loadings left the sample capillary filled and excess sample in the larger splitter capillary with insignificant sample entering the column because of the flow resistance. To transfer sample onto the column, the second valve was closed and the sample capillary reconnected to high pressure by switching the first six-port switching valve. After the

sample was loaded onto the column, the second valve was switched to the smaller i.d. splitting capillary. This splitter served to: 1) allow faster displacement of mobile phase in the sample capillary to give more prompt response to the gradient, and 2) to provide extra pulse dampening to reduce the pumping noise. For all of the separations and injections approximately 1.3 MPa was applied onto the separation column giving a flow-rate of ~ 2 nl/s and a linear velocity of 0.6 cm/s.

To maintain the best detection limits and minimal drift from large volume injections the aqueous buffer was prepared fresh and filtered everyday before the experiment. In addition, after loading the column was rinsed with 5% solvent B-95% solvent A for 5 min before gradient elution started. Gradient elution started at 5% solvent B, linearly changed to 50% solvent B in 5 min, kept at this composition for 2 min, and then stepped back to 5% solvent B.

Electrochemical Detection

A 9 μm diameter, 2 mm long carbon fiber electrode was used as the detector electrode [Kaw93]. The detector electrode was inserted into the outlet of the column using a micropositioner. The outlet of the column was mounted in a cell containing 1.0 M NaCl as electrolyte and fitted with a Ag/AgCl reference electrode. It was found that the position of the electrode related to the capillary wall was very important. Since the capillary i.d. was very small, a great deal of effort was made to avoid the contact of electrode to the capillary column inner wall. Figure 3-4 shows the rms noise of the carbon fiber microelectrode in different positions. Unless stated otherwise, the detector electrode potential was set at 1.0 V *versus* this reference using a battery and voltage divider. The detector current was amplified by a SR570 Current Preamplifier (Stanford

Research Systems, Sunnyvale, CA, USA). Data were collected using a 486 personal computer (Gateway, Sioux City, SD, USA) and data acquisition board (AT-MIO-16F-5, National Instruments, Austin, TX, USA). Software was developed in house using LabWindows (National Instruments).

Microdialysis

Microdialysis sampling was performed using CMA/10 probes (CMA/Microdialysis, Acton, MA, USA) made from polycarbonate membrane material with a 20 kDa cut-off. The concentric probes had 0.5 mm diameters and 4 mm tip lengths. Per manufacturer specifications, the probe was rinsed with methanol and then buffer for 5 min each before use. It was found that an overnight rinse with aCSF buffer further decreased impurity peaks in chromatograms of dialysate. During experiments, the probe was perfused with aCSF using a microliter syringe pump (Harvard Apparatus 553206, South Natwick, MA, USA) at 0.6 µl/min unless stated otherwise. Dialysate samples were collected every 5 min and immediately stored at -4 °C. Samples were equilibrated to room temperature before capillary LC-ECD analysis.

Surgical Preparation and Procedures

Male Sprague-Dawley rats weighing 300-425 g were anesthetized with subcutaneous injections of 100 mg/ml of chloral hydrate. The initial injection was 4.0 ml/kg. Booster injections of 2.0 ml/kg were given every 30 min until the animal no longer exhibited limb reflex. After surgery, the rat was kept unconscious with subcutaneous administration of 1.0 ml/kg chloral hydrate as needed. Once the rat was secured in the stereotaxic apparatus, the microdialysis probe was placed in the globus pallidus ventral pallidum to the coordinates -1.0 mm anterior-posterior, -3.0 mm medial-

lateral, +9.0 mm dorsal-ventral from bregma [Pel67]. Basal level chromatograms were taken until they stabilized which was typically 2 h after insertion of the dialysis probe.

Data Processing

To correct for drift in the chromatographic traces, some chromatograms were processed using a variant of median filtering described elsewhere [Moo93]. For typical chromatograms where the data acquisition rate was 5 Hz and the peak width was 15 s, a window size of about twice the peak width was used to calculate the medians of raw data. By subtracting the corresponding medians from raw data, the baseline drift could be greatly eliminated. If more than one peak was inside the filter window, and the total peak width (sum of each peak width) was more than 50% of the selected window size, a larger median filter window was chosen.

Results and Discussion

Electrochemical Detection of Met-enkephalin

For detection of met-enkephalin, the best signal-to-noise ratio was obtained with +1.0 V applied to the electrode (see figure 3-5). The conversion efficiency was calculated to be 100% at this voltage and flow-rate. For example, for injection of 2.0 fmol, the peak area was 191 $\pm$ 13 pC. Assuming a 1 electron transfer, we would expect an area of 193 pC at 100% conversion. Under these conditions, the root mean square (RMS) noise level was typically 300 fA and the detection limit, calculated as the amount of analyte injected that would yield a peak three times the RMS noise, was 40 amol or 2 nM for a 20 nl injection. Detection limits for capillary LC-ECD have been reported as low as 1 to 10 amol [St.85] and for CE-ECD as low as 0.5 amol [Ole90, Par95] for catechols. The higher detection limit for met-enkephalin was due to several reasons. First, the detection

of tyrosine-containing peptides required higher voltages than catechols which in turn increased the background noise. The noise increase is exacerbated by the fact that EDTA, a commonly used mobile phase additive to reduce background noise, actually caused an increase in background and noise when the detector electrode was higher than +0.8 V (data not shown). A second reason for the higher detection limit was that the gradient used during the separation increased the background drift and noise relative to the other cases where isocratic separations were performed. Considering these factors, it is expected that the detection limit in this case would be comparable to that achieved for derivatized amino acids (36 amol) in a similar chromatographic system [Oat89].

In order to maintain the lowest detection limits and stable responses, it was necessary to avoid electrode deterioration caused by the peptide. Electrode fouling caused a 20% decrease in response after injection of 1 fmol of met-enkephalin. Fouling of electrodes has been seen before with electrochemical detection of tyrosine-containing peptides and can be attributed to adsorption of oxidation products [Par97]. The fouling effect was eliminated by applying a triangular waveform between -0.90V and +1.10V at 300 Vs^{-1} for 20 s at the beginning of a series of chromatograms. After this pretreatment, the electrode stability was improved so that six consecutive injections of 1 fmol met-enkephalin gave a relative standard deviation of 7.4% (see figure 3-6). This electrode waveform has previously been reported by Edmonds and Ji [Edm83] for activating carbon electrodes.

Use of Large Injection Volumes

The mass detection limit of 40 amol for met-enkephalin by capillary LC-ECD is superior to that obtained by RIA thus suggesting its possible application to assay of

microdialysis samples; however, the relatively high concentration detection limit of 2 nM with a 20 nl injection would make capillary LC-ECD unsuitable for that application. Therefore, we explored on-column preconcentration to further improve the concentration detection limit.

The ease of preconcentration is a key advantage of capillary LC over CE for detection of trace-level analytes in biological samples such as microdialysates and is the main reason that we chose capillary LC instead of CE for this application [Vis96]. In on-column preconcentration, the sample is injected in a weak mobile phase so that it is retained at the head of the column and concentrated. Analytes are eluted with a stronger mobile phase after the less retained solutes are washed out. The greater the retention factor (k') for analyte in the sample solution, the greater the preconcentration that can be achieved. When the k in the injecting solution is too low, the peaks can begin to migrate down the column during a large volume injection resulting in broadening or breakthrough giving rise to variable retention times and peak areas or excessive peak widths.

We found that the Alltima C-18 stationary phase allowed excellent retention of met-enkephalin when injected in dialysate solutions as illustrated by the data in Figure 3-7, figure 3-8 and Table 3-1. In this experiment, the total amount of analyte was kept constant while the injection volume was increased. As shown by the figures and quantified in the table, a constant peak area was obtained indicating no loss of the analyte during preconcentration. The retention time was also unaffected by the injection volume indicating that the met-enkephalin did not elute during the sample loading. Finally, the variances of the analyte peak were also unchanged indicating no broadening of the zone during preconcentration. These results show that even with a sample volume of 2 µl,

Table 3-1. Effect of large injection volume on characteristics of met-enkephalin peak

Injection volume (nl)	Concentration of sample (nM)	Retention time (s)	Height of peak (pA)	Limit of Detection (pM)	Variance of peak (s^2)
10	80.0	382	23.1	4200	0.13
30	26.7	383	24.2	1300	0.14
100	8.00	387	20.4	470	0.14
500	1.60	386	21.5	89	0.13
1000	0.80	388	23.3	41	0.14
2000	0.40	384	22.1	22	0.13

which is equivalent to at least 59 column volumes (capillary volume is estimated to be 34 nl), the met-enkephalin did not significantly migrate through the column. These results indicate that the concentration detection limit can be improved by over 100-fold when compared with an injection volume of 20 nl on the column (see Table 3-1).

For all subsequent work we utilized 1 μl injection volumes. Larger injection volumes could be used for better concentration detection limits; however, this would result in a diminishing return in concentration detection limit for injection time. For example, increasing injection volume from 0.2 μl to 1 μl improves the detection limit 5-fold to 40 pM for an increase in injection time of 6.6 min. (At 2 nl/s, the injection time was 1.6 min for 0.2 μl and 8.3 min for 1 μl.) A further 2-fold improvement in detection limit to 20 pM would require another 8.3 min for injection for a total of 16.6-min injection time. This time is significant relative to the total analysis time.

Quantitative aspects of the system were explored using 1 μl injection volumes. To achieve complete loading of 1 μl onto the column using a 1 μl sample capillary, it was found 3 μl of sample had to be injected into Valve 1 (see Figure 3-9). Presumably, this overfilling requirement was due to dead volume and inefficient rinsing of the tubing used in the system and a more efficient design could reduce the amount of sample needed to make 1 μl injections. Using 1 μl injections, the system had linear dynamic range for met-enkephalin from 100 pM to at least 10 nM. A typical calibration curve covering this concentration range was given by the following equation: Peak Area (pC) = 88.4 pC/nM × concentration (nM) + 14.4 pC with a correlation coefficient of 0.998.

The large preconcentration used with these capillary columns resulted in several practical problems. The first was that the preconcentration step concentrated impurities

in the water and buffers resulting in baseline drift and extra background peaks. For example, in Figure 3-7 a large broad peak, presumably due to detection of preconcentrated impurities, increased with injection volume. It was found that many of these interferences could be decreased by rinsing the column with 5% Solvent B for 5 min as described in the Experimental section. A comparison of injections with and without the rinsing step illustrating the decrease in background is shown in Figure 3-11. Even with rinsing, a significant background peak remained as shown in Figure 3-11. Furthermore, this peak was somewhat variable as seen by comparing the chromatograms of Figure 3-7 and Figure 3-11 which were obtained on different days. This variability was presumably due to different levels of impurity caused by differences in filtering and water quality. Another problem encountered with large volume injections was that the electrode sensitivity decreased by up to 50% after loading a 1 µl sample dissolved in high salt solutions such as aCSF. The reason for this deactivation is unclear; however, it was avoided by setting the potential of the detector electrode at 0.0 V during the loading of large samples. Despite these problems, the method allowed reliable detection of trace-level of met-enkephalin with a simple large-volume injection technique.

Characterization of Microdialysis Probe

Temporal resolution in microdialysis sampling is typically limited by the mass sensitivity of the analytical method and the absolute recovery of the probe. Absolute and relative recoveries for met-enkephalin at 37 °C by the probe utilized in this work are shown in Figure 3-12. In order to maximize signal and temporal resolution, we used a flow-rate of 0.6 µl/min since at this flow-rate the absolute recovery begins to level off. At this flow-rate the relative recovery was 63 $\pm$ 3%. Below this flow-rate, less analyte

will be removed per unit time and temporal resolution will be compromised. Above this flow-rate, we will see more dilution and larger samples would need to be injected. Thus, temporal resolution may be enhanced at a higher flow-rate, but this will be achieved at the expense of disproportionately longer injection times.

In Vivo Measurements

The requirement of 3 μl of sample for injection and a dialysis flow-rate of 0.6 μl/min suggested that samples could be collected as often as every 5 min if the system had sufficient detection limits to allow determination of the peptide of interest. Based on our detection limit of 40 pM for 1 μl injections, the high relative recovery of the probe at 0.6 μl/min, and previous observations by RIA [Mai89], it seemed likely that we could use 5-min sampling times for *in vivo* measurements of met-enkephalin. Figure 3-13 shows chromatograms obtained from *in vivo* experiments utilizing 5-min sampling times. This figure illustrates chromatograms obtained for injection of dialysate under basal conditions, dialysate during perfusion with high K^+, a standard sample, and a blank solution. The large drift in the baseline makes it difficult to discern the peaks unless the median filter is used over the section of interest as seen in Figure 3-14B. As shown, the chromatogram from dialysate at basal conditions has a peak that matches the retention time of met-enkephalin at a level just above the detection limit. Furthermore, this peak increases with increasing K^+ in the dialysis probe as expected for a neurotransmitter under depolarizing conditions. Based on the matching retention time, the response to K^+, and the results of experiments in which authentic met-enkephalin was spiked into the dialysate samples (not shown), this peak has been attributed to the detection of met-

enkephalin. Using this technique, the dialysate concentration of met-enkephalin was determined to be 111 $\pm$ 35 pM (n = 13) under basal conditions.

Figure 3-15 illustrates the results of monitoring met-enkephalin concentration *in vivo* in a single rat with 5-min temporal resolution during an infusion of K^+ in the probe. Figure 3-16 shows similar data averaged from 5 different rats. During infusion of K^+ the met-enkephalin level was immediately elevated to an average of 3.2 $\pm$ 1.8 times the basal level. After the K^+ stimulant was removed, the met-enkephalin level lowered, but it did not always stabilize at the basal level.

The met-enkephalin levels obtained in this work are in good agreement with previous results obtained using microdialysis sampling with RIA [Mai89, Mai91] and MS [Emm95] if the differences in relative recovery are taken in to account. In addition, the change in met-enkephalin is comparable to that previously reported during K^+-stimulation [Mai89, Emm95]. The LC-ECD system however, allowed samples to be collected with 6-fold higher temporal resolution than either the RIA or the MS method. This difference can be attributed to a mass detection limit that was 5-fold lower and a smaller sample volume requirement. The higher temporal resolution allowed several novel observations to be made. For instance, these results show that neuropeptide concentration increased within the first 5 min of K^+-stimulation. Furthermore, our results show that within the 30-min stimulation period, the release of met-enkephalin is sustained at a constant level. With only 30-min sampling intervals, such observations would not have been possible. In combination with behavioral studies or pharmacological manipulations, the improved temporal resolution should be more valuable.

Conclusion

The work presented here demonstrates that aqueous samples can be preconcentrated by over 100-fold on-column to give concentration detection limits as low as 20 pM for met-enkephalin. This sensitivity and sample requirement allow capillary LC-ECD combined with microdialysis sampling to be used for monitoring met-enkephalin *in vivo* with 5-min temporal resolution. The prospects for improving temporal resolution to less than 1 min seem good. First, the sample injector wasted 66% of the 3 μl samples, therefore a three-fold gain could be made by utilizing all of the sample for injection. A system compatible with higher pressures could allow larger volumes to be injected quicker which, in turn, would allow practical use of larger volume samples. Thus, higher dialysis flow-rates, with subsequent higher absolute recovery, could be used resulting in better temporal resolution. Finally, the possibility of derivatizing peptides using the biuret reaction for electrochemical detection offers the possibility of extending this approach to non-electroactive peptides [War89, Tsa91].

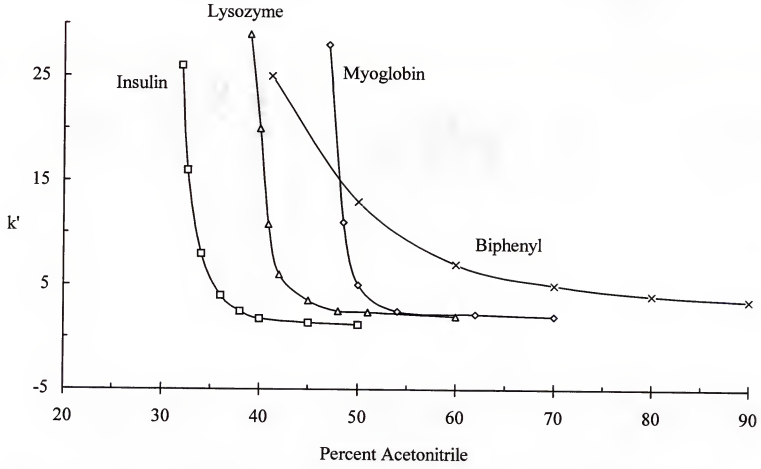

Figure 3-1. Effect of organic modifier content on analyte retention. [Handbook of Analysis And Purification of Peptides And Proteins by Reversed-Phase HPLC, Vydac Technique Note, 1991]

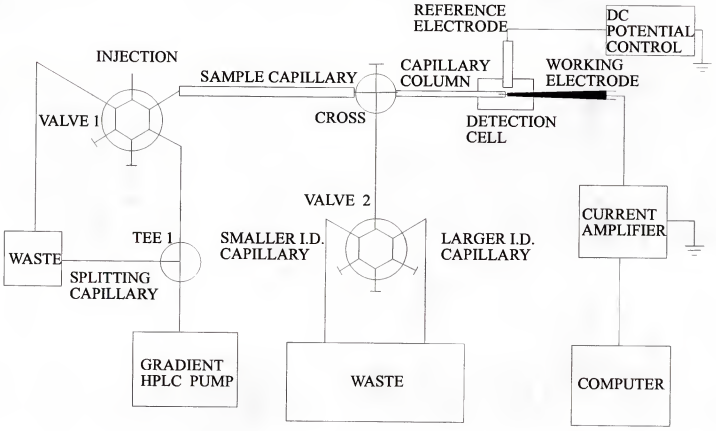

Figure 3-2. Block diagram of capillary LC/ECD

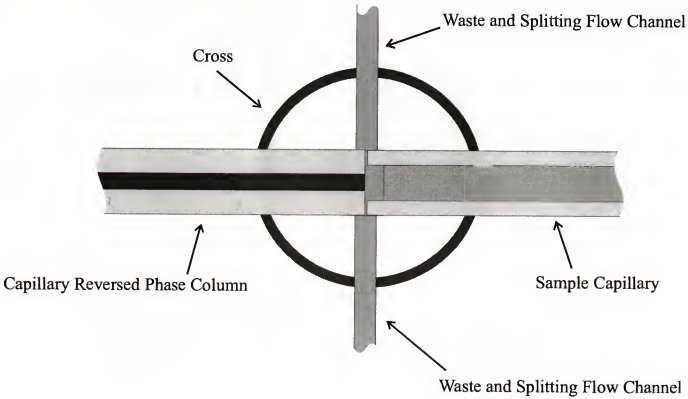

Figure 3-3. Detailed structure of cross used in figure 3-2.

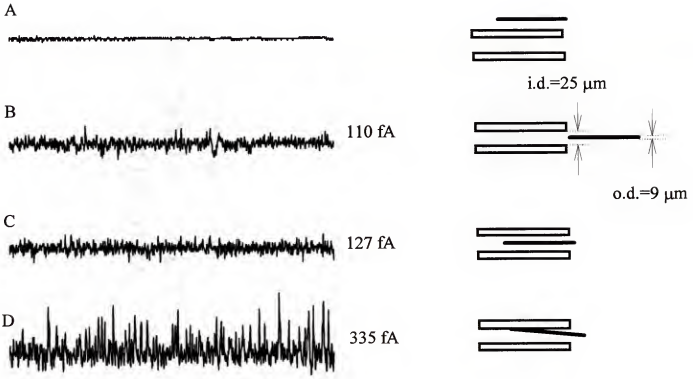

Figure 3-4. Effect of electrode positioning on rms noise. The rms noise was calculated over 100 seconds period. The right portion illustrated the relative positioning of the microelectrode to that of capillary column.

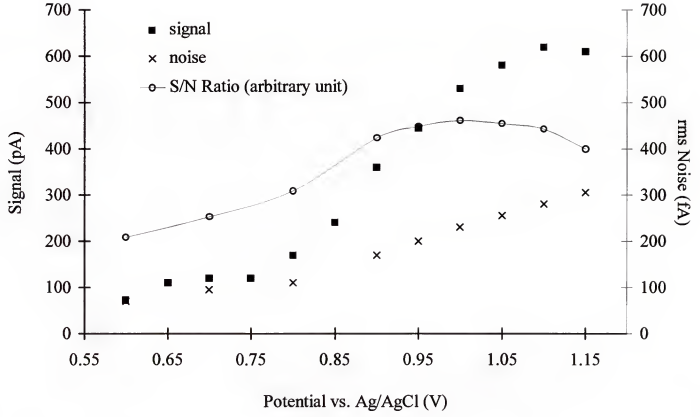

Figure 3-5. Hydrodynamic voltammogram of met-enkephalin.

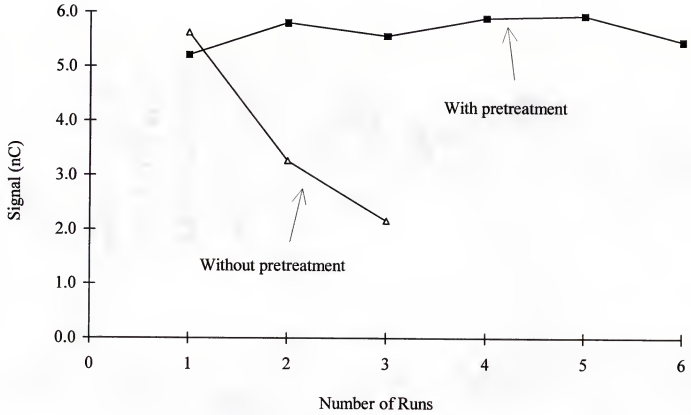

Figure 3-6. Electrochemical pretreatment on microelectrode stability.

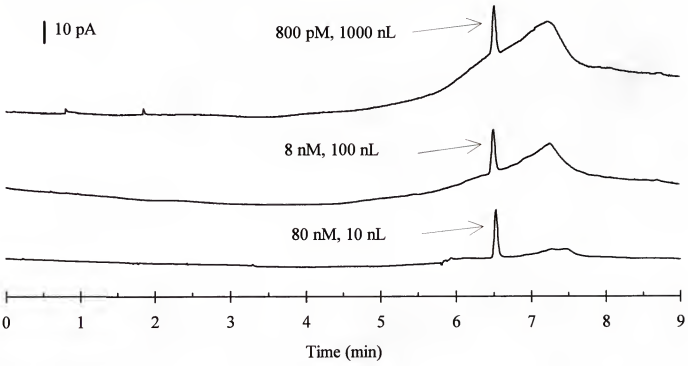

Figure 3-7. Chromatograms from different sample volumes. Detailed explanation see text.

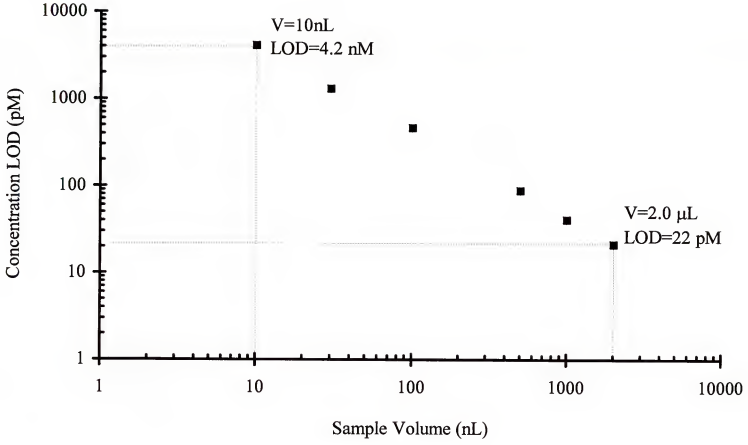

Figure 3-8. Preconcentration effect on concentration limit of detection.

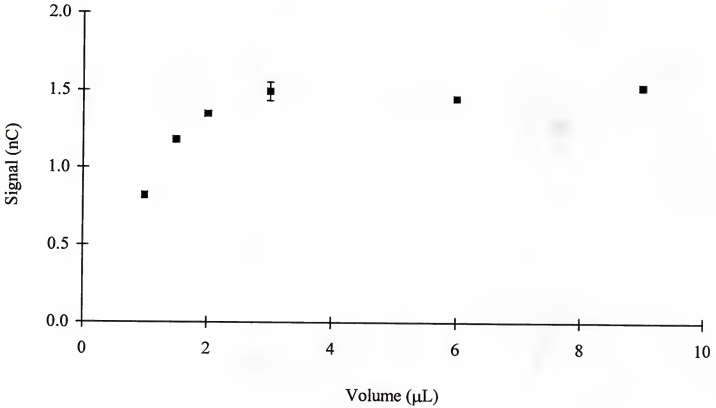

Figure 3-9. Effect of loading sample volume.

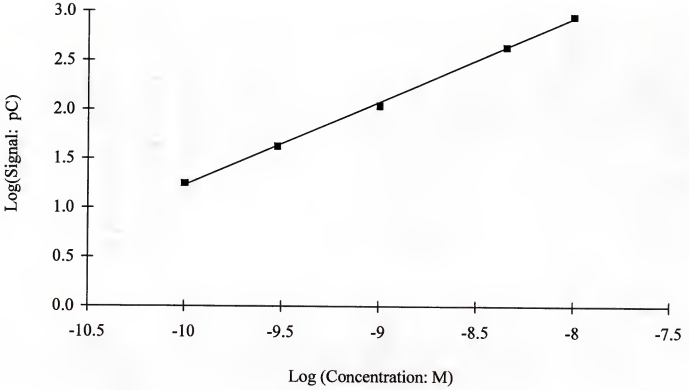

Figure 3-10. Calibration curve of capillary LC/ECD determination of met-enkephalin.

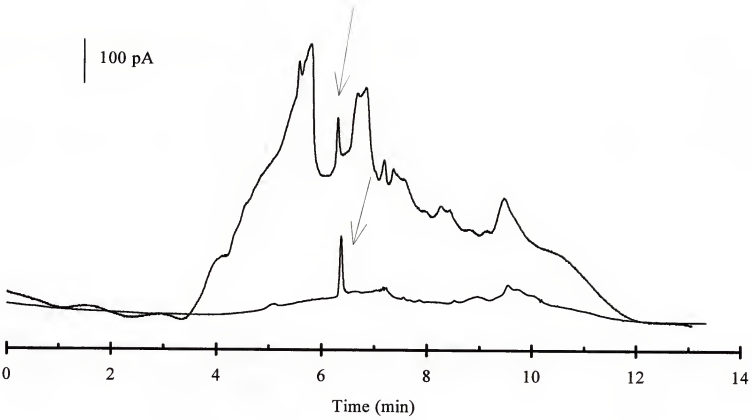

Figure 3-11. Extensive low organic mobile phase rinsing decreases impurities but leaves the met-enkephalin peak intact (pointed by the arrows)

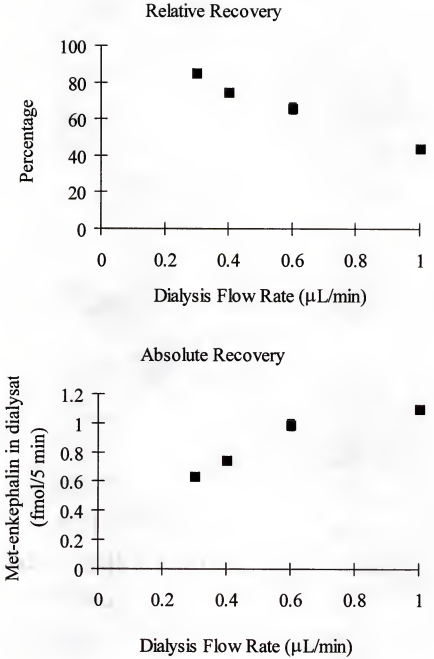

Figure 3-12. Relative and absolute recovery of met-enkephalin with 20 kD cut-off microdialysis probe at 0.60 µl/min flow rate. See text for detailed explanations.

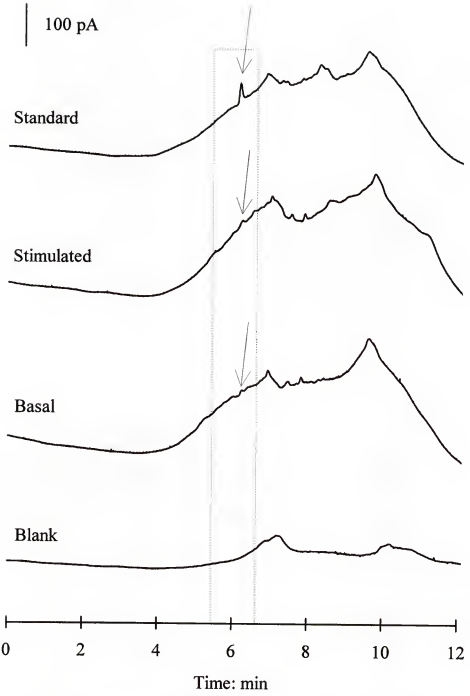

Figure 3-13. Chromatograms of *in vivo* dialysate obtained by microdialysis coupled with capillary LC/ECD.

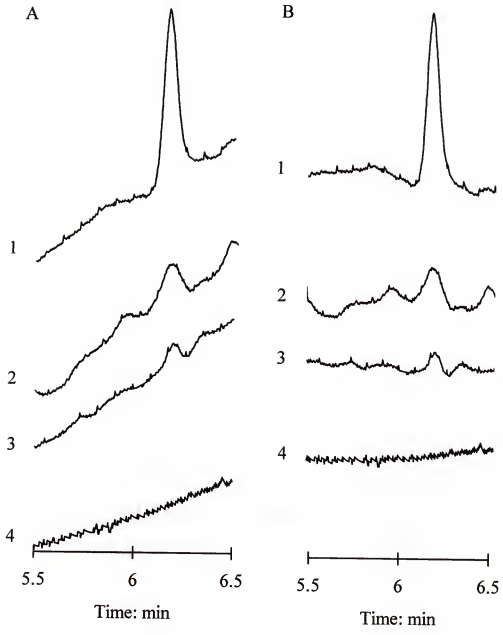

Figure 3-14. Expanded view of dashed-region in *in vivo* dialysate chromatograms. (A) original chromatograms, (B) median filtered chromatograms in A.

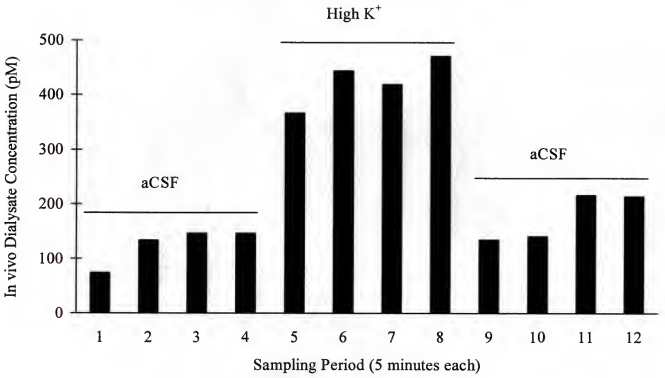

Figure 3-15. Monitoring of met-enkephalin *in vivo* in rat brain (single rat). There was 20 minutes time interval between the sampling of basal level (indicated by aCSF) and that of stimulated level (High K^+) for correcting the dead volume of microdialysis delivery tubing.

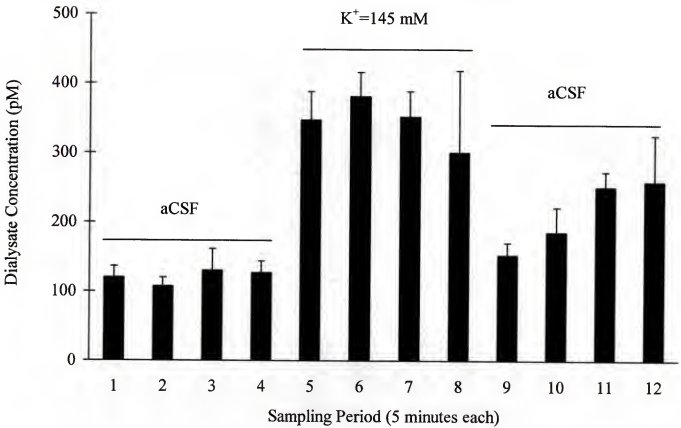

Figure 3-16. In vivo monitoring of met-enkephalin secretion from rat brain. Error bars represent standard deviation of the mean of 5 rats.

CHAPTER 4
MONITORING BOTH ELECTROACTIVE AND NON-ELECTROACTIVE NEUROPEPTIDES WITH CAPILLARY LC/ECD THROUGH PRE-COLLUMN BIURET DERIVATIZATION

Introduction

Neuropeptides are a group of peptides present in the central nervous system functioning as neuromodulators, neurotransmitters, and neurohormones. The study of these neuropeptides is of great importance in understanding brain function. However, due to their low concentrations in the brain, the analysis of these peptides presents great analytical challenges. So far the most popular method for dynamic monitoring these neuropeptides is radioimmunoassay (RIA) coupled with microdialysis sampling. Though the RIA is very selective and suitable for batch processing, its sensitivity is usually limited to the upper attomole range and a single analysis will take several hours even days to finish. The temporal resolution was limited by the mass detection limit of the method as well as by the dialysis recovery. For example, in an *in vivo* analysis of a brain peptide such as vasopressin, the RIA based method has mass detection limit of about 0.1 fmol and achieved temporal resolution of 30 minute when coupled with microdialysis sampling [Lud92]. Since the neuronal events occur on much faster time scales than current methods can follow, it is of interest to develop alternative approaches to monitoring that allow better temporal resolution. To improve the temporal resolution of dynamic monitoring, better mass detection limit is required.

For electroactive neuropeptides, such as met-enkephalin, a tyrosine containing pentapeptide, an analytical method based on capillary liquid chromatography (LC) with a microelectrode detector has been developed [She97b]. This method is based on the oxidation of the electroactive group, or tyrosine, to be specific, in the peptide and can generally be applied to other electroactive peptides. This capillary LC/ECD based method improved temporal resolution for *in vivo* met-enkephalin monitoring from 30 minute to 5 minute when coupled with microdialysis. This improved temporal resolution is mainly attributed to the low mass limit of detection of capillary LC/ECD compared to that of RIA.

In addition to the electroactive peptides, there are also brain peptides that are not electroactive and therefore cannot be detected by the above method without derivatization. These non-electroactive peptides, such as substance P and bradykinin, to name just two, also play very important roles in brain function. In order to take advantage of low mass limit of detection of capillary LC/ECD, a derivatization is required.

There are numerous ways of derivatizing peptides to achieve either electrochemical or fluorescence detection. Fluorescence based detection has established itself as one of the most sensitive methods for bioanalytical applications. For low concentrations, fluorescence of derivatized peptides, e.g., o-phthalaldehyde (OPA) and naphthalene-2,3-dicarboxaldehyde/CN- (NDA) derivative products have been reported [Orw91, Car86] and as low as 10^{-10} M concentration detection limit has been achieved [Orw95]. However, peptide derivatives usually do not have as high a sensitivity as amino acids due to the differences in the photophysical properties of isoindole derivatives. For

example, a recent published study on determination of bradykinin with fluorescence detection coupled with conventional HPLC had detection limit of 5 to 10 fmol [Kan97]. Also, successful derivatization relies on the presence of a primary amine in the peptide or protein. Therefore, even though a fluorescence based approach is very sensitive but it will not be applicable to detecting proteins and peptides that do not have reactive amines. Even further, the above method will respond to all kinds of amines instead of selectively for peptides. This non-selective derivatization detection scheme will impose great demands on separation power when all the derivatives must be separated.

Margerum [Mar83] published a study on formation of biuret complexes between peptides and copper in the basic solution as well as other properties, including electrochemical properties. Copper ion (M^{2+}) and peptide (L) can form a metal-N(peptide) bond and release peptide hydrogen ions:

$$M^{2+} + H_xL \leftrightarrow M(H_{x-n}L)^{2-n} + nH^+ \qquad 4\text{-}1$$

where the value n is the total number of hydrogens that were released from the nitrogen of the peptide. For copper (II) - peptide complex, the initial pH can be as low as 3 to 6 to form a complex. As the pH of the solution increases, the peptide will further ionize and lose more hydrogen ions into the solution. The formed peptide-copper complex (biuret complex) can significantly decrease the oxidation potential of the copper (II) to copper (III). As the solution pH increases, the oxidation potential of copper (II) to copper (III) becomes even lower [Mar83, Che95b]. As an example, for copper - tetraglycine, (see figure 4-1), as the pH of the solution increases, the complex undergoes a change from structure I to structure II and the oxidation potential decreases from 0.67 V (structure I) to 0.42 V (structure II) [Che95b]. Both oxidation potentials are much lower than that of free

copper ions in solution. This change enables the detection of copper (II) in the complex at the electrode surface through its oxidation under moderate potential. Since only copper (II) in the biuret complex can be detected at a moderate potential, the oxidation signal of copper (II) is directly proportional to the amount of peptide that complexes with the copper (II). These copper derivatives provide an alternative way of analyzing non-electroactive peptides with electrochemical detection. This method does not rely on the presence of primary amine and is selective to peptide instead of all the amines and therefore holds great promise to be a universal detection scheme for peptides.

Weber and co-workers have published a series of studies on the electrochemical detection of peptides based on the biuret complex following HPLC separations [War89, Tsa90, Tsa91, Tsa92, Che95d]. In the studies, glassy carbon electrodes were coupled with conventional HPLC reversed phase columns to detect the biuret complex through either pre-column or post-column derivatization. Typically the detection limit of their system were 6 to 100 fmol through a narrow bore reversed phase column coupled with a glassy carbon disk electrode. As discussed in the first chapter, decreased column inner diameter will improve the mass sensitivity of concentration sensitive detection. If smaller i.d. capillary column is used, the mass detection limit can be in the low attomole range.

With this biuret derivatization, both electroactive and non-electroactive peptides can be analyzed by capillary LC/ECD. With improved mass limit of detection, both electroactive and non-electroactive peptides can be monitored with higher temporal resolution. As mentioned before, bradykinin, a nonapeptide present in different brain region as well as many other parts of the body, has been implicated in the genesis of inflammation, cardiovascular shock, hypertension, pain, and even rheumatoid arthritis

[Sny80]. It is believed that bradykinin is probably the most potent pain-producing substance known. Its release by tissue damage and action at specific receptors on sensory neurons has been suggested as a first step in pain perception [Sny80].

An immunohistochemical study revealed the bradykinin distribution throughout the brain region and at low concentrations. For example, the content of bradykinin in the rat hypothalamus was determined as 255 ± 71 fmol per gram tissue weight. Considering the average weight of the hypothalamus in a rat is about 63 mg, this can be translated into that total bradykinin in the rat hypothalamus was only 16 fmol [Kar85]. So far only the content of bradykinin in different brain locations and in serum has been reported [Kar85]. However, the capability of *in vivo* monitoring of its release in various locations will greatly enhance the understanding of its function in the biological system.

Also in the same region presents other neuropeptides such as vasopressin. Vasopressin is synthesized predominantly in the hypothalamic supraopic and paraventricular nuclei. Behavioral studies suggested a role for vasopressin in learning and memory [DeW79]. Also in clinical trials, vasopressin may improve memory in brain-damaged human subjects [Sny80]. However, as said in the beginning, currently RIA based monitoring can only achieve the temporal resolution of 30 minute [Lud92, Lan92]. This limited the capability of following these neuronal functions in a more timely manner.

Reported here is the study of the development of a capillary LC/ECD system to improve mass sensitivity of peptide copper biuret complexes. A comparison between glassy carbon disk electrode and carbon fiber microelectrode was also made. The established method was further used in the application of *in vivo* monitoring of both

bradykinin and vasopressin in 5 min temporal resolution by coupling with microdialysis sampling.

Experimental

Reagents and Mobile Phase

Unless specified otherwise, all chemicals were purchased from Sigma (St. Louis, MO, USA). The aqueous portion of the mobile phase (solvent A) for reversed-phase capillary liquid chromatography was 40 mM sodium carbonate buffer in 0.75 mM sodium potassium tartrate and 0.25 mM cupric sulfate adjusted to pH 10.5 with sodium hydroxide. The organic phase (solvent B) was prepared by mixing 40% (v/v) of aqueous buffer with 60% acetonitrile. The mobile phase was degassed by helium before and during use (The BOC Group, Inc., Murray Hill, NJ, USA). Artificial cerebral spinal fluid (aCSF) used for microdialysis perfusion consisted of 145 mM NaCl, 2.68 mM KCl, 1.01 mM $MgSO_4$, and 1.22 mM $CaCl_2$. The high K^+ perfusate solutions for stimulation experiments consisted of 2.62 mM NaCl and 145 mM KCl with other salts the same as aCSF. The copper derivative reagent for biuret complex consists of 40 mM boric acid buffered with sodium hydroxide at pH 10.5 and 3.75 mM sodium potassium tartrate and 1.25 mM cupric sulfate. All buffers were made fresh and filtered with 0.22 μm pore size hydrophobic Teflon filter membrane (MSI, Westboro, MA, USA) before use. The use of this Teflon based filter membrane enabled the filtration of basic solution and at the same time removed some of the hydrophobic impurities.

Capillary Liquid Chromatography (LC)

Preparation of Capillary Reversed Phase Columns. Capillary columns were prepared by previously described techniques [Ken89] using 15 to 20 cm lengths of 25 μm

inner diameter (i.d.), 360 μm outer diameter (o.d.) fused silica capillaries (Polymicro Technologies, Phoenix, AZ, USA) as the column blanks. Columns were slurry-packed with 5 μm Astec C-18 (Alltech, Deerfield, IL, USA) reversed-phase particles (slurries consisted of 10 mg packing material in 3 ml acetonitrile) at 2.4 to 3.0 MPa using a pneumatic amplifier pump (Cat. No. 1666, Alltech).

The detailed packing procedure was the same as that stated in the previous chapter. The use of Astec particles, a polymer based C-18 reversed phase particles, facilitated the basic separation conditions. The Astec particle also has high carbon loading, which is very critical to our preconcentration requirement. Even under basic conditions, where the peptides were ionized and complexes with metal were formed, the capacity factors of these peptides were still large enough to allow up to 1 μl sample loading which was 50 times of the column void volume.

Capillary LC system operation. A schematic of the capillary LC system used in this work is shown in Figure 4-2. Mobile phase flow was generated using a SSI 232D HPLC gradient pump (Scientific Systems, State Collage, PA, USA) and a Varian high pressure loading pump through three splitter tees. A two 6-port valve injection system was designed to minimize dead volume between the sample capillary and the column and also to maximize sample usage. The first six-port two position valve (Valco Instruments, Houston, TX, USA) was used to direct the flow into the second valve from either the Varian high pressure loading pump or SSI 232D HPLC gradient pump depending on purpose. This valve together with the second valve controls the loading and separation of the system. A sample capillary was used to connect this second six-port valve to the separation capillary column through a peek cross. The outlet of the sample capillary was

inserted into a cross (Valco) which was constructed so that 360 μm o.d. capillaries fit snugly inside. One port of the cross was connected to the separation column, and the other two ports were connected to a three port purge valve (Valco), which has a splitter capillary (50 μm i.d. by 15 cm long) attached. The sample capillary and column were positioned inside the cross under a microscope with a minimum gap between them in order to minimize dead volume. The use of a cross instead of a tee facilitated easy capillary positioning.

Large volume sample loading. Injections were made by switching the sample capillary from the high pressure flow path using the second valve to connect the sample capillary to a microsyringe with the purge valve open. Such loadings left the sample capillary filled and excess sample in the splitter capillary with insignificant sample entering the packed capillary reversed phase column because of the flow resistance. To transfer sample onto the column, the purge valve was closed and the sample capillary reconnected to high pressure loading pump by switching both the first and second six-port valve. After the sample was loaded onto the column, the purge valve was opened to the splitting capillary and valve one was switched again to the gradient HPLC pump. The loading pressure was set as high as 4000 psi to ensure fast sample loading while the separation was carried out at pressure generally below 1000 psi to achieve better resolution and detection. The two pump configuration eases the concerns of damaging the pulse damper in the HPLC gradient pump when fittings fail at high pressure. The splitter attached to the purge valve served to: 1) allow faster displacement of mobile phase in the sample capillary to give more prompt response to the gradient, and 2) to provide extra pulse dampening to reduce the pumping noise. The capillaries from the two

ports of the cross will greatly decrease the unswept volume inside the cross and thus minimize the memory effect of the system. The system usually has a flow rate of over 3 nl/s for sample loading and 0.6 nl/s during separation.

Gradient separation. To maintain the best detection limits and minimal drift from large volume injections the aqueous buffer was prepared fresh and filtered everyday. In addition, after loading, the column was rinsed with 5% solvent B-95% solvent A for 2 min before gradient elution started. Gradient elution started at 5% solvent B, linearly changed to 35% solvent B in 5 min, kept at this composition for 2 min, and then stepped back to 100% solvent A.

Biuret Complex Formation and Detection

Previous research showed that for small peptide, biuret complex can form instantly at room temperature upon the addition of copper to peptide solution under basic condition. However, for larger peptide, heating was required for the formation of biuret complex [Tsa91]. Due to the technical difficulty of post column derivative reagent addition in a capillary LC with column i.d.'s as small as 25 μm, the pre-column derivatization approach was used. Except for the post-column derivatization scheme in the dual detector conventional HPLC design, in which, small peptides (number of amino acid groups ≤ 5) were used, all derivatization was carried out by heating the sample solution at 60 °C before it was loaded into the capillary LC system. The standard biuret complexes were prepared by dissolving a specific concentration of peptide in the aqueous mobile phase. The relatively large volume solution (typically 1 to 2 ml) was then heated in a water bath of 60 °C for 20 minutes in a glass vial to minimize possible adsorption of peptides to the container.

For *in vivo* dialysate determination, a polypropylene microvial was used. A 20 μl polypropylene pipette tip end was heated and sealed by flame. During the experiment, 2.5 μl dialysate was collected in this polypropylene microvial and 0.50 μl copper derivative reagent was added. Also in this copper derivative reagent there was 6% of acetonitrile which made the final acetonitrile content in the sample as 1%. This acetonitrile was added to prevent possible adsorbing of analytes into the container. The solution was then incubated in a water bath at 60 °C for 8 minutes immediately before the sample loading.

Electrochemical Detection

Cylindrical carbon fiber microelectrode detector. A 9 μm diameter, 1.2 mm long carbon fiber electrode was used as the detector electrode [Kaw93] and was inserted into the outlet of the column using a micropositioner. The outlet of the column was mounted in a cell containing 100 mM NaCl as electrolyte and fitted with a Ag/AgCl reference electrode. Unless stated otherwise, the detector electrode potential was set at 0.60 V *versus* this reference using a battery and voltage divider. The detector current was amplified by a SR570 Current Preamplifier (Stanford Research Systems, Sunnyvale, CA, USA). Data were collected using a 386 personal computer (Gateway, Sioux City, SD, USA) and data acquisition board (AT-MIO-16F-5, National Instruments, Austin, TX, USA). Software was developed in house using LabWindows (National Instruments).

Dual detector scheme. In the experiment, a dual-detector design was set up to compare the detection of biuret complex at both a glassy carbon electrode and a carbon fiber microelectrode. In this scheme, a conventional C-18 reversed phase column was used and the biuret derivatization was performed in a post-column format. As seen in

figure 4-3, first, the eluant from the reversed phase column was mixed by a post-column copper derivative reagent to introduce copper (II) ions into the eluant as well as to adjust its pH. Second this eluant was then splitted into two flow paths to be detected at both detectors in parallel. The glassy carbon electrode adopted a thin layer detection cell design while the carbon fiber microelectrode detection was performed by inserting the microelectrode into the outlet of the tubing. For detecting peptide without copper derivatization, the experimental design was kept the same only that copper was absent from post-column copper derivative reagent. The signal from both electrodes was registered and analyzed to compare the difference between the two electrodes. In this study, both electrode were held at 0.80 V *versus* Ag/AgCl reference electrode and the post-column solution pH was controlled at 10.2 with final copper ion concentration in the post-column effluent be 2.0 mM. The same data acquisition instrument set was used.

Microdialysis

Microdialysis sampling was performed using CMA/10 probes (CMA/Microdialysis, Acton, MA, USA) made from polycarbonate membrane material with a 20 kDa cut-off. The concentric probes had a 0.5 mm diameter and 4 mm tip length. Per manufacturer specifications, the probe was rinsed with ethanol and then aCSF for 5 min each before use. It was found that an overnight rinse with aCSF buffer further decreased impurity peaks in chromatograms of dialysate. During experiments, the probe was perfused with aCSF using a microliter syringe pump (Harvard Apparatus 553206, South Natwick, MA, USA) at 0.5 μl/min unless stated. After 10 minutes of collecting basal level dialysate, the perfusion solution was changed to high potassium aCSF and hold for 30 minutes then returned to normal aCSF. Dialysate samples were collected

every 5 min and immediately stored at -4 °C. The sample was thawed immediately before derivatization and analysis.

Surgical Preparation and Procedures

Male Sprague-Dawley rats weighing 300-450 g were anesthetized with subcutaneous injections of 100 mg/ml of chloral hydrate. The initial injection was 4.0 ml/kg. Booster injections of 2.0 ml/kg were given every 30 min until the animal no longer exhibited limb reflex. After surgery, the rat was kept unconscious with subcutaneous administration of 1.0 ml/kg chloral hydrate as needed. Once the rat was secured in the stereotaxic apparatus, the microdialysis probe was placed in the supraoptic nucleus (SON) of the rat brain to the coordinates 1.1 mm posterior to bregma 1.7 mm lateral to midline 9.1 mm below the surface of the skull [Lud92]. Basal level chromatograms were taken until they stabilized which was typically 2 h after implantation of the dialysis probe into the brain.

Results and Discussion

Biuret Complex Electrochemical Detection

Carbon Fiber Microelectrode vs. Glassy Carbon Electrode. It has been reported that glassy carbon electrode can be used to detect copper biuret complex under moderate potentials after HPLC separation of peptides [Che95b, Che95c]. The compatibility of glassy carbon electrode to the organic component in the reversed phase HPLC allows detection of these biuret complexes. For electroactive peptides, i.e. the peptides that contain tyrosine or tryptophan, the formed biuret complexes can improve detection. It has been explained that both the electroactive amino groups and the copper (II) in the

complex were oxidized and therefore the signal on the electrode was the sum of both and the signal was enhanced over 100% [Tsa91].

Microcolumn separation was used in the research to achieve better mass sensitivity. The best electrochemical detector to date for coupling with capillary column separation is the cylindrical carbon fiber microelectrode. Although the glassy carbon electrodes have been used extensively in the detection of biuret complex following HPLC separation, the biuret complex oxidation behavior on the carbon fiber microelectrode is still unknown. A study was conducted to investigate the similarity and the difference of biuret complex oxidization on glassy carbon electrode and carbon fiber microelectrodes. Both electroactive and non-electroactive peptides were used. Figure 4-4 shows the result of peptide biuret complex oxidation obtained with a glassy carbon disk electrode and with a cylindrical carbon fiber microelectrode. For both electrodes, the signal of des-tyr-met-enkephalin, a non-electroactive tetrapeptide, was negligible compared to the signal of its biuret complex. (see figure 4-4A) It is clear that the copper (II) present in the solution at basic conditions facilitated the detection of non-electroactive peptide such as des-tyr-met-enkephalin at both electrodes. For met-enkephalin (figure 4-4B), an electroactive pentapeptide, the signal on the two electrodes behaved differently. The met-enkephalin itself can be detected at both electrodes under experimental condition without the presence of copper. With copper (II) added into the post-column derivatization reagent, the signal on the glassy carbon disk electrode increased almost 100%. Assuming the pentapeptide forms biuret complex with copper in a 1:1 ratio, the increased signal can be interpreted as the sum of peptide itself and copper in its biuret complex provided they both are oxidized at the specific potential. Since copper promoted the detection of met-

enkephalin on the glassy carbon electrode, there should be no doubt of the formation of the biuret complex in this post column derivatization scheme. However, the difference of the met-enkephalin signals with copper (II) and without copper (II) on the carbon fiber microelectrode was insignificant. The average signal of biuret complex seemed to increase compared to that of met-enkephalin itself. But a t-test concluded that the difference between the detection of met-enkephalin itself and its biuret complex on carbon fiber microelectrode was insignificant (α=0.05).

A partial conclusion of this study is that although the copper improves the detection of both electroactive and non-electroactive peptides on glassy carbon disk electrode, the same cannot be said for the cylindrical carbon fiber microelectrode. With the formation of biuret complex, non-electroactive peptides can be detected on the carbon fiber microelectrode. Nevertheless, for the tyrosine containing peptide, met-enkephalin, the formed biuret complex did not enhance the signal of the peptide on the carbon fiber microelectrode.

Cyclic voltammetry. Cyclic voltammetry was used to further explore the difference between the glassy carbon and carbon fiber microelectrode. Weber and co-workers showed that the cyclic voltammograms of biuret complex will exhibit two wave form on oxidation of electroactive peptides [Tsa92]. The cyclic voltammograms of met-enkephalin biuret complex obtained in our lab shows two oxidation peaks with carbon fiber microelectrode too. In figure 4-5A, the oxidation peak is at 500 mV and there is no reduction peak can be observed on the voltammogram. Figure 4-5B shows the voltammogram of met-enkephalin copper (II) complex. There are two oxidation peaks shown in the voltammogram, first is at 560 mVand the second is at 850 mV. It seems

that the complex shift the oxidation potential to higher potential. Also presented in this figure is a reduction peak which is at 330 mV. This can be attributed to the reduction of copper (III) in copper-met-enkephalin complex. Figure 4-5C and D show the voltammograms of des-tyr-met-enkephalin and bradykinin biuret complexes. Both voltammograms show oxidation peaks at around 600 mV and reduction peaks at about 300 mV. It is obvious that these two peptides are detected due to their biuret complexes. In figure 4-5, it shows that biuret complex promote the detection of non-electroactive peptide such as des-tyr-met-enkephalin and bradykinin. For met-enkephalin, the two oxidation peaks indicate that both tyrosine and copper (II) in the complex are oxidized and the reduction peak at 350 mV confirms the existence of copper (III) due to the oxidation of copper (II). Due to fact that second oxidation peak located at 850 mV and the highest potential we used to detect met-enkephalin was 800 mV on carbon fiber microelectrode, a possible explanation is that only one oxidation happened during the detection. This may explain that detection of copper met-enkephalin biuret complex on the carbon fiber microelectrode was not promoted by the presence of copper.

Hydrodynamic Voltammograms. Due to the fact that copper did not enhance the detection of electroactive peptide such as met-enkephalin on a carbon fiber microelectrode, a further hydrodynamic voltammetry study of other electroactive and non-electroactive peptides was carried out. Among those peptides, vasopressin, oxytocin and neurotensin are electroactive while bradykinin is non-electroactive. It was found that for bradykinin, pre-heating was required for the detection of its biuret complex. Samples were derivatized in a pre-column approach as indicated in the experimental section. After incubation, the sample was loaded into the system and separated and detected. Figure 4-6

and 4-7 showed the hydrodynamic voltammograms of these peptides both with and without copper.

It is common to see baseline drift during gradient elution when electrochemical detection is coupled with reversed phase HPLC. The use of basic condition and the excess copper present in the mobile phase caused both background current increase and baseline gradient drift. For this reason, detection potentials higher than 0.80 V were not used due to the large background current as well as the gradient baseline drift.

The results from these hydrodynamic voltammograms were similar to that obtained in the last section. The biuret complex can promote the detection of non-electroactive peptide, such as des-tyr-met-enkephalin and bradykinin, on the carbon fiber electrode. To closely examine the copper effect on hydrodynamic voltammograms of electroactive peptides, the same set of data is re-plotted as in figure 4-8. It seems that copper (II) ion suppresses the signal of neurotensin at low potential (0.50 V to 0.75 V) but does not change that of the other two significantly. It was also noticed that, for the other two electroactive peptides, vasopressin and oxytocin, there might be limited enhancement due to formation of the biuret complexes under the experimental potential range. However, the enhancement, if any, was not as obvious as that on glassy carbon disk electrode reported in the reference literature [Tsa92]. The difference between glassy carbon disk electrode and cylindrical carbon fiber microelectrode on detection of biuret complex of electroactive peptide was distinct though the reason is still unknown.

Sample pH. Both literature and the study conducted in this lab revealed that pH plays an important role in the detection of biuret complexes. Figure 4-9 shows the effect of pH on the detection of bradykinin and des-tyr-met-enkephalin. For both peptides,

there was a plateau from pH 9.8 to 10.5 range. As previous research showed, the larger the peptide, the higher the pH required to achieve electrochemical detection of its biuret complex. In our experiment, the pH of both copper derivative reagent and aqueous mobile phase was chosen as 10.5 ± 0.1.

Copper concentration. Since detection is based on the formation of copper-peptide complex, the copper concentration effect was also measured. Two non-electroactive peptides, des-tyr-met-enkephalin and bradykinin, were selected as sample peptides in the test. As the copper concentration increased, the signal of both peptide first increased as well and then started to level. However, the signal to noise ratio reached a maximum and then declined as the copper concentration further increased, see figure 4-10. This can be explained by the increased noise level with high concentration copper in the mobile phase. The optimal copper concentration for both peptide was determined between 0.2 to 0.3 mM when the pH was set at 10.5 and the potential was set at 0.60 V. The copper concentration in the mobile phase was fixed at 0.25 mM hereafter.

Sample incubation. Due to the small sample volume, a microvial made from a polypropylene pipette tip was used to derivatize the peptide into their biuret complex for *in vivo* analysis. Because of its small size, heat transfer was more efficient than that in a relatively large volume glass container. A study concerning the optimal incubation time was conducted. Figure 4-11 shows the effect of incubation time with this microvial. The results are the average of 3 measurements. For bradykinin, as the incubation time increases from 2 to 8 minutes, the signal clearly increases. As the incubation time further increases from 10 minute to 20 minutes, the signal actually decreases. This could be explained by possible adsorption of peptide on the polymer surface. For both vasopressin

and oxytocin, the short incubation time did not enhance their detection on the carbon fiber microelectrode. Since they were both electroactive, this non-enhancement was in good agreement with previous results that the formed biuret complex did not promote the detection of electroactive peptide. Signal from both vasopressin and oxytocin decreases as the incubation time further increases, which, can also be explained by peptide adsorption.

Optimal detection. Experiments demonstrated that a mobile phase containing copper would generate larger rms noise at high potential. Figure 4-12 shows the copper effect on the noise profile at pH = 10.5. The rms noise level for both mobile phase were about the same at low potential. However, the rms noise of copper mobile phase started to increase at 0.70 V, unlike that for the mobile phase without copper, which remained relatively constant until 0.85 V. Also from the above experiment, signal to noise ratio was plotted (see figure 4-13) and the potential of 0.60 V to 0.65 V was chosen as the optimal detection range vs. Ag/AgCl reference electrode for the peptides studied. For the *in vivo* experiments later, a potential of 0.60 V was applied to perform end column electrochemical detection, since vasopressin, bradykinin and oxytocin were selected as our target peptides.

Capillary LC Coupled with Electrochemical Detection

Preconcentration and separation. A reversed phase gradient separation was established to accommodate the separation of the peptides of interest from each other as well as from other interferences. Shown in figure 4-14 are the chromatograms of the peptide standards. The use of polymer based Astec C-18 packing material allowed high pH mobile phase to be used to carry out the separation. This Astec C-18 particle also

facilitated large volume sample loading, even at high pH when the peptides formed complexes with copper (II) and ionized. Chromatograms of different sample loading volume are also shown in figure 4-14. With the total mass for each analyte kept the same for all three analyses, as the sample volume increased from 10 nl to 1000 nl, both retention time and peak shape remains unchanged. This consistency in retention time and peak shape revealed high capacity factors for these peptide complexes and served as the basis for on-column preconcentration for large sample loading without sacrificing their separation efficiency.

Similar to that in the chapter 3, the problems of preconcentration of trace impurities associated with large sample volume also presented in this study. However, due to the low potential setting used in detection, the number of interfering peaks were much less and their size were much smaller as can be seen in the chromatogram of 1 μl sample load in figure 4-14. The filtering of mobile phase with a hydrophobic membrane also helped to remove some of the hydrophobic impurities that would retain on the column otherwise. With a shorter (compared to that in the chapter 3) pre-gradient low organic mobile phase rinsing, the chromatograms were relatively clean.

This preconcentration capability greatly improved the concentration limit of detection for these peptides. Figure 4-15 shows the inversely linear dependence of concentration limit of detection of bradykinin on preconcentration volume. As sample loading volume to increase from 10 nl to 1 μl, the correspondent concentration limit of detection changed inversely proportionally. Figure 4-16 shows the calibration curve of the four peptides. Tested linear dynamic ranges were 2 to 3 orders of magnitude with 1 μl sample loading for this capillary LC/ECD system.

System reproducibility. The reproducibility of the system was also determined. With 1 μl sample loading, the standard deviation of the signals of 6 consecutive analyses were below 7% and the concentration limits of detection for vasopressin, bradykinin, oxytocin and neurotensin were 7, 5, 20 and 59 pM respectively. Another phenomenon that is worth to pointing out is that electrode fouling is limited in comparison to that of neutral pH. The signal decrease due to electrode fouling was only about 15% without sweeping the electrode between sample analysis (comparing to that of 40% fouling in chapter 3). A mild electrochemical treatment by sweeping the carbon fiber microelectrode between -0.40 V to 1.6 V for only four cycles in a rate of 1 V/s between runs will eliminate this signal loss. The reason of this less severe fouling could be partially attributed to the basic mobile phase used in the analysis. At high pH, the adsorption of analyte on the electrode surface will probably be less severe compared to that of neutral pH.

Characterization of Microdialysis Probe

Temporal resolution in microdialysis sampling is typically limited by the mass sensitivity of the analytical method and the absolute recovery of the probe. Absolute and relative recoveries for the three peptides, which we were interested, e.g. vasopressin, bradykinin, and oxytocin, at 37 °C by the probe utilized in this work are shown in Figure 4-17A and Figure 4-17B. In order to maximize signal and temporal resolution, we used a flow-rate of 0.5 μl/min because at this flow-rate the absolute recoveries begin to level off. At this flow-rate the relative recoveries were 59% ± 7% for vasopressin, 55% ± 4% for bradykinin and 53% ± 4% for oxytocin. The recovery of neurotensin was not measured

due to its relatively high detection limit and its low extracellular concentration in the brain region to be explored.

In Vivo Application

For further validation, this capillary LC/ECD system was used to determine the *in vivo* concentration of several neuropeptides of interest through microdialysis sampling. Since 3 μl samples were required for loading into the capillary LC/ECD, a 5 minute sample collection time will be used to provide dialysate from rat brain. Based on previous research of monitoring brain neuropeptide by RIA with microdialysis sampling, it seemed that the concentration detection limit of capillary LC/ECD system is adequate for monitoring these peptide release with 5 minute temporal resolution.

Figure 4-18 shows the chromatograms of neuropeptide release from supraoptic nucleus (SON) in rat brain. By comparing the chromatogram of peptide standard to that of *in vivo* dialysate, vasopressin and bradykinin can be identified based on their retention time. Vasopressin clearly increased with the stimulation of high concentration potassium aCSF perfusion. However, the same cannot be said for that of bradykinin. The bradykinin peak had no observable changes during the course of high concentration potassium stimulation. For the peak with the retention time the same as that of oxytocin, no obvious change has been observed during the high concentration potassium stimulation either. Also note that the oxytocin peak co-eluted with another wide peak which made the measurement of oxytocin peak difficult. Also based on the previous RIA analysis, the amount of oxytocin recovered in 5 minute was just above the detection limit of the system. All these factors contributed to the irreproducibility in quantification of oxytocin in the dialysate.

Our previous experiment clearly showed that the copper peptide biuret complex would promote the detection of non-electroactive neuropeptide such as des-tyr-met-enkephalin and bradykinin. Figure 4-19 shows the effect of copper derivatization on dialysate. Comparing trace A and trace B in Figure 4-19, the peak corresponding to the retention time of bradykinin shows up clearly in trace B while it is almost invisible in trace A. Recall that the formation and detection of bradykinin will require the excessive heating of the mixture. This is another piece of evidence that the corresponding peak was bradykinin. At the same time, the peaks corresponding to vasopressin and that of oxytocin did not increase with the incubation of copper derivative reagent. This is also in good agreement with the results obtained from electrode characterization.

In addition to the peaks identified by retention time of the peptide standards, there are other peaks that noticeably increase after the sample is incubated with copper derivative reagent, such as the peak with the retention time of 441 seconds, and that of 470 seconds. Since monoamine would not form a biuret complex with copper ions, this increased peak must not be due to the presence of monoamine neurotransmitters. Also by the fact that these peak retained very well even under high pH, they were very likely peptides that were acquired through the *in vivo* microdialysis. The small peaks shown in trace A could be explained by the slow formation of the biuret complexes between copper and peptides. The incomplete formation will give partial signal of peptide. With extensive heating, the biuret complex formation will be sped up and a large signal will be detected due to biuret complex (trace B). Further investigation will be required to identify these peaks, hopefully, with the help of mass spectrometry.

Shown in Figure 4-20 is the monitoring profile of *in vivo* vasopressin release in the rat SON region. The first arrow points at the time when the perfusion fluid was switched from normal aCSF to high potassium aCSF. According to the manufacturer's specification, the microdialysis probe used has 4 μl of dead volume in the probe. Also the dead volume in the Teflon tubing is 3.6 μl before the probe and 1.8 μl after the probe. So overall dead volume will be approximately 9.4 μl. This volume is about the dialysate collected in 4 sampling periods and therefore a delay should be expected in monitoring response upon the application of high potassium stimulation. As in Figure 4-20, the measured vasopressin concentration starts to increase at sampling period 9 and reaches its maximum at period 10. As high potassium stimulus continues, the vasopressin concentration stays above the basal level. After the potassium stimulus is removed, the vasopressin returns to its basal level.

The measured basal vasopressin release by capillary LC/ECD coupled with microdialysis sampling was in the same range as previous results obtained by RIA [Lud92]. The basal vasopressin level in SON determined by Landgraf was about 550 ± 150 pM. The vasopressin level in the first 6 dialysis samples in our study averaged 410 ± 120 pM. Additionally, the average vasopressin increase for the 30 minutes of high potassium stimulation was determined as 2.1 fold over that of basal level. This can be directly compared to RIA results of 2.4 fold enhancement for the first 30 minute or 1.9 fold for the second 30 minutes sapling period. However, due to the improvement of mass detection limit, temporal resolution of *in vivo* measurement can now be shortened to 5 minute instead of 30 minutes with RIA. This improved temporal resolution allows the

observation of vasopressin release change in 5 minute intervals rather than the average of 30 minutes upon stimulation by high concentration potassium.

Figure 4-21 shows the monitoring profile of bradykinin. The release of bradykinin seemed unchanged upon stimulation with high concentration potassium aCSF. As stated, its change was insignificant. The average *in vivo* bradykinin level measured by capillary LC/ECD was 240 ± 56 pM. This unchanged bradykinin level during the potassium stimulation suggested that bradykinin may not function as a neurotransmitter in this brain region.

Conclusion

The work presented here demonstrates that the capillary LC/ECD can be used to measure both electroactive and non-electroactive peptides. For those non-electroactive peptide such as bradykinin, des-tyr-met-enkephalin, electrochemical detection can be achieved through copper biuret derivatization. Low picomolar detection limits were achieved for both electroactive and non-electroactive peptides. The application of this system to monitoring vasopressin and bradykinin achieved 5 minute temporal resolution which is a 6 fold improvement over that of RIA for vasopressin. The improvement can mainly be contributed to the high sensitivity of the capillary LC/ECD system. Another improvement is the capability of simultaneously multiple analytes determination which is hard to realize by RIA without multi-labeling.

The developed capillary LC/ECD method based on copper biuret derivatization should be applicable to other peptide determinations as well. However, there exists the potential of further improvements based on 1) the use of smaller separation columns, 2)

faster separations, and 3) better understanding of biuret complex oxidation mechanism to achieve better detection.

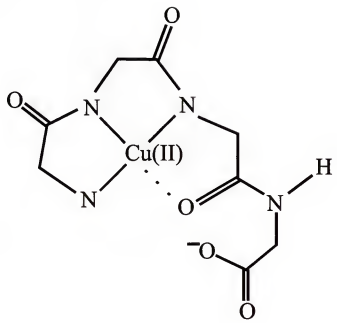

I

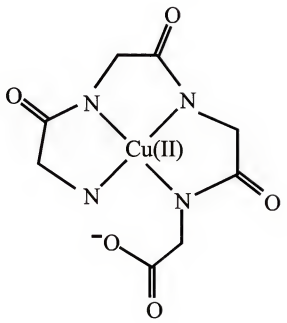

II

Figure 4-1. Structures of Peptide - Copper Biuret Complexes at Different pH. Adopted from ref. [Che95].

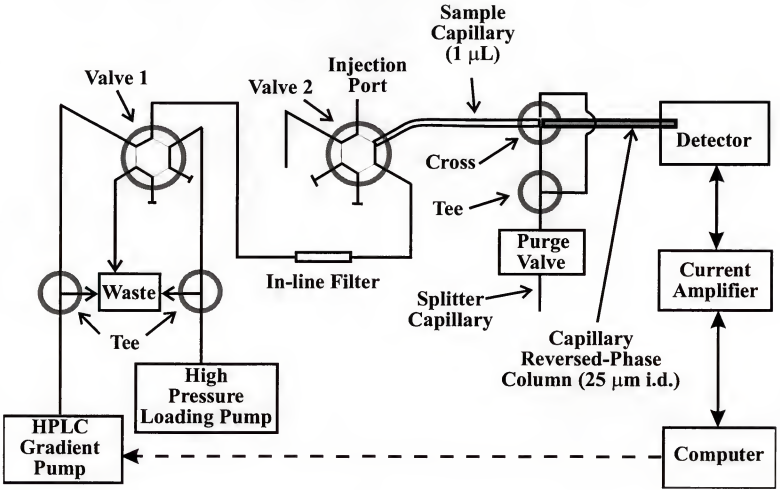

Figure 4-2. Block diagram of on-column preconcentration capillary LC/ECD

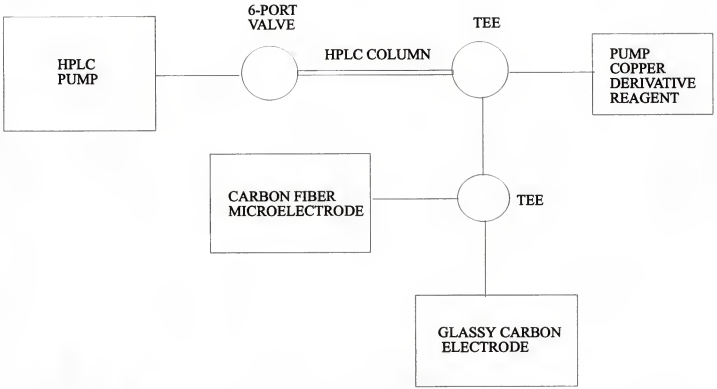

Figure 4-3. Block diagram of dual-detector HPLC system.

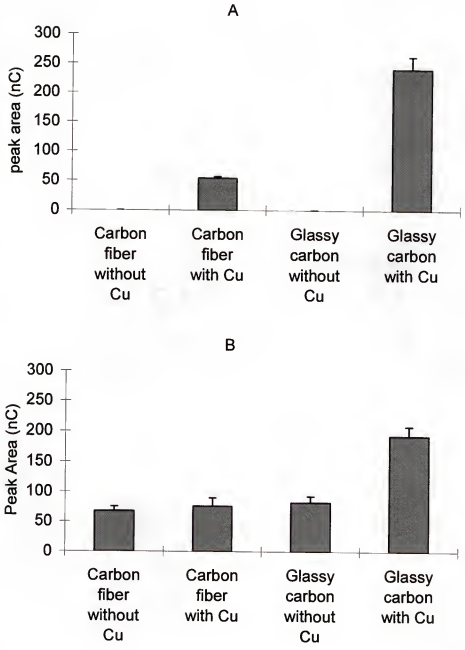

Figure 4-4. Detection of des-tyr-met-enkephalin (A) and met-enkephalin (B) at both glassy carbon electrode and carbon fiber microelectrode. Same amount of peptide was loaded both with copper and without copper.

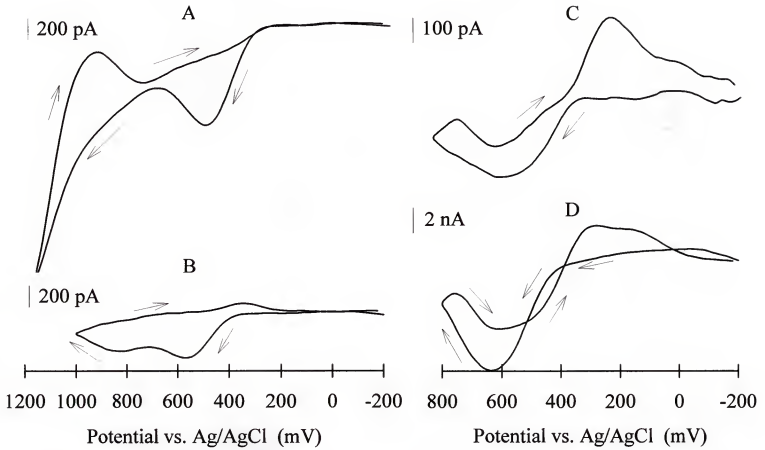

Figure 4-5. Fast scan voltammograms of (A) met-enkephalin without copper and (B) with copper, (C) des-tyr-metenkephalin with copper, and (D) Bradykinin with copper. All peptide concentration = 50 μM. Same mobile phase as in capillary LC.

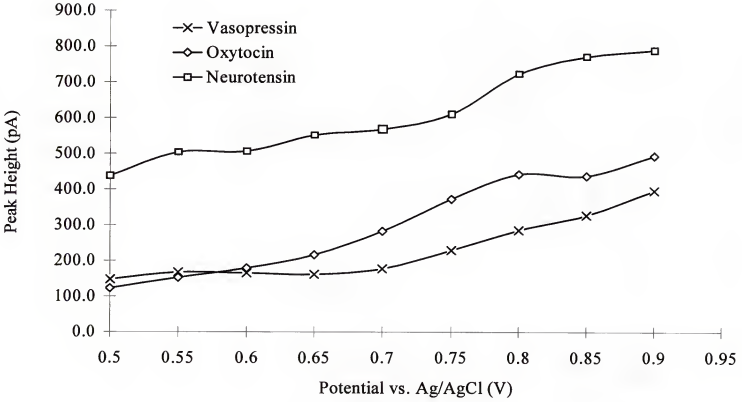

Figure 4-6. Hydrodynamic voltammograms of peptides at pH=10.5. Peptide concentration were as follow: neurotensin, 5 μM; oxytocin, 2 μM and vasopressin, 0.5 μM. Injection volume was estimated as 5 nL.

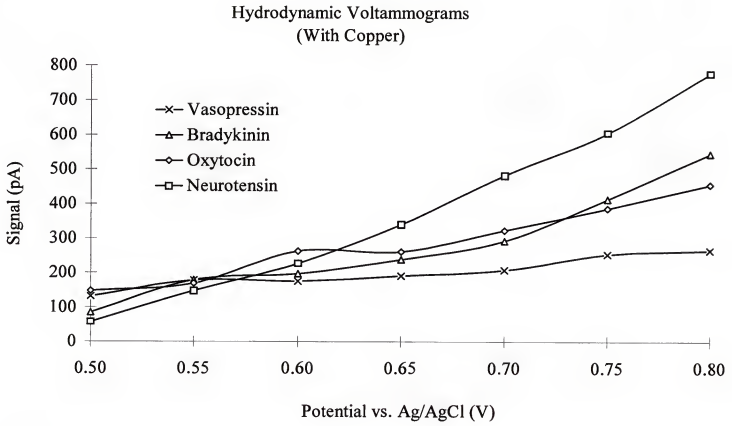

Figure 4-7. Hydrodynamic voltammograms of peptide copper biuret complexes at pH=10.5, [Cu]=0.25 mM. Same peptide concentration and sample volume as described in legend for figure 4-6. Bradykinin concentration: 0.5 μM.

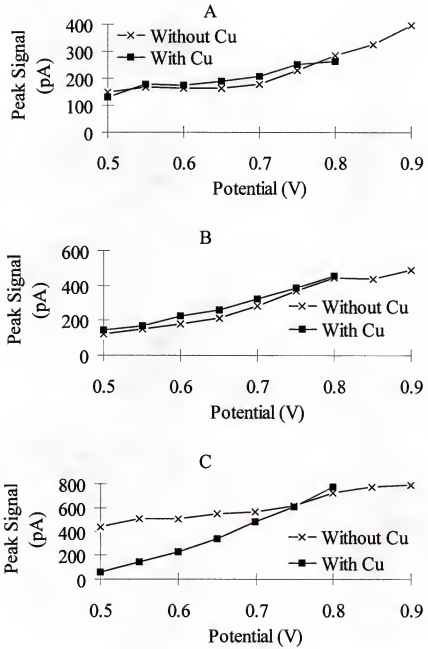

Figure 4-8. Hydrodynamic voltammograms of vasopressin (A), oxytocin (B) and neurotensin (C) with copper and without copper. pH=10.5. $[Cu^{++}]$=0.25mM where applicable.

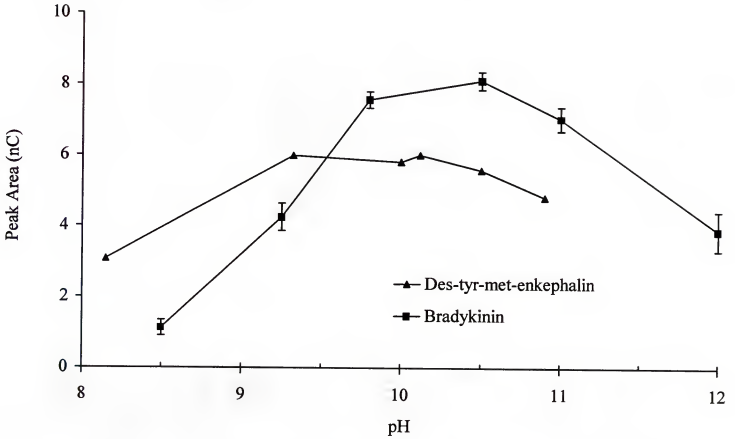

Figure 4-9. pH effect on peptide biuret complexes detection. [Cu]=1.0 mM, V=0.60 V.

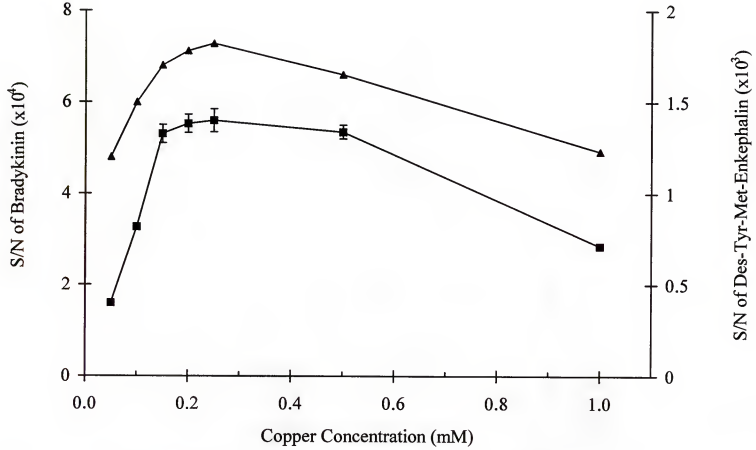

Figure 4-10. Effect of copper concentration on peptide detection. Potential = 0.60V, pH=10.5

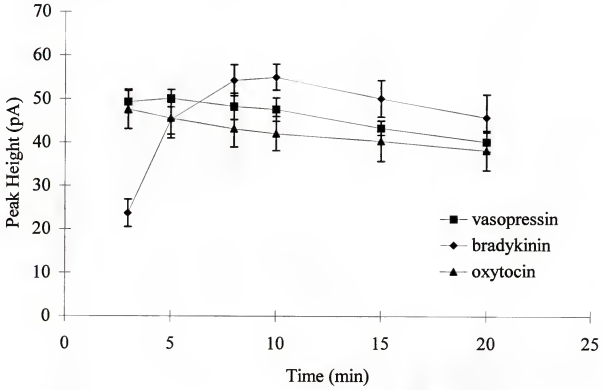

Figure 4-11. Effect of sample incubation. Peptide concentrations: bradykinin 1 nM, vasopressin 1 nM and oxytocin 4 nM. Sample volume was 1 μL. [Cu++]=0.25 mM, V=0.65V.

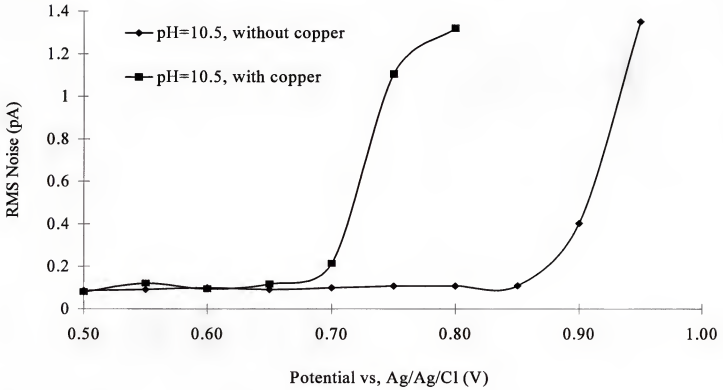

Figure 4-12. Norse level of mobile phase with copper and without copper.

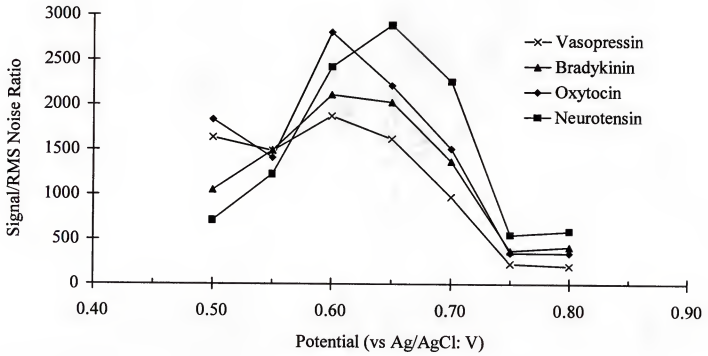

Figure 4-13. Signal-to-noise ratio of peptide determination.

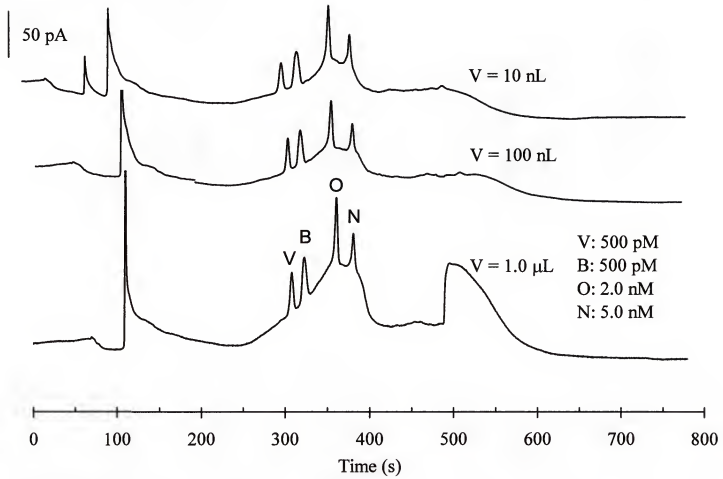

Figure 4-14. Capillary LC/ECD peptide determinations. The total amount for the specific peptide holds constant for all three chromatograms with the concentration of each peptide varied according to the sample volume.

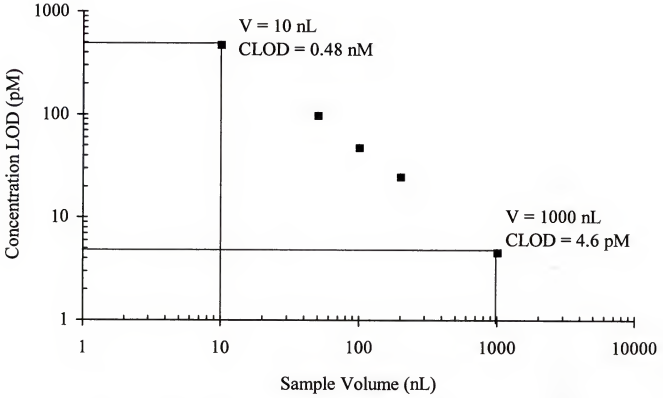

Figure 4-15. Effect of preconcentration on concentration limit of detection. Bradykinin copper biuret complex is used as an example.

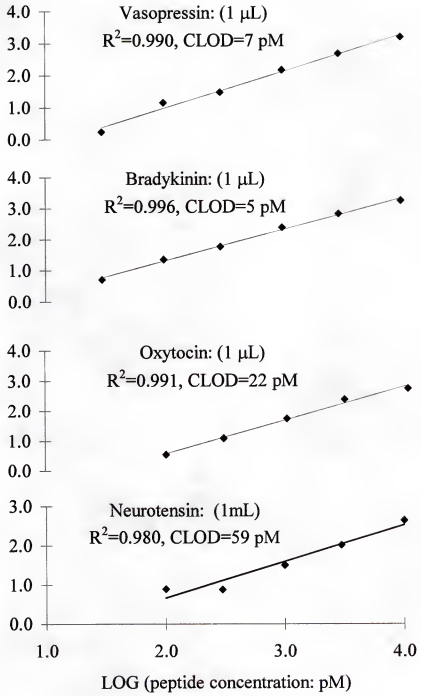

Figure 4-16. Calibration curve of capillary LC/ECD peptide determination.

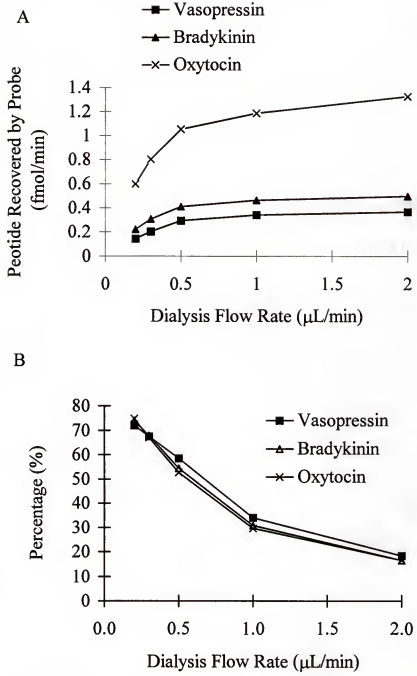

Figure 4-17. Characterization of microdialysis probe. At 0.50 μl/min flow rate, the relative recoveries are vasopressin: 59% ± 7%, bradykinin: 55% ± 4%, and oxytocin: 53% ± 4% respectively.

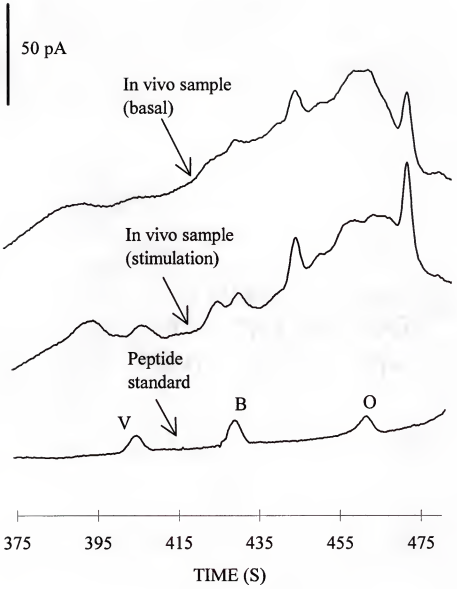

Figure 4-18. Monitoring peptide *in vivo* by capillary LC/ECD. Peptide standard concentrations: vasopressin (V), 250 pM; bradykinin (B), 250 pM and oxytocin (O), 1 nM.

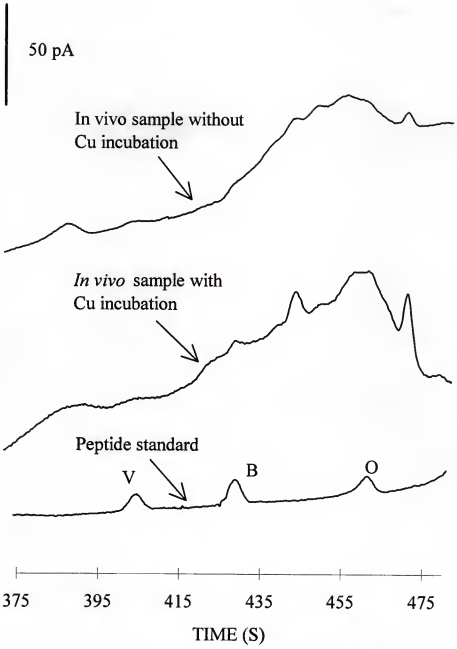

Figure 4-19. Copper effect on in vivo dialysate determination. Concentrations of peptide standard were the same as in figure 4-18.

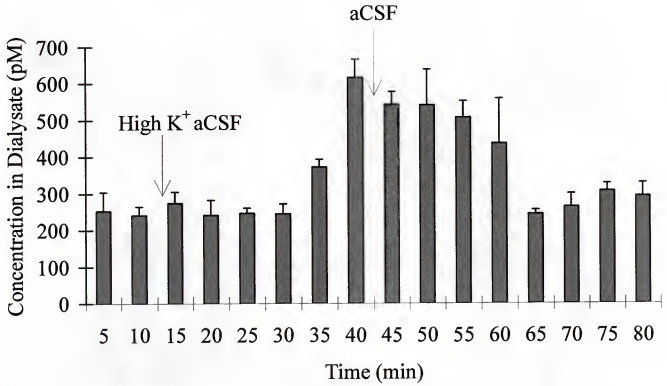

Figure 4-20. Monitoring of vasopressin release *in vivo* with 5 minute temporal resolution. The error bar represent the standard deviation of the mean of 5 rats. High concentration K^+ is applied at first arrow and second arrow indicates the start of normal aCSF perfusion.

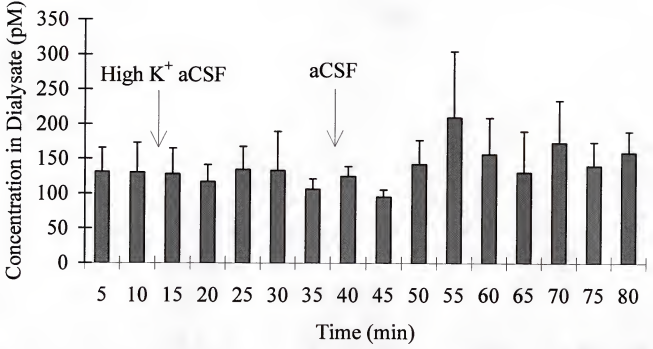

Figure 4-21. Monitoring of bradykinin release *in vivo* with 5 minute temporal resolution. The error bar represent the standard deviation of the mean of 5 rats. High concentration K^+ is applied at first arrow and second arrow indicates the start of normal aCSF perfusion.

CHAPTER 5
CAPILLARY ELECTROPHORESIS WITH DUAL UV ABSORBANCE AND ELECTROCHEMICAL DETECTION FOR THE ANALYSIS OF PEPTIDE BIURET COMPLEXES

Introduction

Capillary LC coupled with electrochemical detection has proven to be a highly sensitive method to perform neuropeptide analysis (Chapters 3 and 4). For both electroactive and non-electroactive peptides, low amol detection limits were achieved (vasopressin, 7 amol and bradykinin, 5 amol) [Chapter 4]. Our research has shown that capillary LC coupled with carbon fiber microelectrode improved mass limit of detection of peptides 1000 fold over that of conventional HPLC/ECD [Chapter 4, Che95, Tsa91]. For example, vasopressin had the mass limit of detection of over 6 fmol in a conventional HPLC/ECD and 7 amol in capillary LC/ECD. For bradykinin, the mass limit of detection was improved from 36 fmol on conventional HPLC/ECD to 5 amol on capillary LC/ECD (based on the conversion of sensitivity data in Che95 and Tsa91). This improvement enabled us to apply this capillary LC/ECD to *in vivo* neuropeptides monitoring with improved temporal resolution [Chapter 4]. Combined with preconcentration capability of capillary LC/ECD achieved concentration limits of detection 7 pM for vasopressin and 5 pM for bradykinin with 1 μL sample loaded. These concentration limits of detection enabled monitoring these neuropeptides *in vivo* with 5-minute temporal resolution.

For a non-electroactive peptide such as bradykinin and des-tyr-met-enkephalin, the formed copper peptide biuret complex enabled the detection of non-electroactive peptides at glassy carbon electrodes [Che95d, Tsa90, Tsa91, Tsa92, War89] and at carbon fiber microelectrodes [Chapter 4] at moderate oxidation potential. It was also noticed that the carbon fiber microelectrode behaved differently to that of glassy carbon electrode when used to detect biuret complex of electroactive peptides. Previous research showed the formed biuret complex enhanced detection of electroactive peptides at glassy carbon electrodes [Che95d, Tsa90, Tsa91, Tsa92, War89]. However, a study in our lab showed that there was a difference between glassy carbon electrodes and carbon fiber microelectrodes when biuret derivatization was used to improve the detection of electroactive peptides [Chapter 4]. On the contrary to that of glassy carbon electrode, the signal of electroactive peptides at carbon fiber microelectrodes experienced no enhancement when the biuret complex was formed. For neurotensin, the electrochemical signal of its biuret complex at carbon fiber microelectrode actually decreased in comparing to that of the free peptide. For further extending this capillary LC/ECD to other neuropeptides, a better understanding the oxidation of formed biuret complex at carbon fiber microelectrode will be beneficial.

It was also suggested that some peptides can form biuret complexes with more than one copper in the complex which was attributed to the different electrochemical sensitivities of different peptide biuret complexes [Tsa91]. For peptide with different structure, the capability of forming multi-copper complex will differ. This difference might affect their relative sensitivities at carbon fiber microelectrode. The knowledge of

electroactivity of different complex forms at carbon fiber microelectrode would help to optimize the detection of these peptides.

To study the different electroactivities of different copper peptide biuret complex forms (including the free form electroactive peptides), they have to be separated first. These peptide complexes differ on the number of Cu^{++} in their complexes and therefore the net charge of the complex. These different complex forms can be separated by the charge-to-mass ratio based separation techniques. The electroactivity of these separated complexes can then be tested at carbon fiber microelectrode individually.

Capillary electrophoresis is suitable for separating different forms of biuret complexes due to its charge-to-mass ratio based separation mechanism. In addition, the geometry of the capillary and the carbon fiber microelectrode makes them a good match in separation and detection. In this study, a UV absorbance detector was used to investigate the complex formation at different copper-to-peptide ratios and to quantify the amount of peptide in different forms. A carbon fiber microelectrode was used to detect these different forms of copper peptide complexes based on their electroactivity. By comparing the signal from microelectrode to that of UV absorbance, the electroactivities of different complex forms can be determined.

Experimental

Reagents and Buffer

Unless specified otherwise, all chemicals were purchased from Sigma (St. Louis, MO, USA). The electrophoresis buffer was 10 mM sodium borate with 3 mM potassium sodium tartrate and its pH was adjusted to 11.0 with sodium hydroxide. The copper derivative reagent was the same buffer with 1 mM cupric sulfate dissolved. Both

solutions were made fresh and filtered with 0.22 μm pore size hydrophobic Teflon filter membrane (MSI, Westboro, MA, USA) immediately before use. The use of this Teflon filter membrane enabled the filtration of the basic solution and at the same time removed some of the hydrophobic impurities. All the peptide standard solutions were first prepared in the same capillary electrophoresis buffer without copper.

Capillary Electrophoresis Apparatus

CE setup and column preparation. The experimental setup is shown in figure 5-1. A fused silica capillary (Polymicro Technologies, Phoenix, AZ, USA) of 30 cm in length, 360 μm o.d. and 50 μm i.d. was used as the separation capillary. A Spellman CZE1000R high voltage power supply (Spellman, Plainview, NY, USA) was used and a Spectra 100 UV-Vis detector (Spectra-Physics, San Jose, CA, USA) was employed to perform on-line detection by removing the capillary coating at the appropriate position. The separation capillary was pretreated first with 1.0 M HCl for 20 min at 200 psi. and then by 1.0 M NaOH for 30 min at the same pressure. The same capillary was rinsed with electrophoresis buffer for 30 min right before the experiment. The separation potential was kept at 15000 V, which was equivalent to 500 V/cm electric field strength, and the separation current was measured to be about 40 μA.

Joint assembly. In order to accommodate electrochemical detection, a de-coupler was used to eliminate the separation electric field prior to the electrochemical detection [Wil87]. Nafion tubing was reported effective in grounding the separation potential [O's92]. The same design was used in this experiment. The separation capillary (30 cm in length, 360 μm o.d. and 50 μm i.d.) was coupled with a piece of 2-cm long, 360 μm o.d. and either 50 μm i.d. or 25 μm i.d. capillary (detection capillary) inside a 2 cm long

Nafion tubing, see the enlarged portion of figure 5-1. Both capillary ends were carefully cut to ensure their flatness which was the key to maintaining a minimum gap between the two capillaries. The Nafion tubing used in the experiment was found to expand when wet. To minimize the possible expansion of the gap between the two capillaries, they were positioned under a microscope when middle portion of the Nafion tubing was wet. Once in position, the Nafion tubing and capillaries were sealed by epoxy and cured overnight at room temperature. This joint served the purpose of grounding the separation potential prior to the electrochemical detection. The Nafion tubing used here allows the transportation of ions but prevents the bulk flow from the capillary system into the grounding buffer. The analytes would then be carried over by the bulk flow to the electrochemical detection cell to be detected electrochemically.

Dual-detection. There are two detectors employed in this experiment, a UV absorption detector and an electrochemical detector. The UV absorbance detection wavelength was set at 210 nm. A window of 0.5 cm was created on the separation capillary by removing its polymer coating by flame. In addition to the UV absorbance detector, an electrochemical detector made of a 9 μm diameter 6 mm in length cylindrical carbon fiber microelectrode was also used. The procedure of preparing this microelectrode is given in the previous chapters. This microelectrode was inserted into the end of the detection capillary with a three-way micro-manipulator under a micro objective to perform electrochemical detection (for a more detailed description, see Chapter 3). A Stanford SR 570 current preamplifier (Stanford Research Systems, Sunnyvale, CA, USA) was used to amplify the signal from the carbon fiber microelectrode. The detection potential was set at 0.65 V verses Ag/AgCl reference

electrode unless specified otherwise. A piece of aluminum foil was used to cover the electrochemical detector to minimize the environmental noise.

Sample preparation and injection

Peptide samples were prepared with different copper-to-peptide ratios (0, 0.5, 1, 2 and 5). Peptide samples were introduced from the anode by electrokinetic injection. This mode of injection was chosen due to its simplicity in operation as well as it reproducibility since the sample discrimination was not a critical issue in our experiment. The actual injection potentials and the injection times varied for different peptide samples as specified in the legend of each figure.

A Gateway 2000 486-66 IBM compatible computer (Gateway, Sioux City, SD, USA) with a National Instrumental data acquisition board (AT-MIO-16F-5, National Instruments, Austin, TX, USA) was used to collect data from both the UV absorbance detector and the electrochemical detector. Data from both detectors were low pass filtered at 3 Hz and collected at 10 Hz. The software used in the experiment was written in-house.

Results and Discussion

System Characterization

Several tests were performed to evaluate the performance of the Nafion joint constructed. One of the main concerns was the effectiveness of the joint as a ground. Figure 5-2 shows the correlation between electrode noise and separation potential. As the separation potential increased, so did the rms noise on the microelectrode. This indicates the possible leaking of electric field into the electrochemical detection cell. Also noticed was that the noise could be reduced by increasing the gap between the two capillaries

inside the Nafion tubing (see figure 5-3). However, increasing the gap would cause band broadening after the Nafion junction. Previous research showed that a smaller i.d. capillary could rapidly quench the electric field at the capillary outlet without a Nafion junction [Wal87]. By decreasing the detection capillary i.d. to 25 μm, the rms noise was decreased from 30 pA to 1.4 pA at 500 V/cm electric field strength while maintaining the minimum gap inside the Nafion junction. The use of a smaller i.d. detection capillary could further benefit the electrochemical detection by means of less band broadening as well as better detection efficiency on the carbon fiber microelectrode.

The system reproducibility was verified with the electrokinetic injection of vasopressin followed by electrophoresis. For six consecutive injections of 100 μM vasopressin (2 seconds at 2000 V), the CE-UV-ECD system generated signals on both UV and carbon fiber microelectrode with relative standard deviations of 4.2% and 6.1% respectively.

Capillary Electrophoresis-UV Absorbance-Electrochemical Detection (CE-UV-ECD) Study of Copper Peptide Complex

As opposed to copper (II) ion, only the peptide bond absorbs at 210 nm. The formation of biuret complex will not affect the UV absorbance of peptide bond at 210 nm. Therefore the signal from the UV absorbance detector can be directly correlated to the amount of peptide, either in free peptide or in peptide-copper complex forms. In the experiment, the UV absorbance detector was used to quantify the amount of peptide in different complex forms at different copper-to-peptide ratios. With the electrochemical detector placed after the UV absorbance detector, the electroactivities of different forms of peptide-copper complexes can be determined. Due to the arrangement of the two

detectors (in series), the migration time of same complex form was different with different detectors.

The peptides used in the experiment are listed in the table 5-1 together with the numbers of amino acid in each peptide, their molecular weight, the presence of electroactive amino acid group (numbers in parentheses) and their disulfide bonds.

Table 5-1. Characteristics of peptide used in experiment.

Peptide Name	Number of Amino Acid	Molecular Weight	Electroactive Amino Acid	Disulfide Bond
Bradykinin	9	1060	none	none
Neurotensin 1-13	13	1672	Tyr.(2)	none
Oxytocin	9	1007	Tyr.(1)	one
Substance P	11	1347	none	none
Vasopressin	9	1084	Tyr.(1)	one

Vasopressin and oxytocin. Vasopressin and oxytocin both contain 9 amino acid groups and one disulfide bond as well as one tyrosine. They were both electroactive and could be detected on the carbon fiber electrode without biuret derivatization (see figure 5-4, and 5-5). For vasopressin, with the increase of copper-to-vasopressin ratio from 0 to 0.5 and to 1 (see figure 5-4 with subtitle of A1, B1, A2, B2, A3 and B3), the peak labeled with free peptide gradually decreased while the peak labeled with complex increased. Further increase of the copper-to-peptide ratio had no obvious effect on the complex peak. The same can be said for oxytocin (see figure 5-5). This suggests the formation of copper peptide biuret complex with a copper-to-peptide ratio of one.

Theoretically, peptides larger than 8 amino acid could form biuret complexes with more than one copper, however, the experiment shows that only one copper containing biuret complex was formed for both peptides. This can be explained by their disulfide bond which forms a ring between the first and the sixth amino acid groups. This ring

structure would prohibit a further conformational change that is critical to the formation of more than one form of copper biuret complexes. [Mar83]

Since both peptides contain tyrosine, an electroactive amino acid, it was expected that they undergo a one electron transfer during oxidation for the free peptide. However, with the formation of biuret complex, copper (II) in the complex can also be oxidized in addition to the peptide. If both copper (II) and peptide were oxidized at the electrode surface, the signal generated on the electrode would be the sum of the two. Form the signals of the UV absorbance detector, the amount of peptide in both forms can be determined. If peptide in both forms (free peptide and complex) only undergoes single electron transfer during their oxidization, the ratio of signals of ECD to that of UV for both forms should be identical. If, however, there were multiple electron transfers in the complex, the ratio of ECD/UV signals (area) would be bigger for the peptide complex than that for the peptide alone. The calculated values of signal ratio (ECD/UV) for free peptide peak and complex peak for both vasopressin and oxytocin are listed in table 5-2 and table 5-3 respectively.

Table 5-2. Signal (peak area) ratio[a] of electrochemical detection to UV absorbance for vasopressin and its copper complex.

copper-to-peptide ratio	free peptide: (ECD)/(UV)	complex: (ECD)/(UV)
0	3.25	-
0.5	3.51	3.30
1	-	3.05
2	-	3.15
5	-	2.84

[a] the ratio has units of pC/mAUFS*S and the same units were used throughout the chapter.

Table 5-3. Signal (peak area) ratio of electrochemical detection to UV absorbance for oxytocin and its copper complex.

copper-to-peptide ratio	free peptide: (ECD)/(UV)	complex: (ECD)/(UV)
0	0.84	-
0.5	0.91	0.78
1	-	0.77
2	-	0.72
5	-	0.75

As can be seen in the table, the actual peak area ratio of complex peak was not bigger than that of free peptide peak. For vasopressin, the ratio for free peptide peak is 3.36 and that of complex peak is 3.08. For oxytocin, the ratio of free peptide peak is 0.87 and that of complex peak is 0.76. The actual decrease in the ratio of complex peak can partially be explained by the migration time difference between the free peptide peak and complex peak. Since complex peak migrates slower than that of free peptide peak, the resident time of complex peak in the UV detection cell is longer than that of free peptide peak. When both peak areas are measured at UV absorbance detector, the complex peak will be bigger than it really is before the difference in migration time is corrected. After both peaks pass through the Nafion joint, they are transferred by the run buffer and their migration flow rate are the same as that of the run buffer, which is driven by pressure and therefore both free peptide peak and complex peak will pass the electrochemical detector at the same flow rate with no discrimination between the two. This phenomenon will cause the discrimination when calculating peak ratios. When signal of ECD to UV ratio for complex is calculated, the ratio will be smaller than it should due to the larger UV area measured. If this effect is taken into consideration, the peak area ratio could be closer than they are in the tables. The above data shows that though the biuret complexes were formed, they did not improve the detection of either vasopressin or oxytocin.

As seen in figures 5-4A2 and 5-5A2, when about 50% copper was added into peptide solutions, two distinct peaks appeared. This fact indicates that the peptide copper complexes were stable and remained as complex even when the free peptides were separated from the complexes. This result indicates either very high formation constant of these peptide copper complex or very slow dissociation kinetic of the formed complexes. Since the complexes formed almost instantly, both hypotheses come to the conclusion that the formed complexes will be very stable.

Neurotensin. For neurotensin, a 13 amino acid peptide, which contains two tyrosine groups and no disulfide bond, multiple copper biuret complexes were formed with excess of copper (see figure 5-6). The uncomplexed neurotensin can be detected on the carbon fiber microelectrode due to its two tyrosine groups, see figure 5-6B1. With the increase of copper to neurotensin ratio, complex I peak and complex II peak start to increase and eventually complex II peak became dominant (figure 5-6A5). In the mean time, the electrochemical signal gradually decreased for the carbon fiber electrode, see figure 5-6B2 to B5. However, there was no indication that complex II peak was detected at the microelectrode. Table 5-4 lists the ratio of ECD signal (sum of free peptide peak and complex I peak) to that of UV. The peak ratio also showed that there was no enhancement for the detection of neurotensin electrochemically with the formation of biuret complexes.

Table 5-4. Signal (peak area) ratio of electrochemical detection to UV absorbance for neurotensin and its copper complexes.

copper-to-peptide ratio	free peptide and complex I: (ECD)/ (UV)
0	5.17
0.5	4.56
1	4.96
2	4.84
5	5.16

Branykinin and substance P. For non-electroactive peptides such as bradykinin and substance P, the formed biuret complexes can be detected on the microelectrode. Figure 5-7 shows the formation and detection of bradykinin copper complexes at both UV absorbance and carbon fiber microelectrode. At copper-to-peptide ratio of 0.5, a total of four peaks were generated, see figure 5-7A2. Adding more copper caused the free peptide peak, which was free form bradykinin, to gradually diminish and the complex I peak to increase. Further increase of copper-to-peptide ratio from 2 to 5, showed no obvious changes on the ratio of complex I to that of complex III (UV signal). Due to the fact that when complex I peak of the UV signal increased, the signal on microelectrode also increased and based on migration time relation as well, it was believed that complex I peak was the one that was detected on the microelectrode. Table 5-5 shows the signal ratio of ECD to that of UV for bradykinin.

Table 5-4. Signal (peak area) ratio of electrochemical detection to UV absorbance for bradykinin and its copper complexes.

copper-to-peptide ratio	complex I peak(ECD)/ (UV)
0	0
0.5	7.1
1	8.1
2	7.3
5	6.9

The relatively constant peak ratio confirmed in another way that only complex I peak was detected at the carbon fiber microelectrode.

Figure 5-8 shows the analysis of substance P with biuret complexes. Like bradykinin and neurotensin, multiple copper-peptide complexes were formed. Substance P has no electroactive amino acid groups and cannot be detected on the electrochemical detector prior to derivatization, see figure 5-8A1 and 5-8B1. With copper added, complex I peak began to develop in UV and was detected at the microelectrode, see figure 5-8A2 and 5-8B2. With the further increase of the copper-to-peptide ratio from 0.5 to 2.0, as seen in figure 5-8A4 and figure 5-8B4, complex II peak began to appear and was detected electrochemically. With copper-to-peptide ratio increase to 5, free peptide peak is almost disappeared and complex II peak further increased.

Also seen in figure 5-8A2 and 5-8A3, where the copper-to-peptide ratios were 0.5 and 1.0, the percentage of peptide in complex I form of total peptide (area, both from UV absorbance) were 24.3% and 48.3% respectively. This is a good indication of the formation of complex with two coppers in one peptide (correspond to complex I peak), since complex II peak was not significant in size at both circumstances.

The signal ratios of electrochemical detection to that of UV absorbance for both complex I and complex II were tabulated in the table 5-5.

Table 5-5. Signal (peak area) ratio of electrochemical detection to UV absorbance for substance P and its copper complexes.

copper-to-peptide ratio	complex I peak: (ECD)/ (UV)	complex II peak: (ECD)/ (UV)
0	-	-
0.5	5.67	-
1	5.03	-
2	5.01	2.53
5	5.75	2.61

In table 5-5, both ratios held constant over the experimental copper-to-peptide ratios. The signal ratio of complex II peak is only about half of that of complex I peak for

substance P. Since complex II peak required further excess of copper to form (compared to complex I peak), the complex represented by complex II peak must have contained no less copper than that of complex I peak. Their electrochemical signal differences can not be explained by the number of copper ions in the complexes. Rather, stereo-hindrance could be a possible reason for low sensitivity of complex II peak on carbon fiber microelectrodes.

Detection of Vasopressin at Higher Potential. A further investigation of detection potential effect was also conducted. When vasopressin and oxytocin were studied, no enhancement was observed due to the formation of peptide copper biuret complex. This phenomenon could be resulted from higher oxidation potential for the complex. An elevated detection potential can be used to test this hypothesis. Vasopressin was chosen as a sample peptide to determine the electrochemical difference of biuret complex at different potentials. Figure 5-9 showed the study of CE-UV-ECD with the working electrode potential set at 0.80 V against Ag/AgCl reference electrode. This potential was chosen based on following considerations: 1) copper (II) in non-electroactive peptide biuret complexes could be oxidized at 0.65V and gave reasonable electrochemical signals as for both bradykinin and substance P. 2) these electroactive peptides such as vasopressin and oxytocin can generate good response at microelectrode at 0.65V too. 3) Weber and coworkers [Che95d, Tsa90, Tsa91, Tsa92, War89] obtained enhanced oxidation signal on the electroactive peptide due to the formation of copper biuret complex at 0.80V at glassy carbon electrode. Table 5-6 shows the signal ratios of different peaks.

Table 5-6. Signal (peak area) ratio[a] of electrochemical detection to UV absorbance for vasopressin and its copper complex (detection potential = 0.80 V).

copper-to-peptide ratio	free peptide peak: (ECD)/ (UV)	complex I peak: (ECD)/ (UV)
0	4.80	4.60
0.5	5.02	4.94
1	-	4.00
2	-	4.64
5	-	4.58

Again, there is no distinguishable difference between the ratio for free peptide peak and that for complex I peak. Even at 0.80 V, there is still no enhancement for the detection of vasopressin electrochemically with the copper biuret complex formed. This means that the non-enhancement effect was not due to the different in oxidation potential shift of copper (II) and electroactive amino acid groups in the complex.

Comparing table 5-6 and table 5-2 shows that the electrochemical signal was higher when the detection potential was set at 0.80 V. This conclusion agrees well with the results from capillary LC studies [Chapter 4].

Estimation of Relative Sensitivity of Peptides on Microelectrode

For those peptide that existed in only one electroactive form, such as vasopressin, oxytocin, bradykinin, and possibly neurotensin, their relative sensitivities on the carbon fiber microelectrode can be estimated as follows. Assume that a 5-fold excess of copper-to-peptide ratio is large enough for all the possible complexes to form, the ratio of electrochemical detector signal(only one detectable peak) to that of UV absorbance (the sum of all the detectable peaks) can be used to determine their relative sensitivities. The higher the ratio, the more sensitive the peptide would be on a microelectrode, see table 5-7.

Table 5-7. Relative sensitivity estimation[a].

Peptide	Ratio	Estimated Relative Sensitivity	Result from Capillary LC/ECD[b]	Result from Glassy Carbon Electrode[c]
bradykinin	3.52	1.00	1.00	-
neurotensin[c]	3.83	1.09	0.08	1.07
oxytocin	0.75	0.21	0.25	0.78
vasopressin	2.84	0.80	0.70	0.70

[a] The estimated relative sensitivity was calculated verses that of bradykinin.
[b] Result from Chapter 4.
[c] From references [Che95], potential was set at 0.80V against Ag/AgCl reference electrode. Assuming relative sensitivity rating of vasopressin as 0.70 for easy comparing.
[d] For neurotensin, the UV absorbance signal due to the different number of peptide bonds was corrected verses other peptides.

As listed in table 5-7, the estimated relative sensitivities of bradykinin, oxytocin and vasopressin agree well with the experimental results from capillary LC [chapter 4]. One exception is that of neurotensin. Although the number of peptide bonds was taken into consideration when calculating its relative sensitivity, the result still differs significantly from that of capillary LC. As shown in figure 5-6A4 and 5-6A5, free peptide peak and complex I peak continued to decrease as more copper was added. It was possible that with more copper added, free peptide peak and complex I peak would further decrease while the complex II peak would increase. This trend would further decrease the ratio of neurotensin signals listed in table 5-7 and make its true relative sensitivity much smaller than estimated.

When compared to the relative sensitivities of these peptides at glassy carbon electrode, the difference was obvious as listed in table 5-7. At carbon fiber microelectrode, bradykinin was the most sensitive peptide when detecting based on their biuret complexes. The neurotensin was the least sensitive peptide at carbon fiber microelectrode. However, neurotensin was most sensitivity at glassy carbon electrode

while bradykinin was the least sensitive among the peptides tested. This unparalleled sensitivity between carbon fiber microelectrode and glassy carbon electrode together with the difference on the electrochemical signal enhancement with biuret complex suggests different biuret complex oxidation mechanisms of these peptides at different electrode materials.

For substance P, its sensitivity would greatly depend on either complex I peak or complex II peak was the final product. If complex II peak was the final product when a huge excess of copper exists, its estimated sensitivity would be very close to that of vasopressin based on their similar signal ratios of ECD to UV.

A precaution needs to be taken when evaluating peptide sensitivities since many factors can introduce minor variations in the comparison of peptide detection sensitivities, such as different peptide complex migration times in CE-UV-ECD, the inequality of peptide bond UV absorbance, and the eluting peptide peak variances of capillary LC, etc.

Conclusions

It has been shown that the formation of copper peptide biuret complex is highly structure dependent. With the disulfide bond and ring structure in the peptides as in the case of vasopressin and oxytocin, even though they have more than 8 amino acid groups, they only form biuret complex with a copper-to-peptide ratio of one. For other peptide without disulfide bond as a restrictor to their structures such as neurotensin, substance P, and bradykinin, multiple biuret complexes can be formed. For non-electroactive peptides (bradykinin and substance P), the formed biuret complexes enabled their electrochemical detection on the carbon fiber microelectrode. The formed biuret complexes showed

either no enhancement (vasopressin and oxytocin) on the detection of peptide with the presence of copper(II), which could be oxidized at moderate potential, or actually decreased the peptide detection sensitivity (neurotensin) due to the formation of multiple non-electroactive complexes.

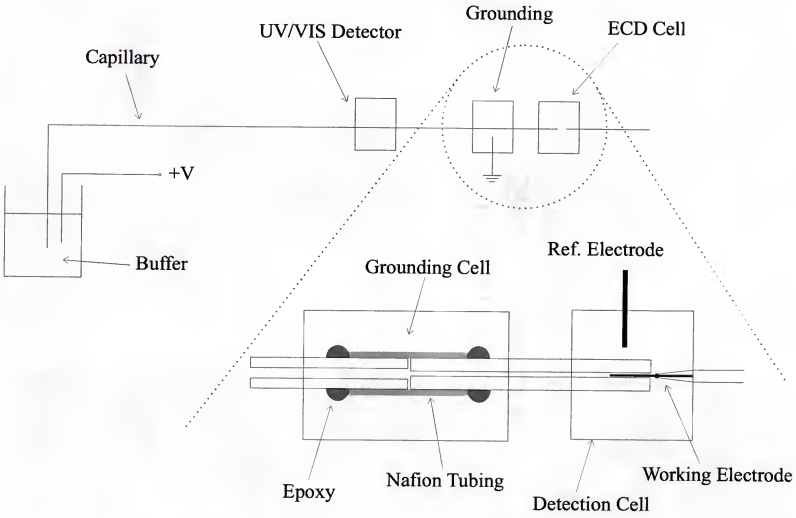

Figure 5-1. Schematic of capillary electrophoresis-UV absorbance-electrochemical detection.

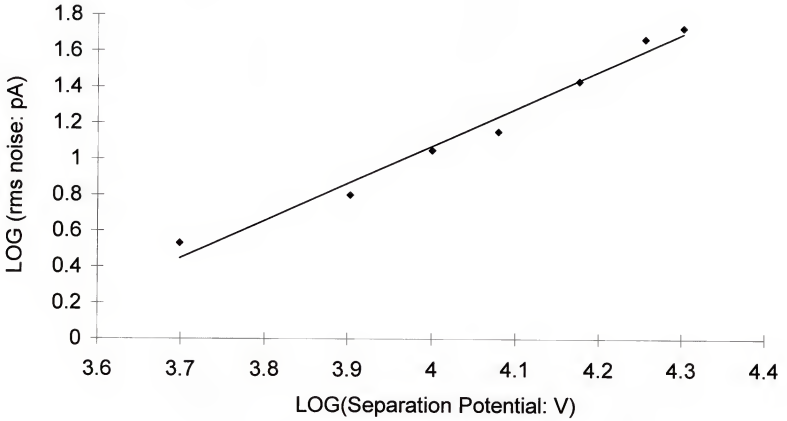

Figure 5-2. Relation between the separation electric field strength and rms noise level on the carbon fiber microelectrode. The detection capillary used here was 360 μm o.d. 50 μm i.d. and 2 cm in length. The gap between the two capillaries was less than 10 μm.

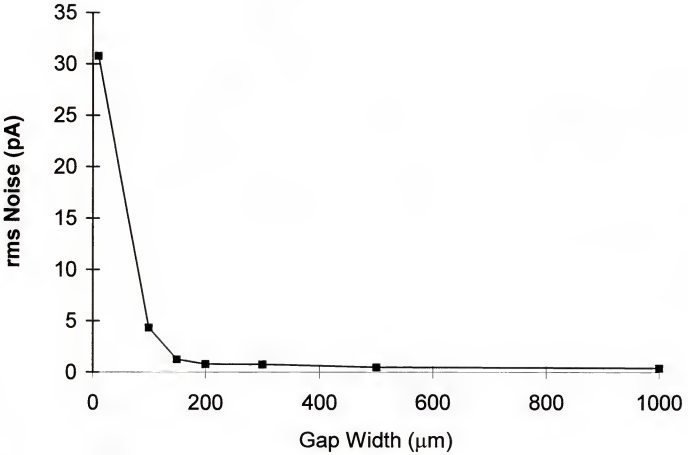

Figure 5-3. Effect of gap width on microelectrode rms noise. The same detection capillary as in figure 5-2 was used but gap widths varied as indicated in the figure. Electric field strength was maintained at 500 V/cm.

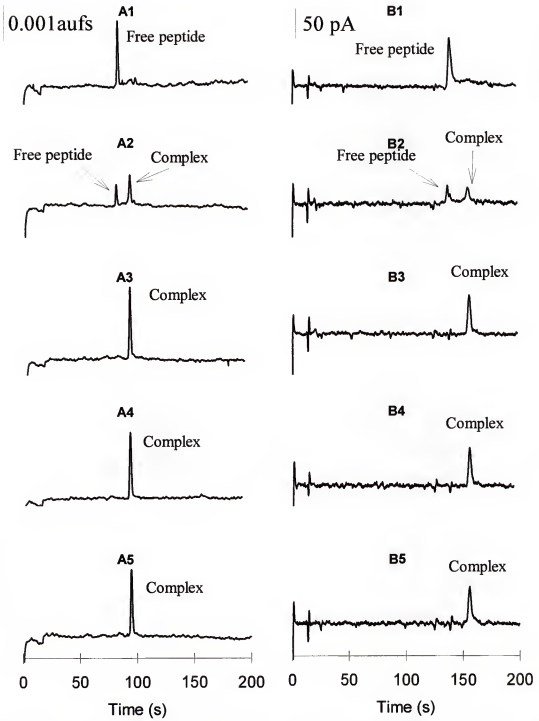

Figure 5-4. CE-UV-EC of vasopressin and its biuret complex detection. Figure A's were from UV and B's were from EC. The copper-to-peptide ratios are 0, 0.5, 1.0, 2.0 and 5.0 for figures with subtitles from 1 to 5. The peptide concentration was 100 μM, injection time was 2 seconds at 2000 V.

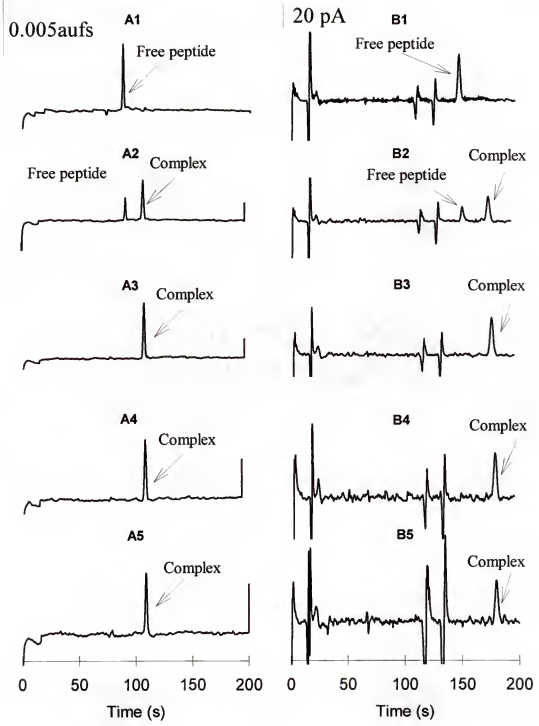

Figure 5-5. CE-UV-EC of oxytocin and its biuret complex detection. Figure A's were from UV and B's were from EC. The copper-to-peptide ratios are 0, 0.5, 1.0, 2.0 and 5.0 for figures with subtitles from 1 to 5. The peptide concentration was 500 μM, injection time was 2 seconds at 5000 V.

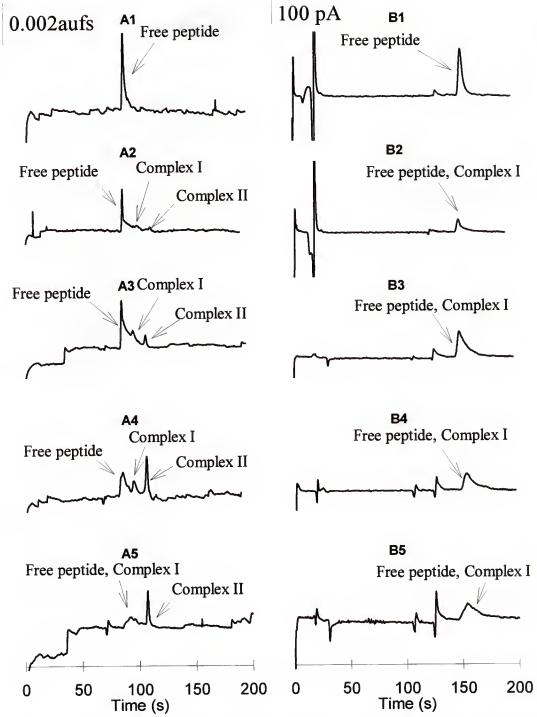

Figure 5-6. CE-UV-EC of neurotensin and its biuret complexes detection. Figure A's were from UV and B's were from EC. The copper-to-peptide ratios are 0, 0.5, 1.0, 2.0 and 5.0 for figures with subtitles from 1 to 5. The neurotensin concentration was 500 μM, injection time was 2 seconds at 5000 V.

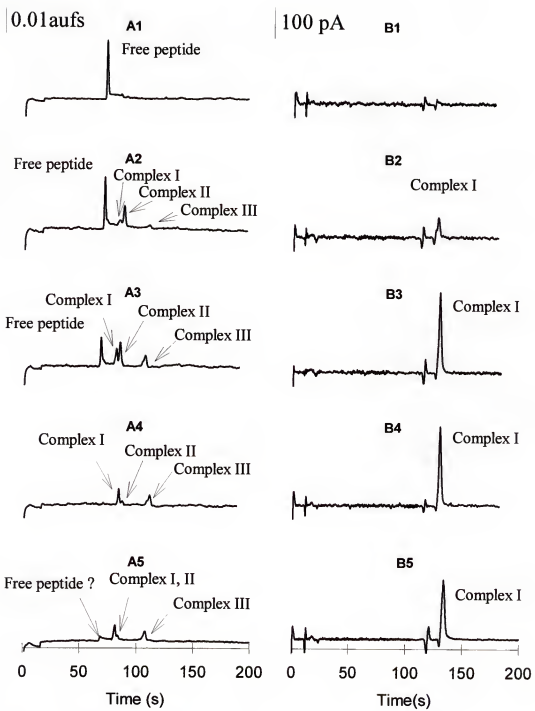

Figure 5-7. CE-UV-EC of bradykinin and its biuret complexes detection. Figure A's were from UV and B's were from EC. The copper-to-peptide ratios are 0, 0.5, 1.0, 2.0 and 5.0 for figures with subtitles from 1 to 5. The peptide concentration was 100 μM, injection time was 2 seconds at 5000 V.

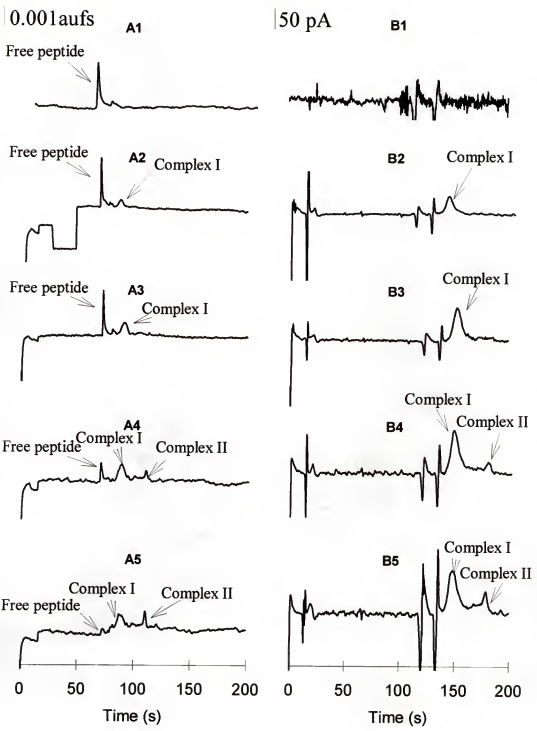

Figure 5-8. CE-UV-EC of substance P and its biuret complexes detection. Figure A's were from UV and B's were from EC. The copper-to-peptide ratios are 0, 0.5, 1.0, 2.0 and 5.0 for figures with subtitles from 1 to 5. The peptide concentration was 500 μM, injection time was 2 seconds at 5000 V.

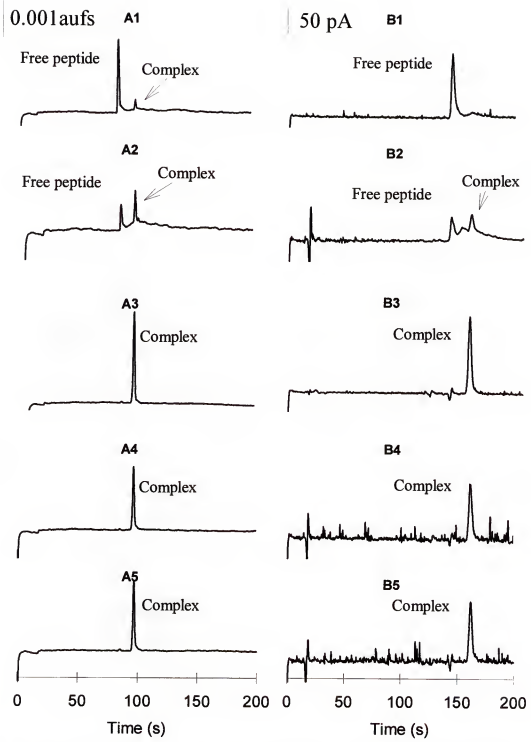

Figure 5-9. CE-UV-EC of vasopressin and its biuret complex detection. Figure A's were from UV and B's were from EC (working electrode was set at 0.80V vs. Ag/AgCl reference electrode). The copper-to-peptide ratios are 0, 0.5, 1.0, 2.0 and 5.0 for figures with subtitles from 1 to 5. The peptide concentration was 100 μM, injection time was 2 seconds at 2000 V.

CHAPTER 6
SUMMARY AND FUTURE DIRECTIONS

The research presented here has focused on bioanalytical method development using capillary liquid chromatography coupled with various detection schemes, including (1) dual microcolumn immunoaffinity/reversed phase chromatography determination of insulin variants; (2) on-line preconcentration capillary liquid chromatography/electrochemical detection (LC/ECD) monitoring of met-enkephalin with microdialysis sampling, (3) monitoring both electroactive and non-electroactive neuropeptides through biuret complexes and (4) determination of electroactivity of peptide copper biuret complexes in different forms by capillary electrophoresis coupled with both UV absorbance and electrochemical detection.

The focus of this dissertation research was to develop low concentration limit of detection method to be applied on bioanalysis. The research demonstrated that in addition to the low mass limit of detection of capillary LC, concentration limit of detection for proteins and peptides in the low picomolar range can be achieved through on-column preconcentration. Up to 1000 fold preconcentration can be achieved through either immunoaffinity interaction or hydrophobic interaction. Coupled with microdialysis sampling, these capillary LC based techniques achieved 5 minute temporal resolution for *in vivo* monitoring of some low concentration neuropeptides such as bradykinin, vasopressin, and met-enkephalin, which was 6 fold improvement compared to that of RIA. With this improved temporal resolution, biological behaviors of these

neuropeptides can be monitored in much short intervals. This improved our capability of obtaining more close to real time biological information that these neuropeptides carry.

In addition to the on-column preconcentration, this dissertation research demonstrated that the formation of copper biuret complex enabled the derivatization and electrochemical detection of non-electroactive peptides at trace concentration. The formed complex can also undergo a on-column preconcentration procedure to improve the concentration limit of detection of non-electroactive peptides (5 pM for bradykinin).

Further improvement of current method seems promising. By further decreasing the inner diameter of capillary column, better limit of detection should be attainable for concentration sensitive detection. Also, the use of laser induced fluorescence detection instead of UV/Vis should further lower the detection limit of DMIA. Other improvements such as shorten overall analysis time, better sample usage (currently 1 μl out of 3 μl collected, which is 33% for the capillary LC/ECD) and on-line coupling system to sampling technique for automation, should also be explored.

As noticed in chapters 4 and 5, there are distinguishable differences between the glassy carbon and carbon fiber microelectrode when they were used to detect biuret complex of electroactive peptides. Glassy carbon can get enhanced signal for electroactive peptides when they form biuret complexes [War89, Tsa90, Tsa91, Tsa92, Che95d]. A glassy carbon based microelectrode will enable us to get better signal for the electroactive peptides. For peptide with more than 8 amino acid groups, the signal could be tripled or even more and this will improve our limit of detection (both mass and concentration) and the temporal resolution of *in vivo* monitoring.

Along with the use of capillary LC, capillary electrochromatography (CEC) is getting more attentions recently due to its liquid chromatographic separation mechanism and capillary electrophoresis like efficiency. With higher theoretical number, the detection limit can also be improved. Combining the improvement from both better electrode material and separation efficiency, the limit of detection might be able to reach the sub attomole level for the capillary LC/ECD peptides analysis. Also, the CEC will enable the use of smaller i.d. capillary without creating the problem of high back pressure in separation.

With currently improved concentration limits of detection for bradykinin, (compared to RIA), 5 minute or less temporal resolution for *in vivo* monitoring of bradykinin in different brain regions can be achieved. By monitoring the change of bradykinin level corresponds to different stimulants, the biological role of bradykinin in the specific brain region can be revealed.

REFERENCES

Adv93 Advis, J. P.; Guzman, N. A. *J. Liq. Chromatogr.*, **1993**,16, 2129-2136.

Afe90 Afeyan, N. B.; Gordon, N. F.; Mazsarofe, D. I.; Varady, L.; Fulton, S. P. *J. Chromatogr.* **1990**, 519, 1-29.

Bag95 Bagdan, B.; Pittman, Q. *J. Neuroscience*, **1995**, 65(3), 869-678.

Bak97 Bakalyar, S. R.; Phipps, C.; Spruce, B.; Olsen, K. *J. Chromatogr. A*, **1997**, 762, 167-185.

Boa83 Boarder, M. R.; Weber, E.; Evans, C. J.; Erdelyi, E.; Barchas, J. *J. Neurochem.*, **1983,** 40, 1517-1527.

Bou94 Bourque, C. W.; Oliet, S. H.; Richard, D. *Front. Neuroendocrinol.*, **1994**, 15(3), 231-274.

Bou97 Bourque, C. W.; Oliet, S. H. *Annu. Rev. Physiol*, **1997**, 59, 601-619.

Bra86 Freeman, W. H. Bradford, *Chemical Neurobiology*, New York, **1986,** 265-316.

Car86a Carlson, R. G.; Srinivasachar R. S.; Matuszewski, B. K. *J. Org. Chem.*, **1986**, 51 3978-3985

Car86b Carr, P. W.; Bergold, A. T.; Hanggi, D. A.; Millei, A. *J. Chromatogr.* Forum, **1986,** Sept/Oct, 31.

Che95a Chen, A.; Lunte, C. E. *J. Chromatogr. A*, **1995,** 691, 29-36.

Che95b Chen, J. G,; Woltman, S. J.; Weber, S. G. *J. Chromatorgr. A,* **1995**, 691, 301-315.

Che95c Chen, J. G.; Vinski, E.; Colizza, K.; Weber, S. G. *J. Chromatorgr. A,* **1995**, 705,171-184.

Che95d Chen, J. G.; Weber, S. G. *Anal. Chem.,* **1995**, 67, 3596-3604.

Chi98 Chiu, D. T.; Lillard, S. J.; Scheller, R. H.; Zare, R. N.; Rodriguez-Cruz, S. E.; Williams, E. R.; Orwar, O.; Sandberg, M.; Lundqvist, A. *Science*, **1998**, 279, 1190-1193

Chu92 Chu, Y. H.; Avila, L. Z.; Biebuyck, H. A.; Whitesides, G. M. *J. Med. Chem.*, **1992**, 35, 2915-2928.

Col93 Cole, L. J.; Schultz, N. M.; Kennedy, R. T. *J. Microcol*, **1993**, 5, 433-442.

Col95 Cole, L. J.; Kennedy, R. T. *Electrophoresis*, **1995**, 16, 549-552.

Coo92 Cooper, B. R.; Jankowski, J. A.; Leszczyszyn, D. J.; Wightman, R. M.; Jorgenson, J. W. *Anal. Chem.*, **1992**, 64, 691-694.

Day81 Dayton, M. A.; Ewing, A.. G.; Wightman, R. M. *Eur. J. Pharmacol.*, **1981**, 75, 141-144.

de93 de-Ceballos, M. L.; Fernandez, A.; Jenner, P.; Marsden, C. D. *Neurosci. Lett.*, **1993**, 160, 163-169.

Dea93 Deacon, M.; O'Shea, T. J.; Lunte, S. M. *J. Chromatogr.* A., **1993**, 652, 377-383.

DeW79 DeWied, D.; Versteeg, D. H. G. *Fed. Proc. Fed. Am. Soc. Exp. Biol.*, **1979**, 38, 2348-2356.

Dov97 Dovichi, N. J. *Electrophoresis*, **1997**, 18, 2393-2399.

Dru85 Drumheller, A. L.; Bachelard, H.; St-Pierre, S.; Jolicoeur, F. B. *J. Liq. Chromatogr.*, **1985**, 8, 1829-1837.

Dur91 During, M. J. in T.E. Robinson and J.B. Justice, Jr. (Editors), *Microdialysis in the Neurosciences* (Techniques in the Behavioral and Neural Sciences, Vol. 7), Elsevier, Amsterdam, **1991**, Chapter 19.

Edm83 Edmonds, T. E.; Ji, G. *Anal. Chim. Acta*, **1983**, 151, 109-121.

Emm95 Emmett, M. R.; Andren, P. E.; Caprioli, R. M. *J. Neurosci. Meth.*, **1995**, 62, 141-147.

Enj79 Enjalbert, A.; Ruberg, M.; Arancibia, S.; Priam, M.; Kordon, C. *Nature*, **1979**, 280, 160-162.

Ewi93 Ewing, A. G. *J. Neurosci. Meth.*, **1993**, 48(3) 215-24.

Ewi94 Ewing, A. G.; Mesaros, J. M.; Gavin, P. F. *Anal. Chem.,* **1994**, 66, 537A-542A.

Fau84 Fausnaugh, J. L.; Kennedy, L. A.; Regnier, F. E. *J. Chromatogr.,* **1984**, 317, 141-155.

Fer96 Fernandez, A.; de Ceballos, M. L.; Rose, S.; Jenner, P.; Marsden, C. D. *Brain*, **1996**, 119, 823-831.

Flu93 Flurer, C. L.; Novotny, M. *Anal. Chem.*, **1993**, 65, 817-824.

Fur95 Furtado, S.; Suchowersky, O. *Can. J. Neurol. Sci.*, **1995**, 22, 5-13.

Gen94 Geng, X. D.; Reginer, F. E. *J. Chromatogr.,* **1994**, 296, 15-30.

Gis87 Gishizky, M. L.; Gerold, G. M. *FEBS Lett.*, **1987**, 223, 227-236.

Gon80 Gonon, F.; Buda, M.; Cespuglio, R.; Jouvet, M.; Pujol, J. F. *Nature*, **1980**, 286, 902-904.

Guo87 Guo, D. C.; Mant, C. T.; Hodges, R. S. *J. Chromatogr.,* **1987**, 386, 205-222.

Hat92 Hattori, T.; Sundberg, D. K.; Morrise, M. *Brain Res. Bull.*, **1992**, 28, 257-263.

Her72 Hertel, P.; Math, J. M.; Nomikos, G. G.; Iurlo, M.; Math, A. A.; Svensson, T. H. *Behavioural Brain Research*, **1972**, 103-114.

Her93 Hernandez, L.; Tucci, S.; Guzman, N.; Paez, X. *J. Chromatogr.* A, **1993**, 652, 393-401.

Hor87 Horsfall, A. C.; Brown, C. M.; Maini, R. N. *J. Immunol. Meth.*, **1987**, 104, 43-51.

Hor95 Horn, T.; Bauce, L.; Landgraf, R.; Pittman, Q. J. *J. Neurochem.*, **1995**, 64, 1632-1644.

Hug75 Hughes, J. T. *Brain Res.*, **1975**, 88, 295-302.

Hur95 Hurst, W. J.; Zagon, I. S. *J. Liq. Chromatogr.*, **1995**, 18, 2943-2949.

Ive79 Iversen, L. L. *Sci. Am.*, **1979**, 241, 118-126.

Jan88 Janis, L. J.; Regnier, F. E. *J. Chromatogr.*, **1988**, 444, 1-12.

Jan89a Janis, L. J.; Grott, A.; Regnier, F.E.; Smith-Gi11, S.J. *J. Chromatogr.*, **1989**, 476, 235-244.

Jan89b Janis, L. J.; Regnier, F. E. *Anal. Chem.*, **1989**, 61, 1901-1917.

Jor81 Jorgenson, J. W.; Lukacs, K. D. *Anal. Chem.*, **1981**, 53, 1298-1304.

Jor83 Jorgenson, J. W.; Lukacs, K. D. *Science*, **1983**, 222, 266-272.

Kad81 Kadekro, M.; Summy-long, J. Y.; Freeman, S.; Harris, J. S.; Terrell, M. L.; Eisenberg, H. M. *Anal. Chem.*, **1981**, 53, 1354-1362

Kan97 Kanazawa, H,; Nagatsuka, T.; Miyazaki, M.; Matsushima, Y. *J. Chromatogr. A* **1997**, 763, 23-29.

Kar74 Karger, B. L.; Martin, M.; Guiochon, G. *Anal. Chem.*, **1974**, 46, 1640-1647.

Kar85 Kariya, K.; Yamauchi, A.; T. Sasaki, T. *J. Neurochem.*, **1985**, 44, 1892-1897.

Kar88 Karlsson, K. E.; Novotny, M. *Anal. Chem.*, **1988**, 60, 1662-1669.

Kaw93 Kawagoe, K. T.; Zimmerman, J. B.; Wightman, R. M. *J. Neurosci. Meth.*, **1993**, 48, 225-240.

Ken72 Kennedy, G. J.; Knox, J. H. *J. Chromatogr. Sci.*, **1972**, 10, 549-556

Ken89 Kennedy, R. T.; Jorgenson, J. W. *Anal. Chem.*, **1989**, 61, 1128-1132.

Ken90 Kendrick, K. M.; *J. Neurosci. Meth.*, **1990**, 34, 35-46.

Kne84 Knecht, L. A.; Guthrie, E. J.; Jorgenson, J. W. *Anal. Chem.*, **1984**, 56, 479-482.

Lad96 Lada, M. W.; Kennedy, R. T. *Anal. Chem.*, **1996**, 68, 2790-2798.

Lan91 Landgraf, R.; Ludwig, M. *Brain Res.*, **1991**, 558, 191-196.

Lau86 Lauer & McManigill, *Anal. Chem.*, **1986**, 58, 166-174.

Li95 Li, X. M.; Tanganelli, F. S.; O'Connor, W. T.; Hasselrot, U.; Ungerstedt, U.; Fuxe, K. *J. Neural Transm.* **1995**, 102, 125-137.

Lom79 Lomedico, P.; Rosenthal, N.;. Efstratiadis, A.; Gilbert, N.; Kolodner, R.; Tizard, R. *Cell*, **1979**, 18, 545-552.

Lu93 Lu, W,; Cassidy, R. M.; Baranski, A. S. *J. Chromatogr.*, **1993**, 640, 433-440.

Lud92 Ludwig, M.; Landgraf, R. *Brain Res.*, **1992**, 576, 231-234.

Lud94 Ludwig, M.; Callahan, M. F.; Neumann, I.; Landgraf, R.; Morris, M. *J.Neuroendocrinol.,* **1994**, 6(4), 369-373.

Lud95 Ludwig, M.; Callahan, M. F.; Morris, M. *Neuroendocrinol.*, **1995**, 62, 619-627.

Lud97 Ludwig, M.; johnstone, L. E.; Neumann, I.; Landgraf, R.; Russell, J. A. *Cell Tissue Rev.* **1997**, 287(1), 79-90.

Ma95 Ma, Y. H.; Wang, J.; Rodd, G. G.; Bolaffi, J. L.; Grodsky, G. M. *Eur. J. Endocrinol.*, **1995**, 132, 370-379.

Mai89 Maidment, N. T.; Brumbaugh, D. R.; Rudolph, V. D.; Erdelyi, E.; Evans, C. *J. Neuroscience*, **1989**, 33, 549-557.

Mai91 Maidment, N. T.; Siddall, B. J.; Rudolph, V. R.; Erdelyi, E.; Evans, C. J. *Neuroscience*, **1991**, 45, 81-93.

Mar83 Margerum, D. W. *Pure & Appl. Chem.*, **1983**, 55, 23-34.

Mon94 Monnig, C. A.; Kennedy, R. T. *Anal. Chem.*, **1994**, 66, 280R-314R.

Moo93 Moore Jr. A. W.; Jorgenson, J. W. *Anal. Chem.*, **1993**, 65, 188-196.

Neu93 Neumann, I.; Ludwig, M.; Engelmann, M.; Pittman, Q. J.; Landgraf, R. *J. Neuroendocrinol.*, **1993**, 58, 637-645.

Neu96 Neumann, I.; Douglas, A. J.; Pittman, Q. J.; Russell, J. A.; Landgraf, R. *J. Neuroendocrinol.*, **1996**, 8, 227-233.

Nov88 Novotny, M. *Anal. Chem.,* **1988**, 60, 500A-510A.

Oat89 Oates, M. D.; Jorgenson, J. W. *Anal. Chem.*, **1989**, 61, 432-441.

Ogo93 Ogorevc., B.; Tavcar, G.; Hudnik, V.; Pejovnik, S. J. *Electroanal. Chem.*, **1993**, 351, 81-90.

Ole90 Olefirowicz T. M.; Ewing, A. G. *Anal. Chem.,* **1990**, 62, 1872-1876.

Orw91 Orwar, O.; Folestad, S.; Einarsson, S. E.; Andine P.; Sandberg, M. *J. Chromatogr.*, **1991**, 566, 39-52.

Orw95 Orwar O. *Anal Chem.*, **1995**, 67, 4261-4268.

O'Sh92 O'Shea, T. J., Greenhagen, R. D., Lunte, S. M., Lunte C. E. *J. Chromatogr.*, **1992**, 593, 305-312

Par95a Park, S.; Lunte, C. E. *Anal. Chem.*, **1995**, 67, 4366-4374.

Par95b Paras, C. D.; Kennedy, R. T. *Anal. Chem.*, **1995**, 67, 3633-3637.

Pel67 Pellegrino, L.; Pellegrino A.; Cushman, A. *A Stereotaxic Atlas of the Rat Brain*, Century Crofts, New York, **1967**, 167-167.

Riv83 Rivier, J.; McClintock, R. *J. Chromatogr.,* **1983**, 268, 112-119.

Rob91 Robinson, T. E.; Justice, J. B. Jr. (Editors), *Microdialysis in the Neurosciences* (Techniques in the Behavioral and Neural Sciences, Vol. 7), Elsevier, Amsterdam, **1991**.

Sag84 Sagar, S. M.; Beal, M. F.; Marshall, P. E.; Landis, D. M. D.; Martin, J. B. *Peptides*, **1984**, 5 suppl. 1, 255-267.

Sar78 Sar, M.; Stumpf, W. E.; Miller, R. J.; Chang, K. J.; Cuatrecasas, P. J. *Comp. Neurol.*, **1978**, 182, 17-25.

Sau84 Sauter, A.; Frick, W. J. *J. Chromatogr.*, **1984**, 297, 215-225.

Sch83 Schroer, J. A.; Bender, T.; Feldmann, R. J.; Kim, K. J.; *Eur. J. Immunol.*, **1983**,13, 693-699.

Sch95 Schultz, N. M.; Huang, L.; Kennedy, R. T. *Anal. Chem.*, **1995**, 6, 924-929.

She97a Shen, H.; Aspinwall, C. A.; Kennedy, R. T. *J. Chromatogr. B*, **1997**, 689, 295-303.

She97b Shen, H.; Lada, M. W.; Kennedy, R. T. *J. Chromatogr. B*, **1997**, 689, 43-52.

Siv91 Sivam, S. P. *Neuropeptides,* **1991**, 18, 210-219.

Slo93 Sloss, S.; Ewing, A. G. *Anal. Chem.*, **1993**, 65, 577-581.

Smi94 Smigol, V.; Svec, F.; Frechet, J. M. J. *Anal. Chem.*, **1994**, 66, 4308-4315.

Sny80 Snyder, S. H. *Science*, **1980**, 209, 976-983.

St.85 St. Claire, R. L.; Jorgenson, J. W. *J. Chromatogr. Sci.*, **1985**, 23, 186-197.

Sue83 Suelter, C. H.; Deluca, M. *Anal. Biochem.*, **1983**, 135, 112-119.

Tao96 Tao, L.; Kennedy, R. T. *Anal. Chem.*, **1996**, 68, 3899-3906.

Toi95 Toide, K.; Iwamoto, Y.; Fujiwara, T.; Abe, H. J. *Pharmacol. Exp. Therap.*, **1995**, 274, 1370-1378.

Tsa90 Tsai, H.; Weber, S. G. *J. Chromatogr. A*, **1990**, 515, 451-457.

Tsa91 Tsai, H.; Weber, S. G. *J. Chromatogr. A*, **1991**, 542, 345-350.

Tsa92 Tsai, H.; Weber, S. G. *Anal. Chem.,* **1992**, 64, 2897-2903.

Tse59 tselivs, A. G. *J. Chromatogr. A*, **1959**, 142, 349-362.

Van89 Vanfleteren, J. R. *Anal. Biochem.*, **1989**, 178, 385-390.

Ver92 Verbalis, J. G.; Dohanics, J. *J. Chromatogr. A*, **1992**, 544, 225-231.

Vis96 Vissers, J. P. C.; de Ru, A. H.; Ursem, M.; Chervet, J. P. *J. Chromatogr. A*, **1996**, 746, 1-13.

Wag86 Wages, S. A.; Church, W. H.; Justice, J. B. Jr. *Anal. Chem.,* **1986**, 58, 1649-1657.

Wal87 Wallingford, R. A.; Ewing, A. G. *Anal. Chem.*, **1987**, 59, 1762-1766.

Wal88 Wallingford, R. A.; Ewing, A. G. *Anal. Chem.*, **1988**, 60, 1972-1975.

Wam80 Wamsley, J.K.; Young, W. S.; Kuhar, M. J. *Brain Res.,* **1980**, 190, 153-160.

War89 Warner, A. M.; Stephen G.; Weber, S. G. *Anal. Chem.,* **1989**, 61, 2664-2668.

Wil94 Wilkinson, M. F.; Horn, T. F. W.; Kasting, N. W.; Pittman, Q. J. *J. Physiology*, **1994**, 481.3, 641-646.

Wol95a Woltman, S. J.; Alward, M. R.; Weber, S. G. *Anal. Chem.,* **1995**, 67, 541-551.

Wot95b Wotjak, C.; Kalsbeek, A.; Buijs, R. M.; Engelmann, M. T.; Landgraf, R. *Brain Res.,* **1995**, 682, 75-82.

Zha96 Zhang, C. X.; Thormann, W. *Anal. Chem.*, **1996**, 68, 2523-2532.

Zho95 Zhou, S. Y.; Zuo, H.; Stobaugh, J. F.; Lunte, C. E.; Lunte, S. E. *Anal. Chem.,* **1995**, 67, 594.

Zim95 Zimmerli, B.; Dick, R. *J. Chromatogr. B,* **1995**, 666, 85-99.

BIOGRAPHICAL SKETCH

Hong Shen was born in Tianjin, China, on September 2, 1963. He spent his happy childhood mostly with his loving grandparents. After 13 years of education he received a Bachelor of Science degree in chemistry from Fudan University, Shanghai, China, in July 1984. After working three years as an engineer at the Institute of Atomic Energy in Beijing, he returned to Fudan University for his graduate study. He obtained a Master of Science degree majoring in radiochemistry in July 1990. During this period he married his lovely wife after being in love with each other for almost 7 years. He came to the United States in 1993 to further his graduate study at the University of Florida. In 1994 one of the most important events in his life happened: the birth of Kevin, "the Hong Jr.," in Gainesville, Florida. He completed his research and was awarded a Doctor of Philosophy degree in May 1998.

I certify that I have read this study and that in my opinion it conforms to acceptable standards of scholarly presentation and is fully adequate, in scope and quality, as a dissertation for the degree of Doctor of Philosophy.

Robert T. Kennedy, Chairman
Associate Professor of Chemistry

I certify that I have read this study and that in my opinion it conforms to acceptable standards of scholarly presentation and is fully adequate, in scope and quality, as a dissertation for the degree of Doctor of Philosophy.

Anna F. Brajter-Toth
Associate Professor of Chemistry

I certify that I have read this study and that in my opinion it conforms to acceptable standards of scholarly presentation and is fully adequate, in scope and quality, as a dissertation for the degree of Doctor of Philosophy.

Richard A. Yost
Professor of Chemistry

I certify that I have read this study and that in my opinion it conforms to acceptable standards of scholarly presentation and is fully adequate, in scope and quality, as a dissertation for the degree of Doctor of Philosophy.

Randolph S. Duran
Associate Professor of Chemistry

I certify that I have read this study and that in my opinion it conforms to acceptable standards of scholarly presentation and is fully adequate, in scope and quality, as a dissertation for the degree of Doctor of Philosophy.

Nancy D. Denslow
Associate Scientist of Biochemistry and Molecular Biology

This dissertation was submitted to the Graduate Faculty of the Department of Chemistry in the College of Liberal Arts and Sciences and to the Graduate School and was accepted as partial fulfillment of the requirements for the degree of Doctor of Philosophy.

May, 1998

_____

Dean, Graduate School